2011

DYNAMIC RESPONSE AND DAMAGE EVOLUTION OF COMPOSITE MATERIALS SUBJECTED TO UNDERWATER EXPLOSIVE LOADING: AN EXPERIMENTAL AND COMPUTATIONAL STUDY

James LeBlanc
University of Rhode Island, James.M.LeBlanc@navy.mil

DYNAMIC RESPONSE AND DAMAGE EVOLUTION OF COMPOSITE MATERIALS SUBJECTED TO UNDERWATER EXPLOSIVE LOADING: AN EXPERIMENTAL AND COMPUTATIONAL STUDY

BY

JAMES LEBLANC

A DISSERTATION SUBMITTED IN PARTIAL FULFILLMENT OF THE REQUIREMENTS FOR THE DEGREE OF

DOCTOR OF PHILOSOPHY

IN

MECHANICAL, INDUSTRIAL AND SYSTEMS ENGINEERING

UNIVERSITY OF RHODE ISLAND

2011

DOCTOR OF PHILOSOPHY DISSERTATION

OF

JAMES LEBLANC

APPROVED:

Thesis Committee:

Major Professor Dr. Arun Shukla

Dr. Martin Sadd

Dr. David Taggart

Dr. K. Wayne Lee

Dr. Nasser H. Zawia

DEAN OF THE GRADUATE SCHOOL

UNIVERSITY OF RHODE ISLAND
2011

ABSTRACT

The dynamic response and damage evolution of composite materials subjected to underwater explosive loading has been studied. The study utilizes both experimental and numerical techniques to aid in the understanding of the behavior of these materials under shock loading conditions. The objective of the project is to develop a better understanding of the response of composite materials when subjected to shock loading conditions leading to more efficiently designed structures. The focus of the work is on performing high fidelity experiments under controlled shock loading and corresponding finite element simulations of the experiments. The work is divided into three phases, each of which build and expand upon the preceding work.

In the first phase of the research the transient response and development of damage mechanisms of E-Glass / Epoxy composite plates is studied. The plates are bi-axial laminates consisting of a non-woven, parallel fiber construction, and are round, flat disks. The work consists of experiments, utilizing a water filled conical shock tube and computational simulations, utilizing the commercially available LS-DYNA finite element code. Two series of experiments have been performed and simulated: (1) a reduced energy series which allowed for the use of strain gages and (2) a series with increased energy which imparted material damage. The strain data obtained from the reduced energy experiments and the corresponding simulations are correlated using the Russell Error measure, a mathematical technique which evaluates the differences in two transient data sets by quantifying the variation in magnitude and phase. It is shown that there is a high level of correlation between the experiments and the simulations when using this measure. Additionally the extent of the damage, including the individual mechanisms, from the high energy experiments and simulations are compared and show good agreement.

The objective of the second phase of the project was to increase the geometrical complexity of the composite plates by shifting from flat to curved mid-sections. The plates utilized in the second part of the study are E-Glass / Vinyl Ester, 0/90 biaxial laminates. The water filled conical shock tube is utilized to impart shock loading to the plates. Computational finite element simulations are performed with the LS-DYNA finite element code. The transient response of the plates was measured using a three-dimensional (3D) Digital Image Correlation (DIC) system, which included high speed photography and specialized post processing software. This ultra high speed system records full field shape and displacement profiles in real time. The transient response of the plates is compared to the simulation results using both point-wise time histories as well as full field deformation profiles. The DIC data and the computational results show a high level of correlation using the Russell Error measure.

The third phase of the project investigates the relative response of three different laminate constructions. The objective is to determine the effectiveness of the laminate variations on increasing the performance of the laminate used in the second phase. Specifically, to improve the dynamic response and mitigate the damage mechanisms that were observed in the experiments from phases one and two. Three laminate constructions have been investigated: (1) a baseline 0°/90° biaxial layup, (2) a 0°/90° biaxial layup that includes a thin glass veil between plies, and (3) a 0°/90° biaxial layup that has a coating of polyurea applied to the back face. The digital image correlation system is used to capture the real-time deformation and velocity response of the plates. The use of polyurea is shown to improve the material performance, while the inclusion of lightweight veils between the plies is shown to negatively affect the response.

ACKNOWLEDGEMENTS

First and foremost I would like to my advisor Dr. Arun Shukla for his guidance, assistance, and patience throughout the duration of my work. His patience and inspiring nature has been a great source of motivation throughout my doctoral studies. Additionally I thank Dr. Sadd, Dr. Taggart, and Dr. Lee for serving as members of my doctoral committee.

I would like to thank my wife Vinessa, my parents Ray and Holly, my siblings Chris, Jennifer, and Allison, and my parent in-laws Vincent and Christine for their understanding nature, and support through this degree program and all of my academic pursuits.

The financial support of the Naval Undersea Warfare Center - Division Newport (NUWCDIVNPT) In-house Laboratory Independent Research program (ILIR) directed by Dr. Anthony Ruffa is greatly acknowledged. Additionally, the support of the Office of Naval Research under ONR Grant No. N00014-10-1-0662 (Dr. Y.D.S. Rajapakse) is acknowledged. Finally, the support provided by NUWCDIVNPT through the Long Term Training program is appreciated.

The help and encouragement from my friends and colleagues are greatly appreciated. I would like to thank all of my lab mates in the dynamic photo-mechanics laboratory. Specifically Nate Gardner, Nicholas Heeder, and Ryan Sekac for their assistance with the usage of the DIC equipment during shock testing. Additionally the departmental support of Nancy Dube, Jen Cerullo, Joe Gomez, and Jim Byrnes is acknowledged. The help and assistance of the NUWC Survivability Lab personnel for their operation of the shock tube facility, measurement equipment, and machining resources; Specifically, Bruce Booker, Brian Ploutz, Steve Morin, Marty Leff, Jim Sinclair, Don Arsenault, and Ken Medeiros. Additionally the support of my supervisors and mentors at NUWC including Kevin Behan and Stephen Turner is acknowledged.

PREFACE

This dissertation is prepared using the manuscript format.

The current study is an investigation into the dynamic response and damage evolution of composite materials subjected to underwater explosive (UNDEX) loading conditions. The research consists of experimental and numerical components to study the material behavior. The composite plates which are used in the study are round discs with both flat and curved mid-sections. A water filled conical shock tube is utilized to impart the shock loading conditions to the plates. The transient response of the plates is captured in real time with strain gages and digital image correlation (DIC). Finite element modeling of the experiments has been performed utilizing the LS-DYNA code available from the Livermore Software Technology Corporation (LSTC). The experimental data and the computational results show a high level of correlation using the Russell Error measure.

Chapter 1 provides a survey of historical and current published literature of subject matter relevant to this dissertation. The topics covered include methods for imparting shock loading to materials, investigations of the effects of shock loading on both metallic and composite materials, and the use of advanced materials to improve the shock response of these materials. The studies which examine the effect of shock loading on materials consist of experimental and computational work. This chapter serves to lay the groundwork for the dissertation and highlight the work that has been done in this field to date.

Chapter 2 presents the effects of underwater shock loading on flat, E-Glass / Epoxy composite plates. The work consists of experiments, utilizing the water filled conical shock tube and computational simulations, utilizing the commercially available LS-DYNA finite element code. Two experimental series have been performed and simulated: (1) a reduced energy series

which allowed for the use of strain gages and (2) a series with increased energy which imparted material damage. The strain gage data and the computational results show a high level of correlation using the Russell error measure. The finite element models are also shown to be able to simulate the onset of material damage by both in-plane and delamination mechanisms. The chapter will follow the formatting guidelines specified by *Composite Structures*.

Chapter 3 presents the response of E-Glass / Vinyl Ester curved composite panels subjected to underwater explosive loading. The work consists of experimental work utilizing the water filled conical shock tube facility and computational simulations with the commercially available LS-DYNA finite element code. The composite specimens are 0/90 biaxial laminates with a thickness of approximately 1.3 mm. The samples are round panels with curved midsections. The transient response of the plates is measured using a three-dimensional (3D) Digital Image Correlation (DIC) system, including high speed photography. This ultra high speed system records full field shape and displacement profiles in real time. The DIC data and the computational results show a high level of correlation using the Russell Error measure. The chapter will follow the formatting guidelines specified by *Composite Structures*.

Chapter 4 investigates the relative response of three E-Glass / Vinyl ester laminates subjected to underwater explosive loading. The plates are round plates with curved midsections. The constructions are: (1) a baseline 0°/90° biaxial layup, (2) a 0°/90° biaxial layup that includes a thin glass veil between plies, and (3) a 0°/90° biaxial layup that has a coating of polyurea applied to the back face. The work consists of experiments utilizing the water filled, conical shock tube facility. The samples are round panels with curved midsections, and are approximately 2.54 mm in thickness. The transient response of the plates is measured using a three-dimensional (3D) Digital Image Correlation (DIC) system, along with high speed

photography. The results show that the performance of the baseline laminate is improved when coated with the polyurea material, but conversely is degraded by the inclusion of the glass veils between plies. The chapter will follow the formatting guidelines specified by *International Journal of Impact Engineering.*

TABLE OF CONTENTS

LIST OF TABLES

TABLE PAGE

CHAPTER 2

CHAPTER 3

CHAPTER 4

LIST OF FIGURES

FIGURE PAGE

CHAPTER 2

CHAPTER 3

FIGURE PAGE

CHAPTER 4

FIGURE PAGE

CHAPTER 1

INTRODUCTION AND LITERATURE REVIEW

1. INTRODUCTION

Composite materials have been widely used in a variety of applications in the marine, automotive, and transportation industries. These materials offer the advantages of high strength to weight ratios, reduced maintenance costs, and improved corrosion resistance. Recently, there has been an increased interest in composite materials for use in military applications including land vehicles (structural components and armor solutions), advanced ship hull designs, and submarine components. The use of these materials in wartime environments requires that they not only be able to withstand the loads produced by everyday use but also those imparted from explosions and high speed projectile impacts. In particular, when used in submarine applications these structures must be able to survive underwater explosion (UNDEX) events. Currently, the response of these materials at static and quasi-static loading rates is well understood. However, the response at the high strain rates that shock and ballistic events can induce is not well understood. This leads to an inherent conservative approach to be taken when these structures are designed and constructed. Typically this results in structures which do not fully realize the weight savings afforded by these materials. This results in a need to understand the behavior of these materials not only at strain rates associated with static load levels ($10^{-4} – 10^{-3}$) but also at loading rates many orders of magnitude higher (10^{-1} - 10^{3}). The focus of the current research is on the response of composite materials subjected to underwater explosions, UNDEX.

The objective of this project is to develop a better understanding of the characteristics of composite materials subjected to shock loading conditions, specifically the dynamic response and damage evolution. The goal was to develop both experimental techniques and

computational modeling methods to aid in the understanding. The experimental aim was to formulate a procedure which subjects the composite material to shock loading conditions in a repeatable and controlled manner while measuring the transient response on the surface of the material. The damage imparted due to the load is also studied. Well instrumented, quality experiments will facilitate and aide in the development of finite element techniques for modeling the dynamic response of composite materials, which can then be extended to large or complicated structures that cannot be easily tested due to size or cost constraints. Validation of these techniques in a controlled laboratory environment and then transitioning them to real structures can make this a powerful tool, equivalent to the currently available prediction tools for metallic structures. Computational modeling techniques utilizing the commercial finite element code LS-DYNA are developed to accurately simulate the experiments. The goal of the development of this methodology was to develop a process which can be applied early in the design phase of new structures to identify any structural inadequacies. An understanding of the ability of these materials to sustain damage while retaining structural integrity is necessary. As the navy is involved in the design and operation of vehicles such as UUV's and composite structures external to the hull of submarines this research would allow for better design of these structures without increasing the danger to personnel or equipment. The over design of these structures could be reduced, resulting in the ability to carry more equipment or simply stronger and lighter structures.

This project is an initial step in bringing the understanding of composite response to UNDEX loading to the maturity level of metallic materials. The behavior of metallic materials during and after a shock event is sufficiently understood such that structures can be designed in a manner which ensures they are not significantly over designed so as to avoid the addition of

unnecessary weight. This work is important as composite structures are rapidly replacing their metallic counterparts as they lend themselves well to manufacturing of complex geometries in a more cost effective manner.

The work is an extension of the previous work in that it includes real time observations of the material response during the loading event itself. These real-time measurements are made using strain gages and digital image correlation. The digital image correlation technique allows for full field shape and displacement profiles to be measured on the composite plates in real time rather than the single point measurements provided by strain gages. Prior work in this field has been limited to observing the amount of damage present after a loading event whereas this work strives to capture the damage progression and transient response of the structure through experimental and computational methods. Furthermore the development and validation of finite element models to simulate the transient response and damage progression in composite plates, with comparison to experimental data, is an area in which there have been minimal publications on which knowledge can be drawn.

2. LITERATURE REVIEW

Interest in the dynamic response of materials and structures to shock loading has continued to increase in recent years. Traditionally, this work has focused on the behavior of metallic materials; however there is now an increased interest in advanced materials including composites. A wide variety of techniques and methods have been developed to aid in the understanding of materials under shock loading conditions. These include experimental methods, development of analytical models, and computational simulations.

Historically, there have been two experimental methodologies used to impart shock loading conditions to structures: (1) explosives and (2) shock tubes. Although the use of

explosives offers an ease of use, there are associated deficiencies such as spherical wave fronts and pressure signatures which are often spatially complex and difficult to capture. Shock tubes offer the advantage of plane wave fronts and wave parameters that are easily controlled and repeated. The current study utilizes a water filled, conical shock tube that replicates the free field pressure wave expansion of an underwater explosion.

Conical shock tubes have historically been designed and built with the intent to replicate the pressure wave propagation as generated by the open water, free field explosion of a spherical charge. The guiding principle is that if the walls of the tube are sufficiently rigid then the radial distribution of the free field pressure wave can be replicated in laboratory setting (Coombs, 1967). Tubes of this type are typically horizontally mounted and water filled, with a conical internal shape. An explosive charge is located at the apex of the cone and is subsequently detonated. The tube geometry represents a solid angle segment of the pressure field that results from the detonation of a spherical, explosive charge. In an open water environment the pressure expands from the charge location as a spherical wave. In the shock tube the rigid wall acts to confine the expansion of the pressure wave in a manner that simulates a conical sector of the pressure field. Using this type of tube, a small amount of explosive is able to replicate the effects of much larger charges in free field environments. An effective amplification factor is typically utilized to relate the weight of the charge in the tube to the weight of a free field charge. This factor is defined by Poche and Zalesak (1992) as the ratio between the weight of a spherical charge, W, required to produce the same peak pressure at a given standoff distance as that produced in the shock tube by a segment of charge weight, w. Further discussion on the development and history of the water filled conical shock tube is provided by Coombs et al (1967) and Filler (1964).

The response of materials subjected to shock and impact loading has been studied over a wide range of loading rates. The effect of shock loading on steel plates subjected to underwater impulsive loads has been presented by Espinosa et al (2006). Nurick et al (1995, 1996) have studied the effects of boundary conditions on plates subjected to blast loading and identified distinct failure modes depending on the magnitude of the impulse and standoff. Studies by Jacinto et al. (2001) and Stoffle et al. (2001) have focused on the dynamic response of plates when subjected to varying levels of blast and shock loading. Experimental studies performed Wierzbicki et al. (1996) aimed at studying the large deformations and failure modes of thin plates subjected to blast loads.

Work by Zaretsky et al (2004) and Yuan et al (2007) has studied the damage characteristics of composite materials when subjected to low velocity impacts. Franz et al. (2002) and Mouritz et al. (1995) studied the effects of an underwater explosion at different standoff distances on a glass composite laminate. The amount of explosive and the standoff distance were varied in order to see the effect of both variables on plate damage. The response of E-Glass and Carbon based composite laminates under shock and explosive loading (including the effects of heat generation during combustion) has been presented by Tekalur et al (2008). Mouritz (2001) studied the effectiveness of adding a light weight, through thickness stitching material to increase the damage resistance of composites subjected to UNDEX loading. LeBlanc et al (2007) have studied the effects of shock loading on three-dimensional woven composite materials. Recently, there has been an increased interest in the study of the effect of shock loading on sandwich structures. These studies include the effects of shock and impact loading conditions (Jackson et al (2011), Schubel et al (2007), Arora et al (2010)).

When composite materials are subjected to loading conditions they may experience damage in the form of several distinct mechanisms occurring in the in-plane and through thickness directions. The in-plane mechanisms consist of fiber breakage and matrix cracking, while the through thickness damage is dominated by delamination of the plies. Composite materials typically have high in plane strengths due to their construction using oriented layers of continuous fibers. The weakness of these materials is found in the through thickness direction. In this direction the material strength is governed by the resin as there are no fibers oriented in this direction. The resin has lower tensile and shear strengths as compared to the fibers. This through thickness weakness typically leads to delamination damage when the plates are subjected to through thickness loading or flexural conditions. Recently, weaving processes have evolved to where it is possible to make structural cloth materials which also include through thickness fibers and show the ability to improve this through thickness weakness (LeBlanc et al (2007), Tekalur et al (2009), Bogdanovich et al (2001)). This damage is increasingly found in composite materials subjected to shock or impact loading. Under shock loading a compression wave will pass through the thickness of the material and then be reflected off of the back face as a tensile wave. Simultaneously there is also a tensile unloading wave passing from the front face of the material toward the back. This unloading wave (also referred to as a release wave) corresponds to the decay phase (negative slope) of the incident loading (Wang, 2004). In reality the incident wave is composed of a loading front followed by an unloading front. If the unloading wave and the reflected wave meet in a ply interface, de-bonding may occur if the waves combine to exceed the tensile strength of the resin. These waves have a greater chance of meeting in composite materials due the lower wave speed compared to metallic parts (Dyka et al.

(1998)). The interaction of the tensile release and reflected waves is the same phenomenon that is often responsible for the formation of surface spalling in metallic materials.

Analytical damage models for composites have been widely developed and are continually being refined and updated. These models typically assign an internal damage variable to each of the types of damage of interest (ie. matrix cracking, fiber rupture) which, in simple form, are ratios of the stress state to a failure criteria (Matzenmiller et al (1995), Zako et al (2003), Dyka et al (1998)). Matzenmiller et al (1995) have presented a mathematical model for damage of composite materials that develops a relationship between the level of material damage and the effective elastic properties of the material. For each of the significant damage mechanisms (fiber rupture, fiber buckling, matrix crushing, and matrix cracking) an internal variable describes the evolution of the damage as a function of loading. Based upon the expression representing each damage variable the effective elastic properties can be degraded when the variable reaches a critical value. Based upon the expression representing each damage variable, the effective elastic properties can be degraded when the variable reaches a critical value. As the mechanical properties must be continually updated to account for the damage degradation this methodology lends itself well to implementation into finite element codes.

The finite element modeling of damage in composites has been performed primarily on models simulating strain rates up to those representing drop test experiments with some work performed at the high strain rate regimes expected in shock loading. Material models are currently being implemented into existing commercial finite element codes (O'Daniel et al (2005), McGregor et al (2007), Williams and Vaziri (2001)) however the validation work with these models has been limited to the low strain rate regime not experienced under blast / shock loading conditions. Recent publications involving computational modeling of damage

progression in composites have utilized LS-DYNA and the Mat_162 (Mat_Composite_OPTION) material model which simulates fiber breakage, matrix cracking and delamination damage. This material model combines the progressive failure theory of Hashin and the damage mechanics approach of Matzenmiller et al (1995). Gama et al (2004) and Xiao et al (2007) have published results from quasi-static punch shear loading experiments which correlate well with simulations utilizing the Mat_162 material model. Simulations of low velocity impact experiments have been documented in the work by Donadon et al (2008) and Hosseinzadeh et al (2006). Furthermore, Batra and Hassan (2007) have studied the response of composites to UNDEX loading through numerical simulations; however there are no comparisons to experimental results. Although the dynamic experiments have been simulated, the results taken from these models have been limited to the prediction of damage area and final deformations rather than comparisons to transient response. Historically the material inputs are determined from quasi-static test data, an assumption which has been shown to be reasonable in simulations of composite materials subjected to high velocity impacts, Chan et al. (2007). This observation has been supported in the current work which investigates the underwater shock loading of composites.

The use of polyurea materials to enhance the failure resistance of materials subjected to explosive loading has recently become a topic of interest. Polyurea is a synthetic, high strength / high elongation coating that is typically spray cast onto existing structures to increase their resistance to shock and ballistic/shrapnel loading events such as those of a bomb blast. The armed forces have begun to investigate the suitability of these materials for use on military and naval vehicles such as Humvees, troop carriers and ship hulls, Hodge (2004). Research efforts have focused on the use of polyurea coatings on steel plates, composite plates, and as inner

layers of sandwich composites. Amini et al (2010, 2010, 2010) have studied the effects of monolithic and polyurea coated steel plates subjected to impulsive loads and showed that polyurea has a positive damage mitigation effect when applied to the back face of the material. They also found that polyurea can enhance the loading and damage levels if applied on the impact side of the plates. Gardner et al (under review, 2011) studied the effect of polyurea in sandwich composites. It was observed that when a layer of polyurea is placed between the foam core and the back face of the sandwich the blast resistance is improved, while conversely if the polyurea is placed between the front face and the foam core the performance is degraded.

CHAPTER 2

DYNAMIC RESPONSE AND DAMAGE EVOLUTION IN COMPOSITE MATERIALS SUBJECTED TO UNDERWATER EXPLOSIVE LOADING: AN EXPERIMENTAL AND COMPUTATIONAL STUDY

by

James LeBlanc and Arun Shukla

has been published in Composite Structures, 92, pp 2421-2430, 2010.

Corresponding Author: James LeBlanc

Naval Undersea Warfare Center (Division Newport)

1176 Howell Street

Newport, RI, 02841

Phone: +1-401-832-7920

Email Address: James.M.LeBlanc@Navy.Mil

Abstract

The effect of underwater shock loading on an E-Glass / Epoxy composite material has been studied. The work consists of experimental testing, utilizing a water filled conical shock tube and computational simulations, utilizing the commercially available LS-DYNA finite element code. Two test series have been performed and simulated: (1) a reduced energy series which allowed for the use of strain gages and (2) a series with increased energy which imparted material damage. The strain gage data and the computational results show a high level of correlation using the Russell error measure. The finite element models are also shown to be able to simulate the onset of material damage by both in-plane and delamination mechanisms.

1. Introduction

Within the naval community there is an interest in constructing new vehicles and structures from composite materials to exploit their high strength to weight ratios, resulting in lighter structural components. In a military environment these structures must be designed in a manner in which they will be able to survive an underwater explosion (UNDEX) event. This results in a need to understand the behavior of these materials not only at strain rates associated with static load levels ($10^{-4} – 10^{-3}$) but also at loading rates many orders of magnitude higher (10^{-1} - 10^{3}). The static response of composite materials is well understood while there is less of an understanding in terms of what happens to the same composite material when subjected to high loading rates. Currently the composite structures in use by the navy are designed with large safety factors to ensure that damage will not occur during a shock event. Due to these large safety factors the structures are often significantly over designed to the point that the full weight savings afforded by composite materials is not realized.

Historically there have been two experimental methodologies used to impart shock loading from a fluid to a structure: (1) explosives and (2) shock tubes. Although the use of explosives offers an ease of use, there are associated deficiencies such as spherical wave fronts and pressure signatures which are often spatially complex and difficult to measure. Shock tubes offer the advantage of plane wave fronts and wave parameters that are easily controlled and repeated.

When composite materials are subjected to loading conditions they may experience damage in the form of several distinct mechanisms occurring in the in-plane and through thickness directions. The in-plane mechanisms consist of fiber breakage and matrix cracking, while the through thickness damage is dominated by delamination of the plies.

Relevant experimental studies on composite materials have studied the material response over a range of loading rates. Work by Zaretsky et al [1] and Yuan et al [2] has studied the damage characteristics of composite materials when subjected to low velocity impacts while Mouritz [3] has studied the damage resulting from high rate UNDEX loading. LeBlanc et al [4] have studied the effects of shock loading on three-dimensional woven composite materials. The results of these experimental studies however are limited to the study of post mortem properties of the materials. Once the loading, low or high rate, has been used to induce damage to the materials, the residual strength or fatigue properties are determined.

The study of damage mechanisms in composite materials can be grouped into three categories: (1) Mathematical formulations, (2) Numerical implementation into finite element software and (3) Experimental studies. Matzenmiller et al [5] have presented a mathematical model for damage of composite materials that develops a relationship between the level of material damage and the effective elastic properties of the material. For each of the significant

damage mechanisms (fiber rupture, fiber buckling, matrix crushing, and matrix cracking) an internal variable describes the evolution of the damage as a function of loading. Based upon the expression representing each damage variable the effective elastic properties can be degraded when the variable reaches a critical value. As the mechanical properties must be continually updated to account for the damage degradation this methodology lends itself well to implementation into finite element codes.

The finite element modeling of damage in composites has been performed primarily on models simulating strain rates up to those representing drop test experiments with some work performed at the high strain rate regimes expected in shock loading. Material models are currently being implemented into existing commercial finite element codes (O'Daniel et al [6], McGregor et al [7], Williams and Vaziri [8]) however the validation work with these models has been limited to the low strain rate regime not experienced under blast / shock loading conditions. Recent publications involving computational modeling of damage progression in composites have utilized LS-DYNA and the Mat_162 (Mat_Composite_OPTION) material model which simulates fiber breakage, matrix cracking and delamination damage. This material model combines the progressive failure theory of Hashin and the damage mechanics approach of Matzenmiller et al [5]. Gama et al [9] and Xiao et al [10] have published results from quasi-static punch shear loading experiments which correlate well with simulations utilizing the Mat_162 material model. Simulations of low velocity impact experiments have been documented in the work by Donadon et al [11] and Hosseinzadeh et al [12]. Furthermore Batra and Hassan [13] have studied the response of composites to UNDEX loading through numerical simulations; however there are no comparisons to experimental results. Although the dynamical experiments have been simulated, the results taken from these models have been limited to the

prediction of damage area and final deformations rather than comparisons to transient response. Historically the material inputs are determined from quasi-static test data, an assumption which has been shown to be reasonable in simulations of composite materials subjected to high velocity impacts, Chan et al. [14]. This observation has been supported in the current work which investigates the underwater shock loading of composites.

2. Composite Material

The composite material studied in this investigation is Cyply® 1002, a reinforced plastic manufactured by Cytec Engineered Materials. The material is a cured epoxy composite which utilizes a non-woven, parallel fiber construction. The fibers are continuous E-Glass filaments. A cross-ply construction has been utilized in this study and has alternating plies of 0° and 90° with each ply having a thickness of 0.254 mm (0.01 in.). The cured material has an areal weight of 0.46 kg/m^2 (0.85 lb/yd^2) per ply (0.254 mm) and a specific gravity of 1.85. The resin content is 36 ± 3%. Thicknesses of 3.3 mm (0.130 in.) and 4.82 mm (0.190 in.) have been chosen for use in the current project with each thickness having 13 and 19 plies, respectively. Due to the odd number of plies there is an additional ply in the 0° direction. The laminate schedule for the 3.3 mm (0.130 in.) material is as follows [0/90/0/90/0/90/0/90/0/90/0/90/0] with a similar schedule for the 4.82 mm (0.190 in.) material, only with 3 more additional 0/90 layers. The material properties for the material are provided in table 1.

Table 1 - Cyply 1002 Crossply - Mechanical Properties

	N/m^2 (lb/in^2)
Tensile Modulus (0°)	23.4e9 (3.4e6)
Tensile Modulus (90°)	23.4e9 (3.4e6)
Tensile Strength (0°)	482e6 (70e3)
Tensile Strength (90°)	482e6 (70e3)
Compressive Strength (0°)	689e6 (100e3)
Compressive Strength (90°)	689e6 (100e3)

3. Shock Loading Apparatus

A conical shock tube (CST) facility located at the Naval Undersea Warfare Center, Division Newport was utilized in the shock loading of the composite materials. The shock tube is a horizontally mounted, water filled tube with a conical internal shape, Figure 1. The internal cone angle of the tube is 2.6 degrees and simulates the free field pressure wave expansion in an open water environment. The tube is 5.25 m (207 in.) long from the charge location to the location of the test specimen and internally contains 98.4 L (26 gallons) of water at atmospheric pressure. The pressure shock wave is initiated by the detonation of an explosive charge at the breech end of the tube (left side of figure) which then proceeds down the length of the tube. A typical pressure profile obtained from the use of the tube is shown in figure 2.

The shock tube has the ability to be configured in two ways: (1) Utilizing a sliding piston, and (2) the piston removed and replaced by a fixed end cap. The purpose of the sliding piston is to absorb energy in order to reduce the loading that the specimen will experience when the weight of the explosive charge cannot be reduced further. The fixed end cap configuration allows the test specimen to absorb the full energy of the pressure wave. Both configurations have been utilized in this study. The reasons will discussed later in the paper.

Mounting fixtures have been designed such that the test specimens are air backed with fully clamped edges. The specimens are 26.54 cm (10.45 in.) in overall diameter with a 22.8 cm (9 in.) unsupported middle section. The mounting arrangments for both tube configurations, slider included and fixed end cap, are shown in figures 3a and 3b respectively.

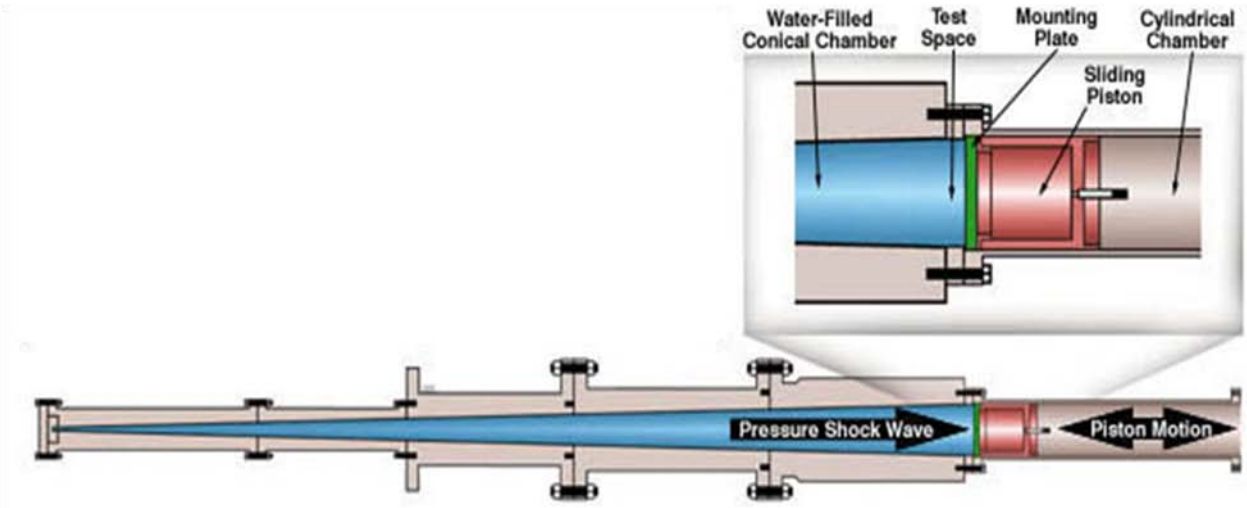

Figure 1 - Conical Shock Tube Schematic

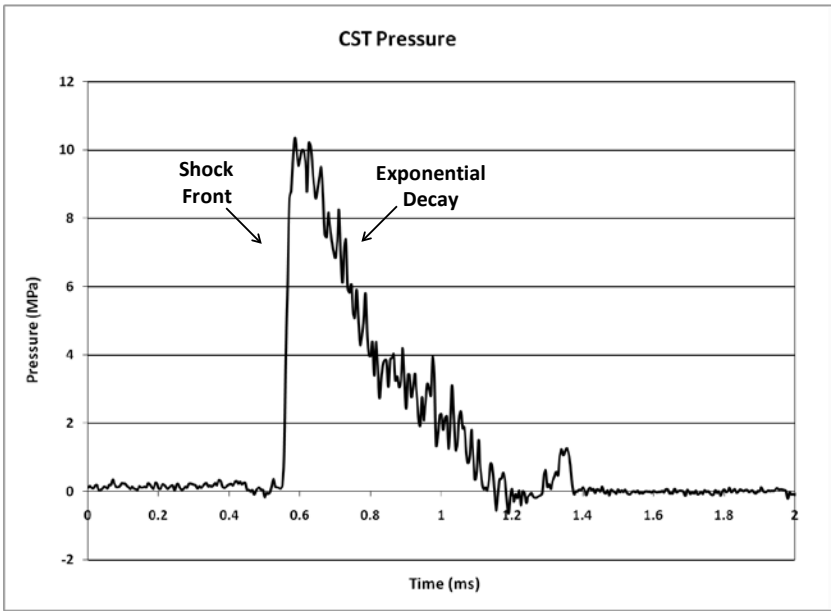

Figure 2 - Shock Tube Pressure Profile

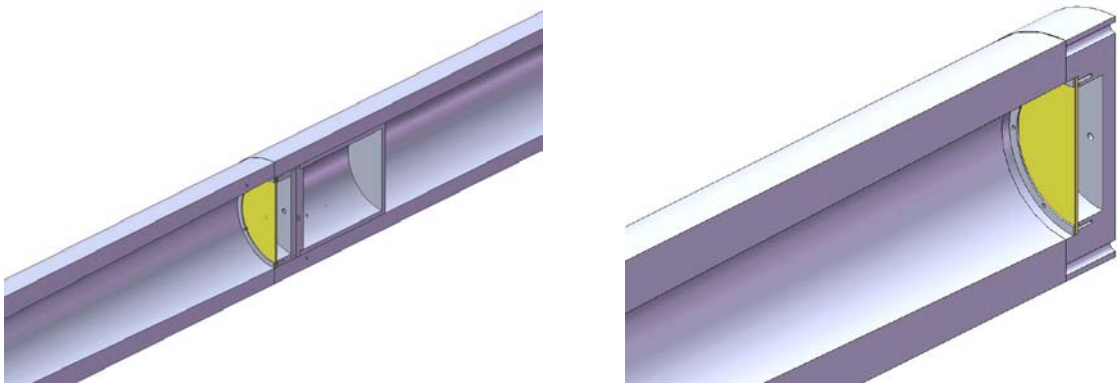

Figure 3 - (a) Slider Mounting Configuration, (b) Fixed Base Mounting Configuration

4. Experimental Testing

Shock testing of the composite material has been performed with the CST in each of the two configurations, slider included and fixed end cap. The reason for utilizing the slider is that a lower loading level of the plates was desired than was possible utilizing the smallest amount of charge permissible (blasting cap only). Although this does not decrease the pressure loading that the plate experiences, the slider does absorb some of the energy that otherwise would be directed into the plate. Lower energy testing was used to decrease the loading level on the plates to the point where it would be possible to instrument the dry face of the test samples with strain gages with the expectation that they would remain attached during the shock event. The strain gage data served to provide a link for correlation between the experimental results and the finite element results to be discussed later. The use of the fixed end cap configuration allows the plate to absorb the full energy level and sustain a suitable level of damage for comparison to the finite element model results.

4.1 Testing with Slider Assembly

A series of two tests was performed utilizing the slider mechanism in order to capture strain gage data on the dry side of test samples. One test was performed with each of the two

thickness materials, 3.3 mm (0.130 in.) and 4.82 mm (0.190 in.). The dry (non-impact) face of each of the samples was instrumented with four (4) tri-axial strain gages, which measured strains in the 0°, 45°, and 90° gage directions. The gages were mounted as seen in figure 4, with one gage located at the center of the panel and three gages located at a 7.62 cm (3 in.) radius from the center along the 0°, 45°, and 90° material directions. For all tests the strains were recorded at a sampling rate of 200 KHz.

For the test performed with the 4.82 mm (0.190 in.) thick test sample 9 of the 12 gages provided suitable output, while the other 3 suffered from de-bonding. In the case of the test performed with the 3.3 mm (0.130 in.) plate only one suitable gage reading was obtained. This being the 0° gage direction on the gage located at a 7.62 cm (3 in.) radius along the 0° material direction. The low survival rate of the gages on the 3.3 mm (0.130 in.) plate can be expected as this plate has more out of plane flexure during the loading than the case of 4.82 mm (0.190 in.) plate. The strain profiles obtained from the test of the 4.82 mm (0.190 in.) plate for the three gages located along the 0° material direction are shown in figure 5.

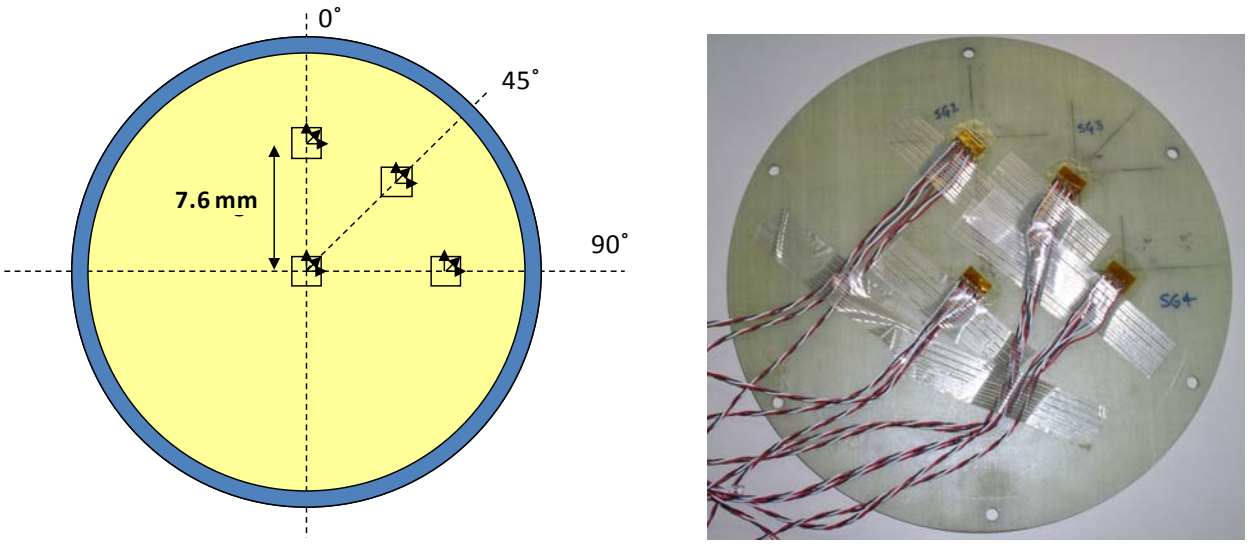

Figure 4 - Strain Gage Mounting Pattern

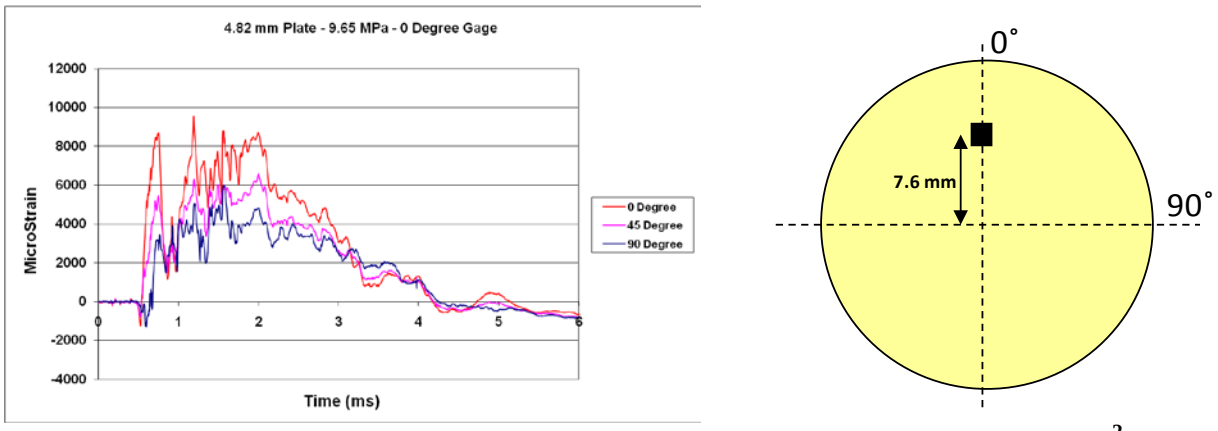

Figure 5- Strain Gage Results, 4.82 mm (0.190 in.) Plate at 9.65 MPa (1400 lb/in^2) Shock Pressure

5. Finite Element Modeling

Finite element modeling of the testing has been performed utilizing the LS-DYNA code available from the Livermore Software Technology Corporation (LSTC). All simulations are generated with Version 971, Release 3.1 and are run in double precision mode.

The composite plate in the simulations is modeled using solid brick elements with a constant stress element formulation (Type 1). The model of the 3.3 mm (0.130 in.) plate is

shown in figure 6 and consists of 7 layers of solid elements. Each layer represents a 0° and 90° combined ply (0.508 mm (0.02 in.) thick) with an additional single 0° layer (0.254 mm (0.01 in.) thick) in the middle of the layup. The holes represent the through bolt holes present in the test samples used for mounting the plate to the fixture. In the through thickness material direction the elements have an edge length of 0.508 mm (0.02 in.). The in plane element edge lengths are approximately 2.54mm (0.1 in.) with 95% of elements having an aspect ratio of 5:1 or less.

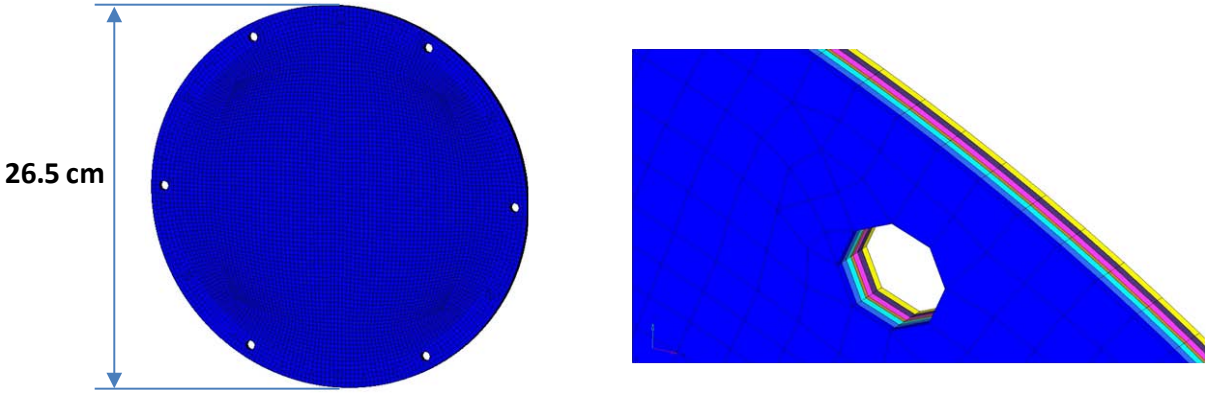

Figure 6 - Finite Element Model of Composite Plate

The LS-DYNA material model that is utilized in this work is Mat_Composite_Failure_*Option*_Model (Mat_059, Option=Solid). This is an orthotropic material definition capable of modeling the progressive failure of the material due to any of several failure criterion including tension / compression in the longitudinal and transverse directions, compression in the through thickness direction, and through thickness shear. Published descriptions of how each failure mode is handled are scarce, however there is some informal documentation available from LSTC. For each possible failure mode there is an internal variable which is checked throughout the analysis to determine if failure in that mode is present. Once failure due to one mode is triggered the load carrying ability of the material in that

direction is reduced to zero. It is important to note that failure in one direction does not cause the element to be deleted. An element is only deleted from the analysis after it has failed in all directions and can no longer carry any load. The input material properties are those provided in table 1. The material model inputs are derived from static tensile and compression testing with no modifications for strain rate effects. It was seen that the static properties provide reasonable results for shock loading conditions. This observation has been seen in literature addressing the ballistic impact problem as well. Chan et al. [14] have shown that the use of static properties is reasonable when applied to composite materials subjected to strain rates associated with high velocity impacts.

In the current modeling effort delamination damage is considered and is taken into account through the use of a surface-to-surface tiebreak contact definition. Using this approach each ply is modeled as a solid layer of elements but the nodes between plies are not equivalenced but rather tied together. The tie break definition initially ties the nodes between plies together to inhibit sliding motion. The nodal force at each node is monitored and checked against a predefined normal and shear force designated in the contact definition. If either the normal or shear force exceeds the defined value then the tie definition for that node is deleted and the node is free to slide. It is important to note that once the tie component of the contact definition is deleted the contact for that node transitions to a standard definition. This allows the slave node to slide and separate from the master surface but not pass through it. Therefore, individual plies can separate but not pass thorough one another.

The complete finite element model of the CST test setup is shown in figure 7. The model consists of the internal fluid of the shock tube, the composite test sample, and the mounting plate

/ slider assembly. No numerical damping has been applied to the model. The fluid within the tube is considered in the simulation so as to capture the fluid structure interaction (FSI) at the interface of the fluid and test plate. As will be shown later, this is a critical interaction to consider as the pressure loading on the plate is not uniform across its face. Only the first 1.01 m (40 in.) of the fluid extending from the test sample towards the charge location are modeled. This was deemed to be acceptable for 2 reasons: (1) the fluid is loaded with the pressure profile measured 50.8 cm (20 in.) from the test sample and (2) a non-reflecting boundary layer is applied at the charge side boundary of the fluid domain. The non-reflecting boundary allows the wave that is reflected from the plate to leave the fluid domain but not reenter. The fluid is modeled with solid elements and a null material definition. The use of the null material allows for the material to be defined with an equation of state (EOS) definition. A linear polynomial EOS is utilized for this model for which only the bulk modulus and density of the water is defined. This allows for an accurate propagation of the pressure wave in the water in a computationally efficient manner. The pressure load is applied as a plane wave at the location of the test pressure transducer. The pressure profile that was measured for each test is applied to the respective model. The fluid structure interaction is handled through the use of a tied-surface-to-surface (LS-DYNA keyword *Contact_Tied_Surface_To_Surface) contact definition. In this method two contact surfaces (*Set_Segment) are defined for which the nodes are tied together. For the coupling of the fluid and composite plate the two surfaces are (1) the fluid face where it contacts the plate, and (2) the plate face where it contacts the fluid. The mounting plate is simulated by a nodal constraint set that forces the nodes in the clamped area of the plate, figure 8, in the first and last ply to move together in the normal direction while they are free to move in-plane independently. The slider mechanism is accounted for through the use of a spring-damper beam

definition. The stiffness and damping properties were determined by running a series of simulations in which the displacement of the mounting plate was compared to the response measured during the test with a linear variable displacement transducer (LVDT) which measured the displacement of the slider during the test.

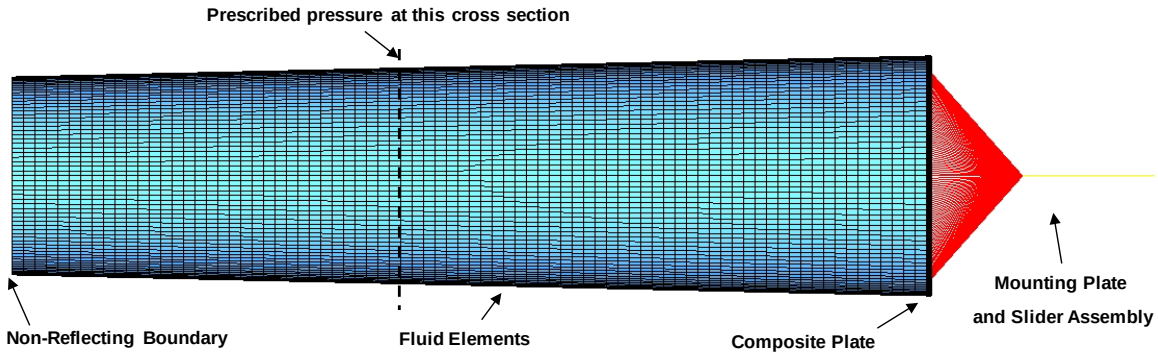

Figure 7 - CST Finite Element Model

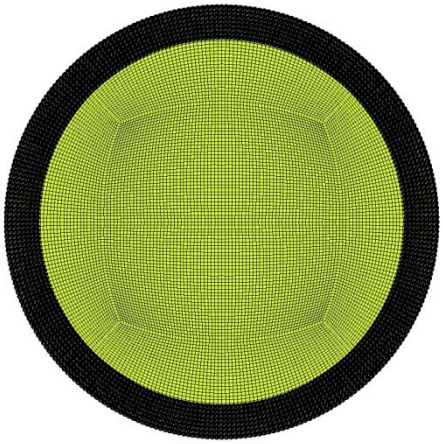

Figure 8- Composite Plate - Clamped Nodes

6. Finite Element Simulation Results

The finite element simulation of the shock tube testing allows for a visual full field representation of the interaction between the pressure wave and the composite plate, whereas the pressure profile obtained from the transducer gives only a single point history. The pressure

field in the fluid as it interacts with and loads the plate, for the case of the 4.82 mm (0.190 in.) plate with the slider mechanism, is shown in the left side of figure 9. The associated plate response is shown in right side of the figure. The time as shown in these figures, is the analysis time with zero taken at the initiation of the pressure field 50.8 cm (20 in.) from the test sample. Figure 9 illustrates several key points. First, although the pressure wave is uniform (planar) prior to its impact with the test plate, the pressure becomes both complex and non-uniform when it interacts with and loads the plate itself. It is evident that there is a low pressure area that develops in the center of the plate while the clamped edge is loaded with high pressure. This can be attributed to the relatively low stiffness of the unsupported area of the plate as compared to the clamped edge of the plate where it is supported by the mounting ring. It is seen that the arrival and full reflection of the pressure wave take place over approximately 0.2 ms. The second point is that the loading of the plate and the associated response can be separated into two distinct time regimes. Where the pressure wave is fully reflected by 0.53 ms, the plate does not start to deform until 0.6ms. The plate reaches full deformation at 1.8 ms and returns to its initial shape at 3 ms. Therefore there is clearly a time lag from when the plate is fully loaded due to the pressure wave, to when plate structurally responds. A similar result is seen for the case of the 3.3 mm (0.130 in.) plate test with the slider, as well as the testing done with the fixed end cap fixture.

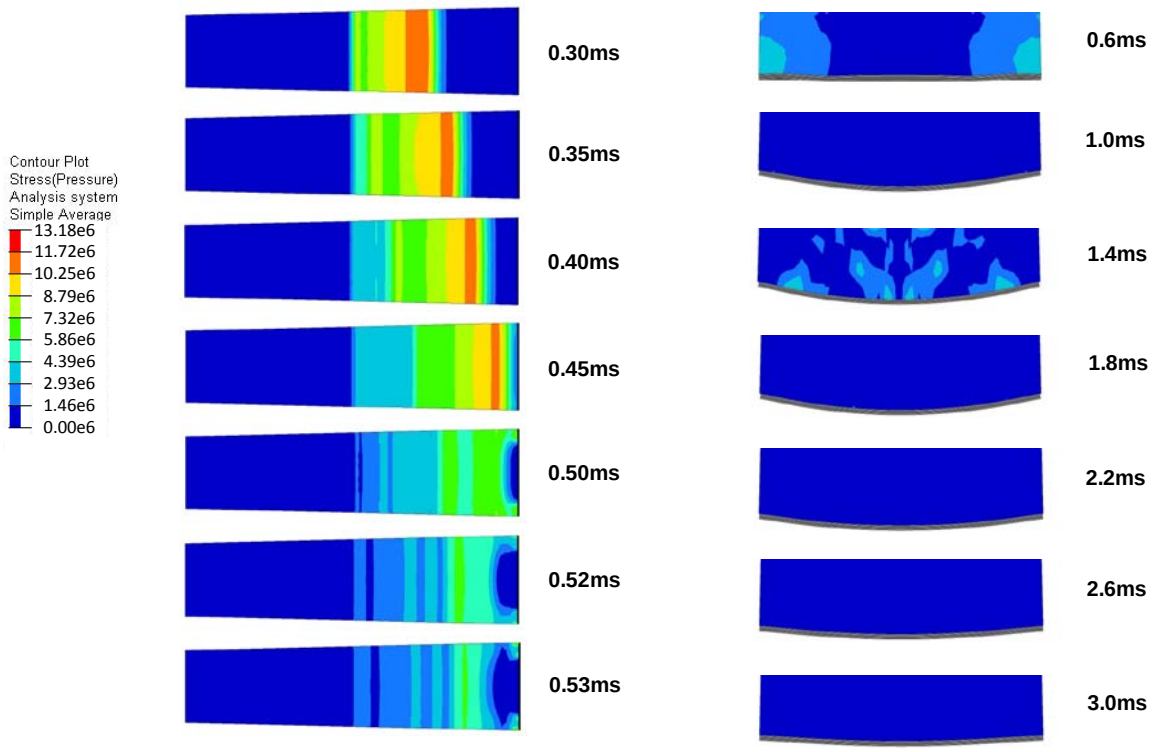

Figure 9- (a) Fluid - Plate Interaction , (b) Plate response (Units of Pa)

6.1 Strain Gage Data – Simulation correlation to Test

The strain gage data that was captured during the experiments performed with the slider assembly is used as a basis to correlate and validate the finite element model results. The quality of the correlation between the test data and numerical results in this study is quantified using the Russell Comprehensive Error measurement. The Russell error technique is one method which evaluates the differences in two transient data sets by quantifying the variation in magnitude and phase. The magnitude and phase error are then combined into a single error measure, the comprehensive error factor. The full derivation of the error measure is provided by Russell [15] with the phase, magnitude, and comprehensive error measures respectively given as:

$$RP = \frac{1}{\pi}\cos^{-1}\left(\frac{\sum c_i m_i}{\sqrt{\sum c_i^2 \sum m_i^2}}\right)$$

$$RM = sign(m)\log_{10}(1 + |m|)$$

$$RC = \sqrt{\frac{\pi}{4}\left(RM^2 + RP^2\right)}$$

In the above equations c_i and m_i represent the calculated (simulated) and measured responses respectively. Excellent, acceptable, and poor correlation using the Russell error measure is given as: Excellent - RC≤0.15, Acceptable – 0.15<RC≤0.28, and Poor RC>0.28. The definition of these criteria levels are the result of a study that was undertaken to determine the correlation opinions of a team in support of a ship shock trial. A summary of the process used to determine the criteria is presented by Russell [16].

The strain gage data comparisons for the shock test performed with the 4.82 mm (0.190 in.) thick plate and slider assembly is shown in figures 10, 11, and 12 for the 0° and 90° gage directions. A summary of the Russell error for each of these tests as well as the gage that survived from the 3.3 mm (0.130 in.) test is provided in table 2. From these graphical comparisons and error summary it is seen that there is a high level of correlation between the experimental results and the computational simulations. Five of the six strain profiles that are compared from the 4.82 mm (0.190 in.) plate thick test fall within the acceptable regime, including 4 in the excellent regime. The gage that remained attached from the 3.3 mm (0.130 in.) test also shows acceptable correlation. This level of agreement between the test and finite element data is encouraging since strain gage data is notoriously difficult to correlate to and match with simulations.

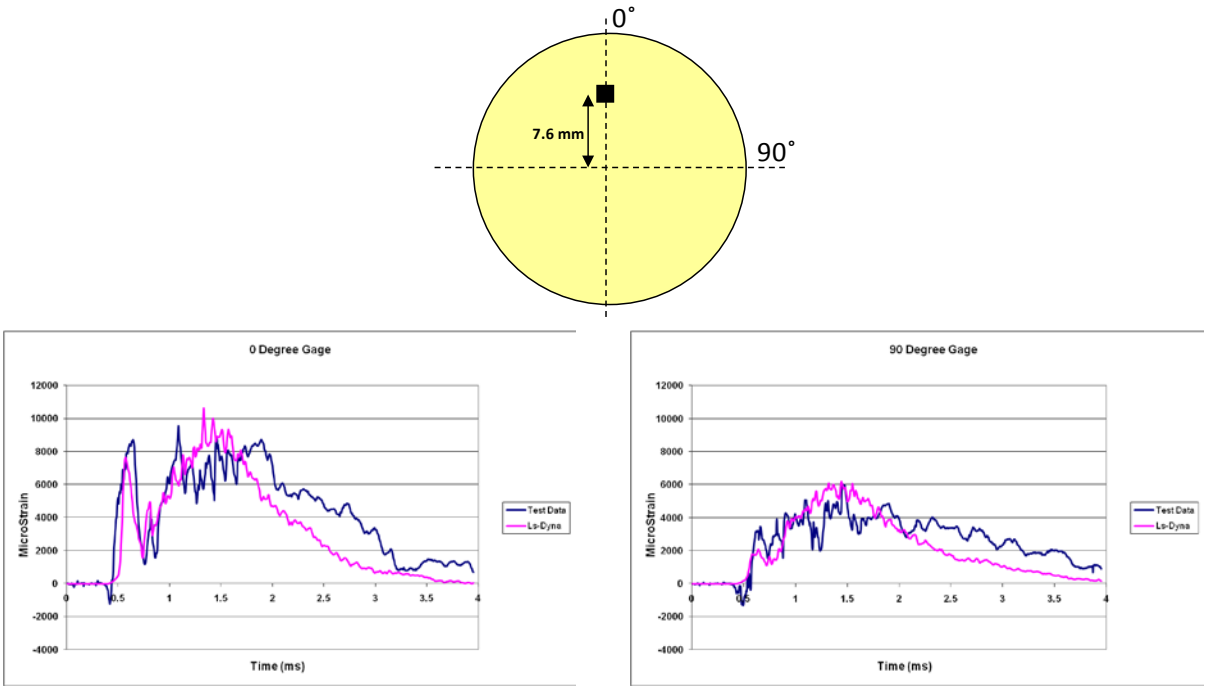

Russell Comprehensive Error = 0.134
(<0.15 Considered Excellent)

Russell Comprehensive Error = 0.124
(<0.15 Considered Excellent)

Figure 10- Material 0 Degree Gage Results

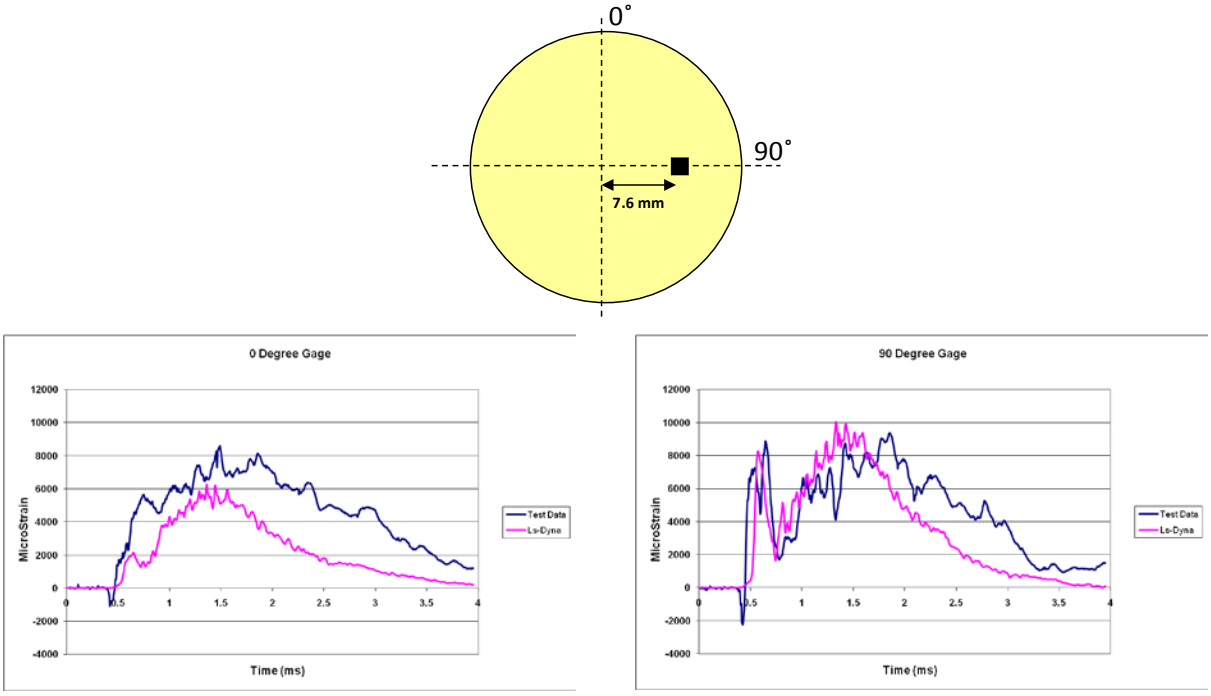

Russell Comprehensive Error = 0.318
(>0.28 Considered Poor)

Russell Comprehensive Error = 0.147
(<0.15 Considered Excellent)

Figure 11- Material 90 Degree Gage Results

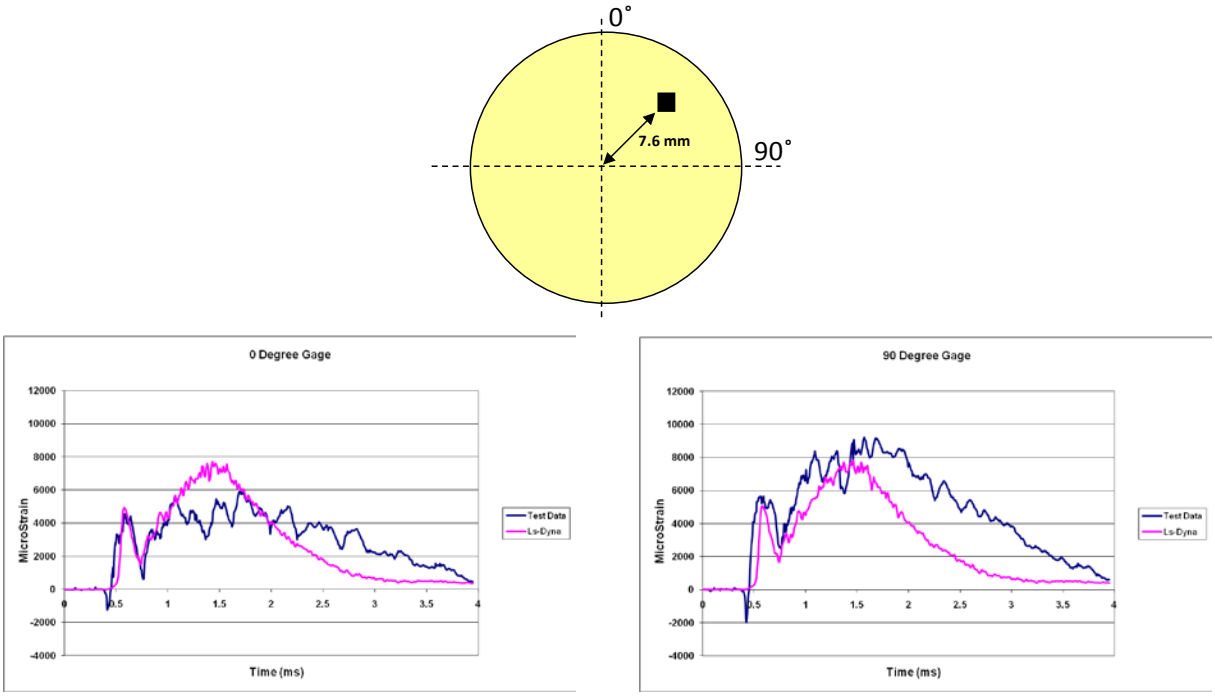

Russell Comprehensive Error = 0.130
(<0.15 Considered Excellent)

Russell Comprehensive Error = 0.249
(<0.28 Considered Acceptable)

Figure 12- Material 45 Degree Gage Results

Table 2 - Russell Error Summary

Russell Error Summary	
4.82 mm Plate – 9.65 Mpa Shock Pressure	
Gage	Comprehensive
4	0.124
6	0.134
7	0.249
9	0.130
10	0.147
12	0.318
3.3 mm Plate – 9.65 MPa Shock Pressure	
6	0.187

<0.15	Excellent
<0.28	Acceptable
>0.28	Poor

7. Damage Mechanisms – Simulation Correlation to Test

The series of testing performed using the fixed end cap mounting fixture allowed for the full energy generated by the explosion to be absorbed by the test panel, as opposed to the slider mechanism which absorbed a portion of the energy. As a result of this increased load on the test plates in this configuration the panels sustained more severe surface and internal damage. The damage that was imparted to the sample during a typical test is shown in the left image of figure 13. This figure is from the 3.3 mm (0.130 in.) thick plate that was tested at a shock pressure of 11.7 MPa (1700 lb/in^2). The corresponding finite element model result is shown in the right side image. The image of the test sample has been backlit to highlight the internal delamination that has occurred.

From these two images several qualitative observations can be made. First, both the experimental and computational results show that there are 2 cracks that initiate from the through holes located at the top and bottom (0° material direction) of the sample. These cracks propagate to a final length of approximately 6.35 cm (2.5 in.) in the experimental test sample and approximately 7.62 cm (3 in.) in the computational result. In both results the cracks run along the 0° material direction. The second observation is that there is material damage located between each of the holes and the edge of the sample, which was also predicted by the simulation. It is important to note that an initial finite element model of the plate was made in which the holes were omitted. This model developed neither the localized damage near the hole locations nor the crack along the 0° direction. This highlights 2 key aspects of this type of experimental and computational work. The first is that the damage that is observed is likely initiated due to the stress concentrations induced by the interaction of the mounting bolts and the

plate as the material flexes and pulls towards the center of the plate during deformation. The second is that when undertaking small scale testing, where edge effects and geometric discontinuities can play a key part in the material response, it is important to include these features in the computational model. Otherwise the amount of damage predicted by the simulation will be less than that seen in the experimental component.

In the left image of figure 13 there is a region of delamination damage that developed along the top edge of the test specimen. This delamination zone extends from the edge of the plate inward to a radial distance of ~50.8 mm (2 in.) between the 10 to 3 O'clock positions. In the computational model this delamination zone also develops, figure 14, but it occurs both along the top and bottom edges. The delamination in the finite element model extends from the edge inward to a radial distance of 7.62 cm (3 in.). Although the amount of delamination is somewhat larger in the computational model than is observed in the test it is encouraging that the model is able to predict the onset of the delamination itself and propagate it to a comparable distance. In the current model the choice of a delamination criterion was taken to be 34.4 MPa (5000 lb/in^2) for both tensile and shear stresses. The choice of this value was based on discussions of the developer of the material model (Materials Sciences Corporation). Based on these discussions it was determined that based on past experience an appropriate knock down factor for the delamination criteria is approximately one-half of the tensile strength of the pure epoxy. The degradation by ½ of the tensile strength accounts for voids and interfacial defects / flaws between the layers of fibers during the manufacturing of the material. The exact epoxy resin formula is held as proprietary by the material manufacturer however published values for the tensile strength of epoxy place the value between 27.5-82.7 MPa (4,000-12,000 lb/in^2). Therefore the choice of 34.4 MPa (5000 lb/in^2) is reasonable. During the development of the

models several values as high as 82.7 MPa (12,000 lb/in^2) were utilized to determine the effect of this value. When a high value is chosen the delamination damage does not occur and all plies remain in tied contact. If a low value is taken then the plies completely delaminate early on in the simulation and the results do not agree with the experimental results. More work is planned into the most efficient way to model the delamination parameters but is outside of the scope of the current study.

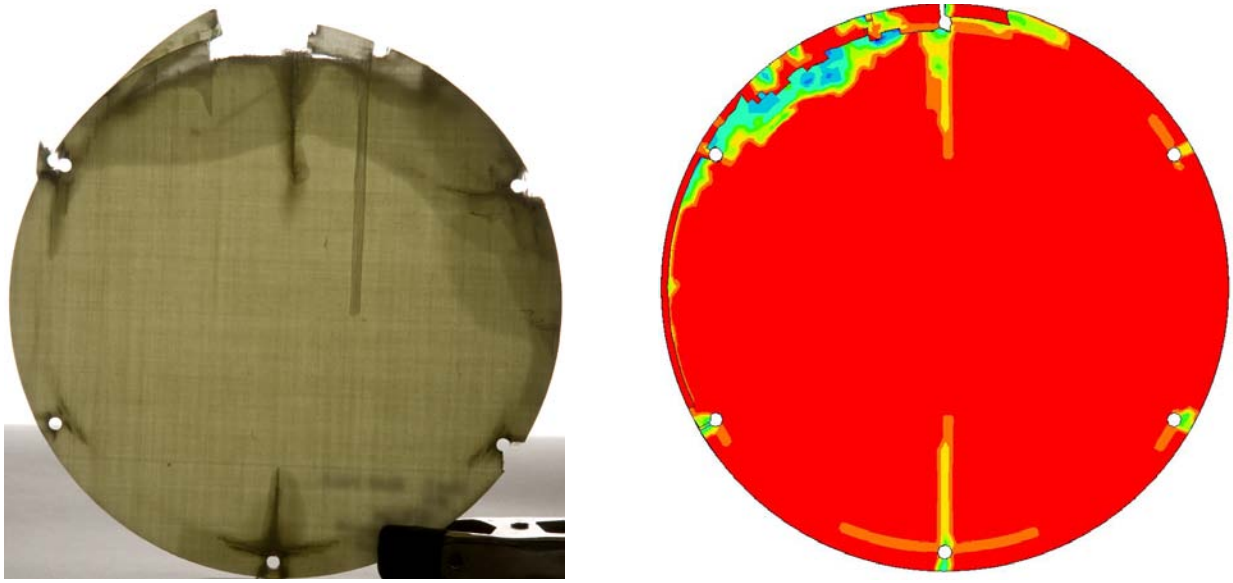

Figure 13- (a) Material Damage during Test, (b) Material Damage from Simulation

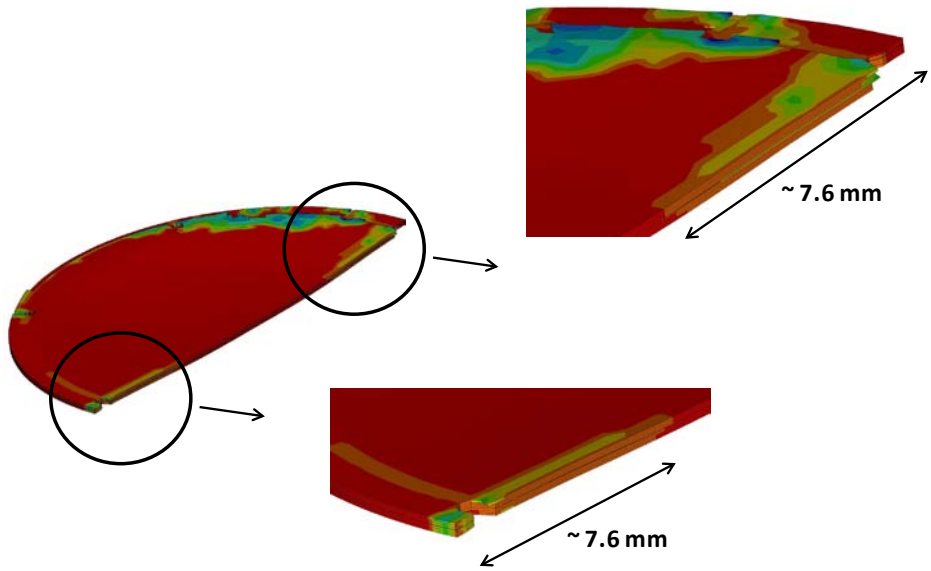

Figure 14 - Finite Element Model Delamination

8. Conclusions

A conical shock tube has been used to study the response of an E-Glass / Epoxy composite material subjected to underwater shock loading. Two test series have been performed along with corresponding finite element model development. One test series was performed in which a slider mechanism was used with the shock tube to absorb a portion of the shock energy. This allowed the energy imparted to the test specimen to be reduced to the point where strain gages bonded to the back face of the specimen would remain attached during the event. The strain gage data recorded during the experiments was correlated to the computational models by utilizing the Russell error. The Russell error comparisons showed that 6 out of 7 of the gages that survived the testing had acceptable error measures with 4 of the gages exhibiting excellent correlation. A second series of testing was performed in which the slider was replaced with a fixed base mounting fixture which allowed for all of the shock energy to be imparted to the specimen. The samples tested with this mounting fixture showed significant damage areas including fiber / matrix breakage as well as internal delamination. The corresponding finite

element simulations were able to simulate the appropriate forms and extents of the damage areas. This work has shown the ability of the LS-DYNA material model Mat_Composite_Failure_Option_Model to realistically model the behavior of a composite material under shock loading conditions. It was shown that the static elastic and strength material properties provide reasonable results for shock loading conditions. This work has served to show that computational tools can serve to support experimental test results and show promise for use as an alternative to testing to support structural designs utilizing composite materials.

Acknowledgements

The financial support of the Naval Undersea Warfare Center (Division Newport) In-house Laboratory Independent Research program (ILIR) directed by Dr. Anthony Ruffa is greatly acknowledged.

References

1. Zaretsky E, deBotton G, Perl M. The response of a glass fibers reinforced epoxy composite to an impact loading. International Journal of Solids and Structures 2004; 41: 569–584.

2. Yuan F,Tsai L, Prakash V, Rajendran AM, Dandeka D. Spall strength of glass fiber reinforced polymer composites. International Journal of Solids and Structures 2007; 44: 7731–7747.

3. Mouritz AP. The effect of underwater explosion shock loading on the fatigue behaviour of GRP laminates. COMPOSITES 1995; 26(1).

4. LeBlanc J, Shukla A, Rousseau C, Bogdanovich A. Shock loading of three-dimensional woven composite materials. Composite Structures 2007; 79: 344-355.

5. Matzenmiller A, Lubliner J, Taylor RL. A Constitutive Model for anisotropic damage in fiber-composites. Mechanics of Materials 1995; 20: 125-152.

6. O'Daniel JL, Koudela KL, Krauthammer T. Numerical simulation and validation of distributed impact events. International Journal of Impact Engineering 2005; 31: 1013–1038.

7. McGregor CJ, Vaziri R, Poursartip A, Xiao X. Simulation of progressive damage development in braided composite tubes under axial compression. Composites: Part A 2007; 38: 2247–2259.

8. Williams KV, Vaziri R. Application of a damage mechanics model for predicting the impact response of composite materials. Computers and Structures 2001; 79: 997 – 1011.

9. Gama B, Xiao J, Haque M, Yen C, Gillespie J. Experimental and numerical investigations on damage and delamination in thick plain weave S-2 glass composites under quasi-static punch shear loading. Center for Composite Materials, University of Delaware 2004.

10. Xiao J, Gama B, Gillespie J. Progressive damage and delamination in plain weave S-2 glass / SC-15 composites under quasi-static punch-shear loading. Composite Structures 2007; 78: 182-196.

11. Donadon MV, Iannucci L, Falzon BG, Hodgkinson JM, de Almeida SFM. A progressive failure model for composite laminates subjected to low velocity impact damage. Computers and Structures 2008; 86: 1232–1252.

12. Hosseinzadeh R, Shokrieh MM, Lessard L. damage behavior of fiber reinforced composite plates subjected to drop weight impacts. Composites Science and Technology 2006; 66: 61–68.

13. Batra RC, Hassan NM. Response of fiber reinforced composites to underwater explosive loads. Composites: Part B 2007; 38: 448–468.

14. Chan S, Fawaz Z, Behdinan K, Amid R. Ballistic limit prediction using a numerical model with progressive damage capability. Composite Structures 2007; 77: 466–474.

15. Russell DM. Error measures for comparing transient data, Part I: Development of a comprehensive error measure, Part II: Error measures case study. Proceedings of the 68th Shock and Vibration Symposium, 3-6 November 1997.

16. Russell DM. DDG53 Shock trial simulation acceptance criteria. 69th Shock and Vibration Symposium, 12-19 October 1998.

CHAPTER 3

DYNAMIC RESPONSE OF CURVED COMPOSITE PANELS TO UNDERWATER EXPLOSIVE LOADING: EXPERIMENTAL AND COMPUTATIONAL COMPARISONS

by

James LeBlanc and Arun Shukla

has been submitted to Composite Structures (January 2011)

Corresponding Author: James LeBlanc

Naval Undersea Warfare Center (Division Newport)

1176 Howell Street

Newport, RI, 02841

Phone: +1-401-832-7920

Email Address: James.M.LeBlanc@Navy.Mil

Abstract

The response of E-Glass / Vinyl ester curved composite panels subjected to underwater explosive loading has been studied. The work consists of experimental testing utilizing a water filled conical shock tube facility and computational simulations with the commercially available LS-DYNA finite element code. The composite specimens are 0/90 biaxial laminates with a thickness of approximately 1.3 mm. The samples are round panels with curved midsections. The transient response of the plates is measured using a three-dimensional (3D) Digital Image Correlation (DIC) system, along with high speed photography. This ultra high speed system records full field shape and displacement profiles in real time. The DIC data and the computational results show a high level of correlation using the Russell Error measure.

1. Introduction

The use of composite materials is becoming increasingly prevalent in naval applications such as advanced ship hull designs, unmanned underwater vehicles (UUVs), and submarine components. The advantages of composite materials include high strength to weight ratios, improved corrosion resistance, and reduced maintenance costs. However, the use of these materials in a military environment, particularly submarine applications, requires that they be able to survive underwater explosion (UNDEX) events. Currently, the response of these materials at static and quasi-static loading rates is well understood. Conversely, the response at the high strain rates that UNDEX/shock events can induce is not well understood. This typically results in composite structures being conservatively designed with large safety factors to ensure that damage will not occur. This inherent conservativeness leads to overdesigns which do not afford the full weight savings possible with composites.

Historically, there have been two experimental methodologies used to impart shock loading conditions to structures: (1) explosives and (2) shock tubes. Although the use of explosives offers an ease of use, there are associated deficiencies such as spherical wave fronts and pressure signatures which are often spatially complex and difficult to capture. Shock tubes offer the advantage of plane wave fronts and wave parameters that are easily controlled and repeated.

When composite materials are subjected to loading conditions they may experience damage in the form of several distinct mechanisms occurring in the in-plane and through thickness directions. The in-plane mechanisms consist of fiber breakage and matrix cracking, while the through thickness damage is dominated by delamination of the plies.

Experimental studies on shock loading of materials have examined the material response over a range of loading rates. Espinosa et al [1] studied the effects of shock loading on stainless steel when subjected to underwater impulsive loads. Nurick et al [2,3] have studied the effects of boundary conditions on plates subjected to blast loading and identified distinct failure modes depending on the magnitude of the impulse and standoff. Tekalur et al [4] investigated the effects of shock loading on both E-Glass and Carbon based laminates. This study used a shock tube to impart pure shock loading as well as a small scale explosion tube to consider the shock load combined with the effects of the heat generated during combustion of the explosive materials. Mouritz [5] studied the effectiveness of adding a light weight, through thickness stitching material to increase the damage resistance of composites. LeBlanc et al [6] have studied the effects of shock loading on three-dimensional woven composite materials. Recently, there has been an increased interest in the study of the effect of shock loading on sandwich

structures. These studies include the effects of shock and impact loading conditions (Jackson et al [7], Schubel et al [8], Arora et al [9]).

Analytical damage models for composites have been widely developed and are continually being refined and updated. These models typically assign an internal damage variable to each of the types of damage of interest (ie. matrix cracking, fiber rupture) which, in simple form, are ratios of the stress state to a failure criteria (Matzenmiller et al [10], Zako et al [11], Dyka et al [12]). Based upon the expression representing each damage variable, the effective elastic properties can be degraded when the variable reaches a critical value. As the mechanical properties must be continually updated to account for the damage degradation this methodology lends itself well to implementation into finite element codes.

The finite element modeling of damage in composites has been performed primarily on models simulating strain rates up to those representing drop test experiments with some work performed at the high strain rate regimes expected in shock loading. Material models are continually being implemented and refined in existing commercial finite element codes (O'Daniel et al [13], McGregor et al [14]). Recent publications involving computational modeling of damage progression in composites have utilized LS-DYNA and the Mat_162 (Mat_Composite_OPTION) material model which simulates fiber breakage, matrix cracking and delamination damage. This material model combines the progressive failure theory of Hashin and the damage mechanics approach of Matzenmiller et al [10]. Gama et al [15] have published results from quasi-static punch shear loading experiments which correlate well with simulations utilizing the Mat_162 material model. Simulations of low velocity impact experiments have been documented in the work by Donadon et al [16] and Hosseinzadeh et al [17]. Furthermore,

Batra and Hassan [18] studied the response of composites to UNDEX loading through numerical simulations; however, there are no comparisons to experimental results. LeBlanc et al. [19] have presented a modeling methodology which simulates composite plates subjected to underwater explosive loading with comparisons to both the transient strain response as well as post mortem damage.

2. Composite Material

The material used in this study is an E-Glass / Vinyl ester composite with a 0°-90° biaxial layup. The glass fabric is a balanced construction of 0° and 90° fibers with the two layers being stitched together rather than woven. The areal weight of the dry fabric is 0.406 kg/m^2 (12 oz/yd^2). The panels which are utilized in the study consist of 3 plys of the fabric, with each ply oriented in the same direction, i.e. the 0° fibers in each ply are parallel. The panels are manufactured using the vacuum infusion process with a vinyl ester resin, AOC Hydropel R015-AAG-00. The finished part thickness is 1.37 mm (0.054 in.) and has a fiber content of 62% by weight. All panels were manufactured by LBI Fiberglass located in Groton, CT. The mechanical properties for the material are provided in table 1. Furthermore, the mechanical properties of the vinyl ester resin are provided in table 2. The pure vinyl ester properties are key, in that they determine the through thickness mechanical properties (modulus, strength) of the laminate.

Table 1 – E-Glass /Vinyl Ester Biaxial Laminate -Mechanical Properties (ASTM 638)

	MPa (lb/in^2)
Tensile Modulus (0°)	15.8e3 (2.3e6)
Tensile Modulus (90°)	15.8e3 (2.3e6)
Tensile Strength (0°)	324 (47,000)
Tensile Strength (90°)	324 (47,000)

Table 2 – AOC Hydropel R015 Vinyl Ester - Mechanical Properties (ASTM 638)

	MPa (lb/in^2)
Tensile Modulus	3.44e3 (500,000)
Tensile Strength	72.4 (10,500)

The geometry of the plates consists of a curved midsection with a flat boundary as shown in figure 1. The convex face of the plate represents the mold line in the manufacturing and has a radius of curvature of 18.28 cm (7.2 in.), an outer diameter of 26.54 cm (10.45 in.), and the curved portion of the plate is 22.86 cm (9 in.) in diameter.

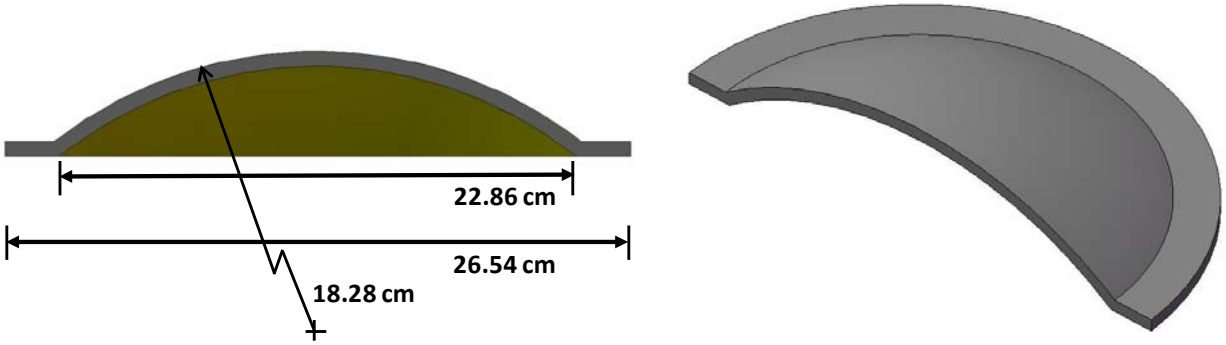

Figure 1 – Composite Plate Geometry (Section View)

3. Shock Loading Apparatus

A conical shock tube (CST) facility located at the Naval Undersea Warfare Center, Division Newport was utilized in the shock loading of the composite materials. The shock tube is a horizontally mounted, water filled tube with a conical internal shape, Figure 2. The tube geometry represents a solid angle segment of the pressure field that results from the detonation of a spherical, explosive charge, Figure 3. In an open water environment the pressure wave expands from the charge location as a spherical wave. In the shock tube the rigid wall acts to confine the expansion of the pressure wave in a manner that simulates a conical sector of the pressure field. In order to compare free field and shock tube pressure values, it is useful to

define an amplification factor which is the ratio between the volume of a spherical charge to the volume of the conical sector charge and is defined by Poche and Zalesak [20] as:

$$AF = \frac{1}{\sin^2\left(\frac{\alpha}{4}\right)}$$

α is the cone angle

This equation assumes perfectly rigid wall conditions which are not fully realized. Therefore, the actual amplification factor is less than the calculated value and is typically reported as an effective weight amplification factor. This is defined by Poche and Zalesak [20] as the ratio between the weight of a spherical charge, W, required to produce the same peak pressure at a given standoff distance as that produced in the shock tube by a segment of charge weight, w. The reduction in the amplification factor is typically attributable to elastic deformation of the shock tube walls. Further discussion on the development and history of the water filled conical shock tube is provided by references 21 and 22.

The internal cone angle of the tube is 2.6 degrees. The tube is 5.25 m (207 in.) long from the charge location to the location of the test specimen and internally contains 98.4 L (26 gal.) of water at atmospheric pressure. The pressure shock wave is initiated by the detonation of an explosive charge at the breech end of the tube (left side of figure) which then proceeds down the length of the tube. Peak shock pressures from 10.3 MPa (1500 lb/in^2) to 20.6 MPa (3000 lb/in^2) can be obtained depending on the amount of explosive charge. A typical pressure profile obtained from the use of the tube is shown in figure 4. This figure illustrates the rapid pressure increase associated with the shock front followed by the exponential decay of the wave. This profile was obtained using a M6 Blasting Cap – 1.32g (.00292 lb) TNT Equivalency and is

measured 0.508 m (20 in.) from the impact face of the test specimen. The length of the tube is sufficient so that plane wave conditions are nearly established at the test specimen.

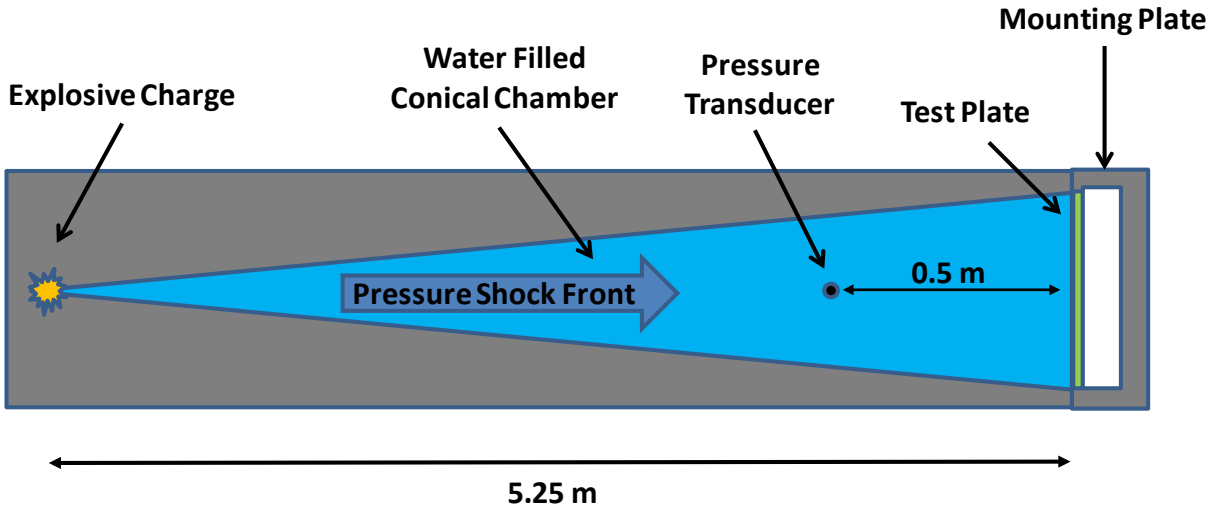

Figure 2 – Conical Shock Tube Schematic (not to scale)

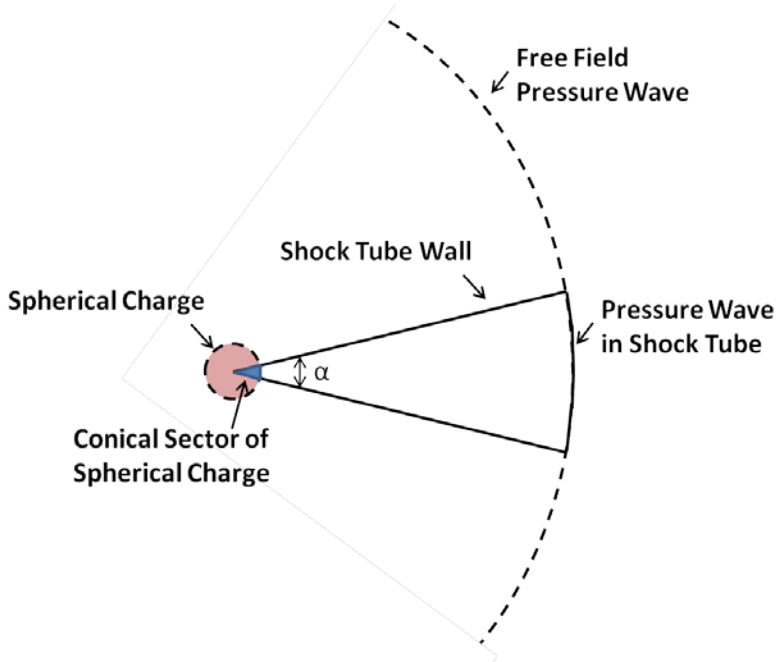

Figure 3 – Explosive Charge in Shock Tube (Poche and Zalesak, 1992)

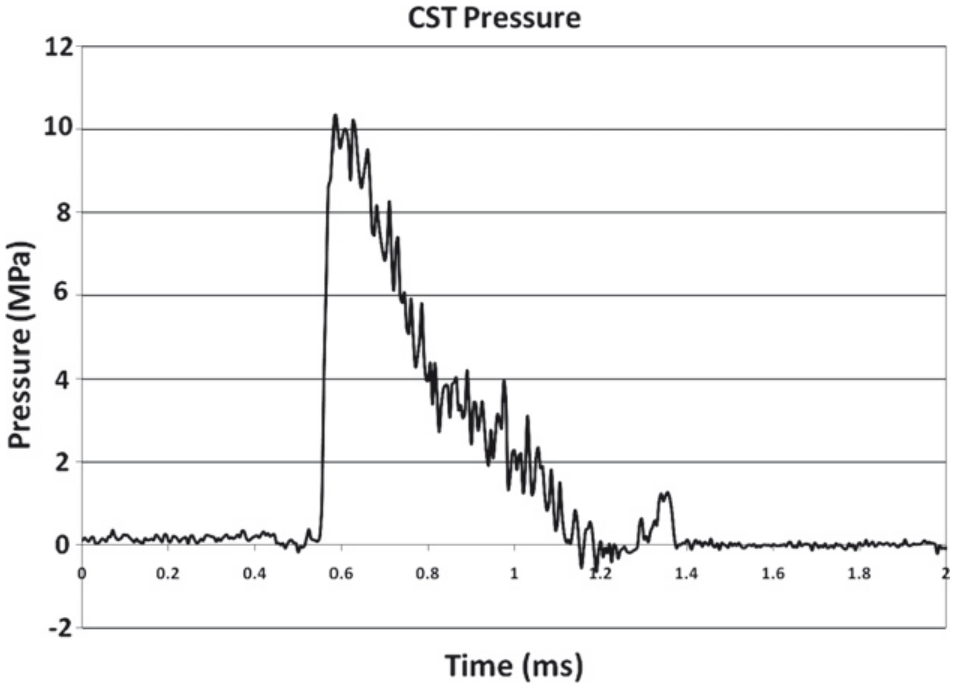

Figure 4 – Typical Pressure Profile Generated in the Conical Shock Tube

A mounting fixture has been designed so the test specimens are air backed with fully clamped edges. The specimens are 26.54 cm (10.45 in.) in overall diameter with a 22.86 cm (9 in.) unsupported middle section. The mounting arrangement is shown in figure 5. The specimens are mounted with the convex surface towards the incoming shock fronts. This is chosen so that the test will represent geometries commonly used in underwater applications with curved surfaces typically facing into the the fluid (i.e. submersible vehicle hull forms).

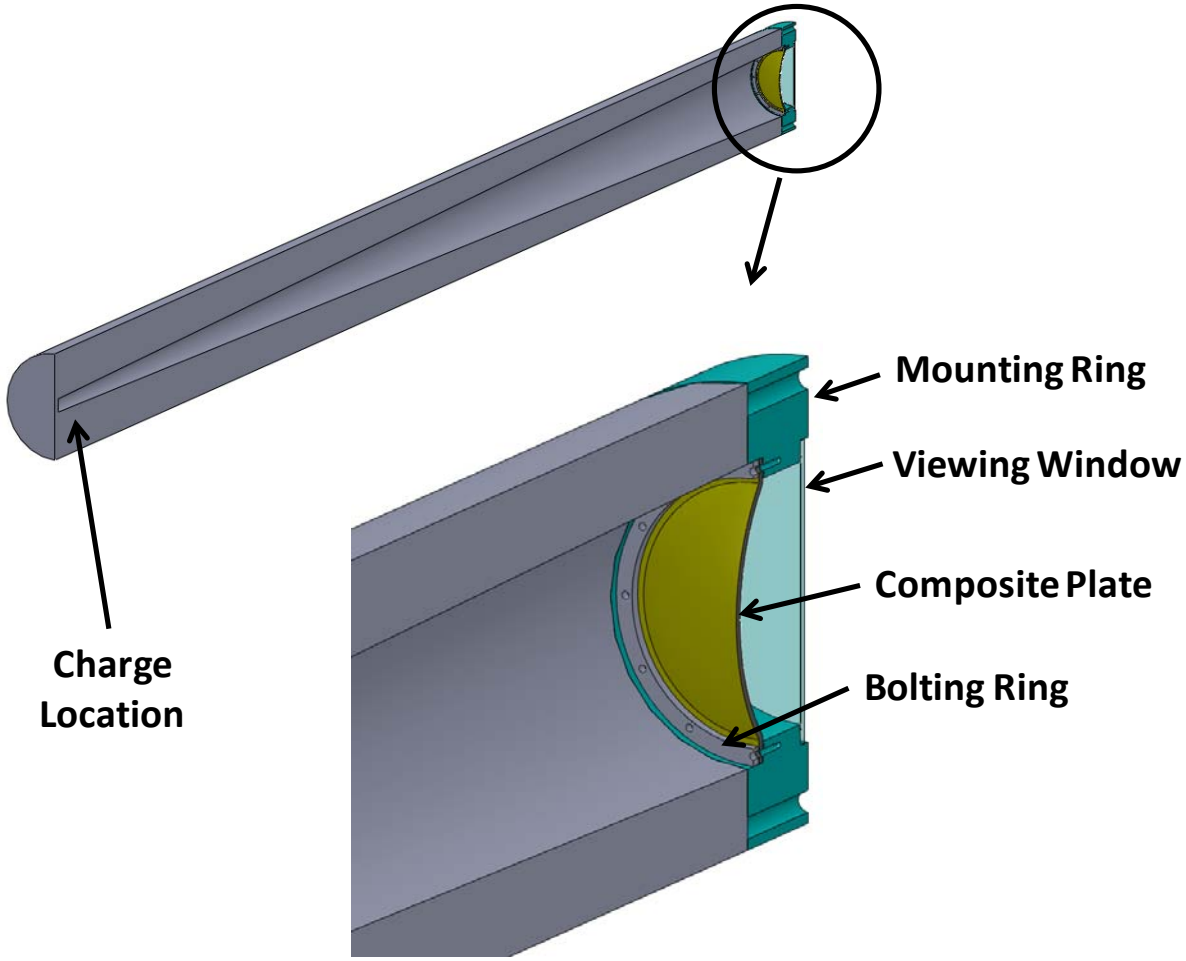

Figure 5 – Shock Tube Mounting Configuration

4. Experimental Procedure

Shock testing of the composite material has been performed with the CST utilizing a fixed end cap. The use of the fixed end cap configuration allows the plate to absorb the full energy level and sustain a suitable level of damage for comparison to the finite element model results. The tube can also be configured with a sliding piston end cap [19] to lower the level of energy the plates absorb, but is not utilized in this study. In the current study high speed photography coupled with a 3D digital image correlation system is utilized to capture the back face transient response during the shock event. This system offers the advantage that it is a

noncontact measurement technique which gives whole field information and eliminates the difficulties of strain gages debonding from the specimens at high shock levels and large plate flexures. The explosive charge used in the study is an M6 blasting cap with a net TNT equivalence of 1.32grams. This yields peak pressures at the sensor location (.508 m in front of the test specimen) of approximately 10.3 MPa (1500 lb/in^2).

The Digital Image Correlation (DIC) technique is used to capture the transient response of the back face (dry) of the plates. DIC is a non-intrusive, optical technique for capturing the full field, transient response of the panels through the use of high speed photography and specialized software. Capturing the three dimensional response of the plates requires that 2 cameras be used in a stereo configuration. To record the transient response with this system the cameras must be calibrated and have synchronized image recording throughout the event. The calibration of the cameras is performed by placing a grid containing a known pattern of dots in the test space where the composite sample is located during the test. This grid is then translated and rotated in and out of plane while manually recording a series of images. As this grid pattern is predetermined, the coordinates of the center of each dot is extracted from each image. The coordinate locations of each dot extracted uniquely for each camera allows for a correspondence of the coordinate system of each camera (Tiwari et al [23]). The DIC is then performed on the image pairs that are recorded during the shock event. Prior to testing the back face of the sample is painted white and then coated with a randomized speckle pattern, Figure 6. The post processing is performed with the VIC-3D software package which matches common pixel subsets of the random speckle pattern between the deformed and un-deformed images. The matching of pixel subsets is used to calculate the three dimensional location of distinct points on

the face of the panel throughout time. This technique has been applied as a full field measurement technique in many applications including shock loading (Tiwari, et al [24])

Two high speed digital cameras, Photron SA1, are positioned behind the shock tube, figure 6. The use of two cameras allows for the out-of-plane behavior to be captured. If a single camera is utilized the data would be limited to the in-plane results. The distance from the lens of the camera to the specimen is 1.44 m (57 in.) and each camera is angled at approximately 7° with respect to the symmetry plane, figure 7. A frame rate of 20,000 was used with an inter-frame time of 50μs.

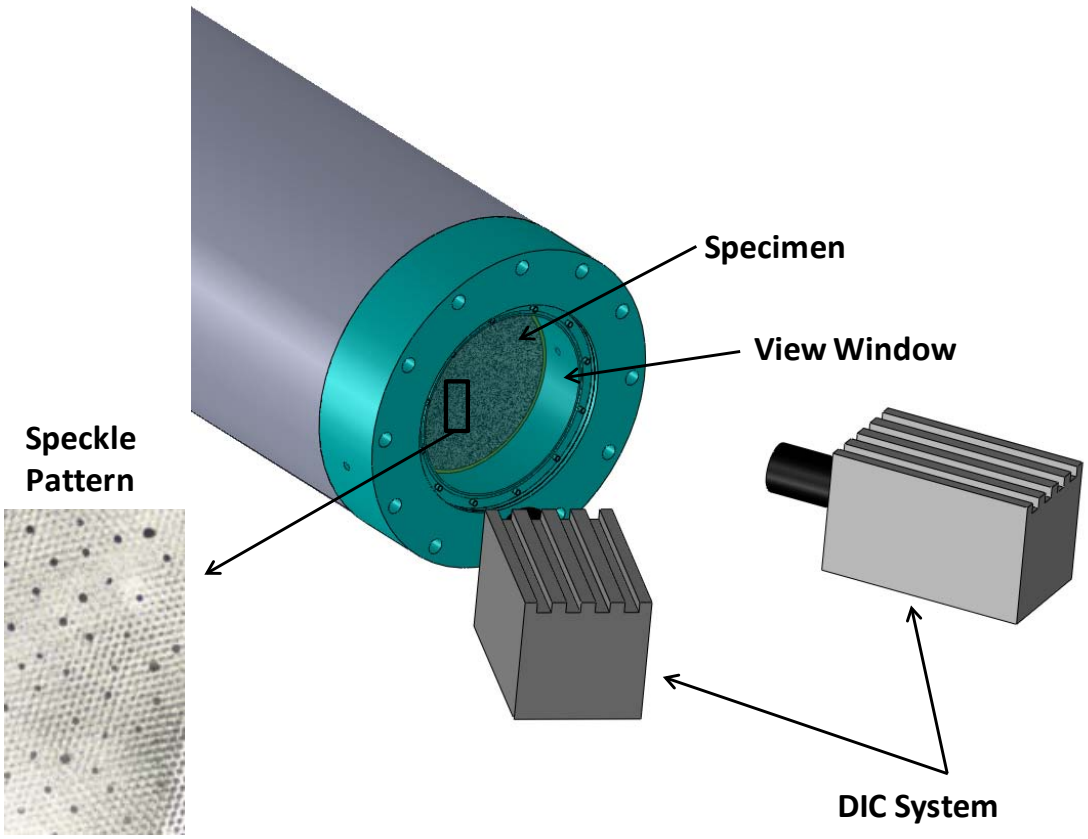

Figure 6 –Digital Image Correlation Schematic

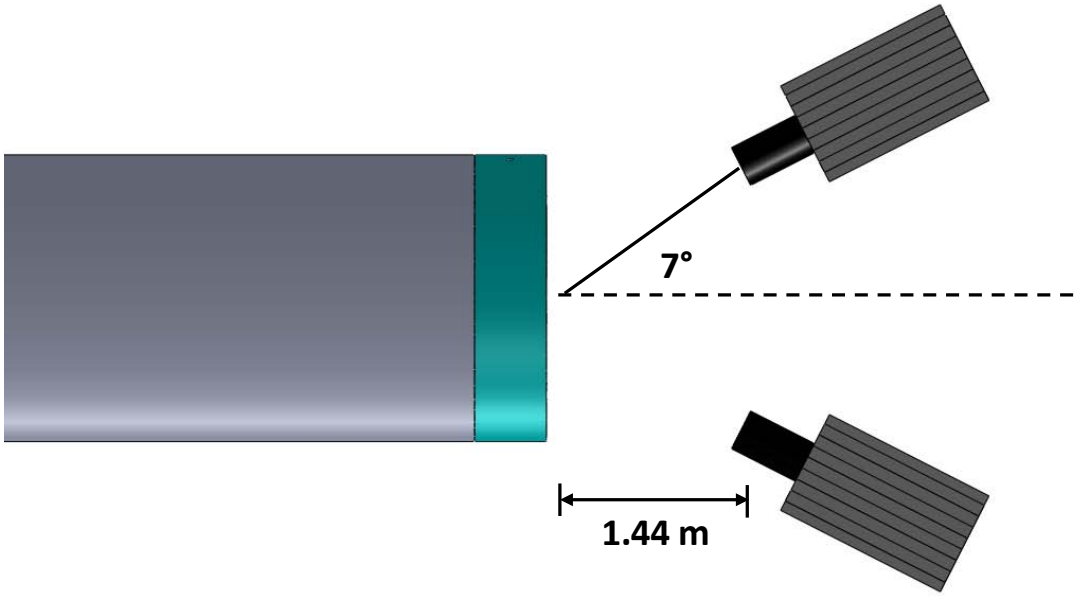

Figure 7 –Digital Image Correlation Setup (Not to Scale)

5. Finite Element Modeling

Finite element modeling of the experiment has been performed utilizing the LS-DYNA code available from the Livermore Software Technology Corporation (LSTC). All simulations are generated with Version 971, Release 4.2 and are run in double precision mode.

The composite plate in the simulations is modeled using shell elements with a fully integrated element formulation (Type 16). The model of the 1.37 mm (0.054 in.) plate is shown in figure 8 and consists of 3 layers of shell elements. Each layer represents a 0° and 90° combined ply with a thickness of 0.457 mm (0.018in.). The mid-surface of each ply is meshed and the individual shell layers are offset by the ply thickness. There are five through thickness integration points for all elements. The holes represent the through bolt holes present in the test samples used for mounting the plate to the fixture. The in-plane element edge lengths are approximately 2.54 mm (0.1 in.) and the maximum element aspect ratio is 2.7:1.

The LS-DYNA material model utilized in this work is Mat_Composite_Failure_*Option*_Model (Mat_059, Option=Shell). This is an orthotropic material definition capable of modeling the progressive failure of the material due to any of several failure criterion including tension / compression in the longitudinal and transverse directions, compression in the through thickness direction, and through thickness shear. Published descriptions of how each failure mode is handled are scarce, however, there is some informal documentation available from LSTC. For each possible failure mode, there is an internal variable which is checked throughout the analysis to determine if failure in that mode is present. Once failure due to one mode is triggered the load carrying ability of the material in that direction is reduced to zero. It is important to note that failure in one direction does not cause the element to be deleted. An element is only deleted from the analysis after it has failed in all directions and can no longer carry any load. The input material properties are those provided in table 1. The material model inputs are derived from static tensile testing with no modifications for strain rate effects. It was seen that the static properties provide reasonable results for shock loading conditions. The DIC strain measurements made during this study show that the in-plane strain rates are on the order of 10-50/s. Although the through thickness strain rate was not measured it is expected to be higher than the in-plane strain rate. Similar observations were made by Chan et al [19] for the ballistic impact problem and by LeBlanc et al for shock loading of flat composite plates [25].

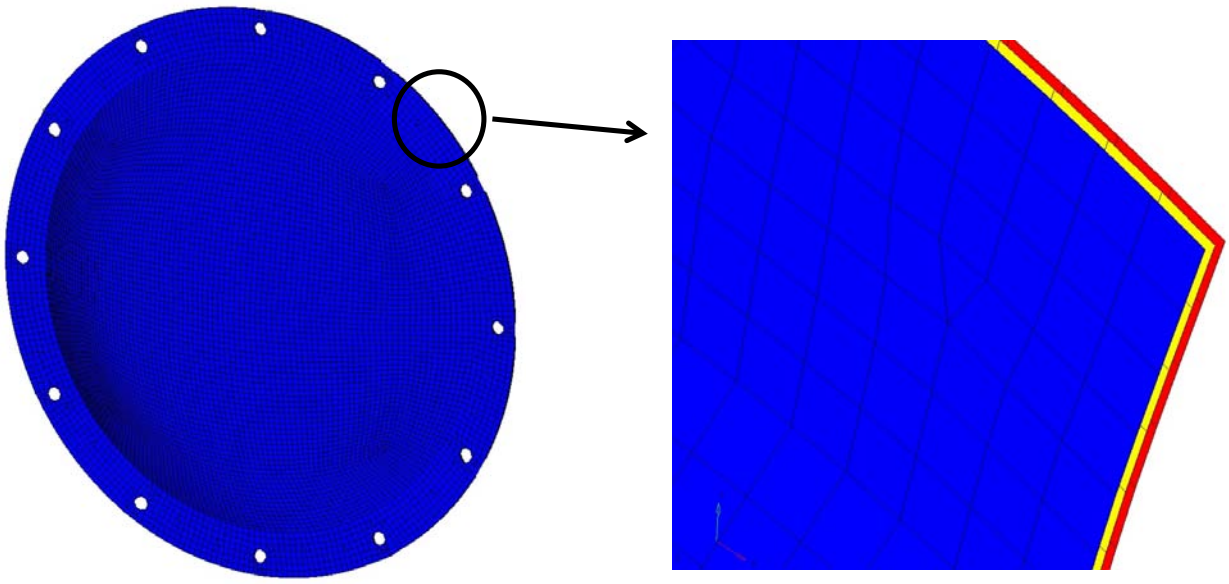

Figure 8 –Finite Element Model of Composite Plate

In the current modeling effort, delamination damage is considered and is taken into account through the use of a surface-to-surface tiebreak contact definition. Using this approach, each ply is modeled as a shell layer of elements representing the mid-surface of each ply and the shell layers are offset by the ply thickness. The tie break definition initially ties the nodes between plies together to inhibit sliding motion. The force at each node is monitored by the software and the corresponding normal and shear stresses are computed. Failure is defined by the following formula:

$$\left(\frac{\sigma_N}{NFLS}\right)^2 + \left(\frac{\sigma_s}{SFLS}\right)^2 \geq 1$$

where: σ_N and σ_S are the computed normal and shear stresses, respectively
NFLS and SFLS are the failure normal and shear stresses, respectively

If the current stress state at any node in the contact definition exceeds the failure criteria then the tie definition for that node is deleted and the node is free to slide. It is important to note that once the tie component of the contact definition is deleted, the contact for that node

transitions to a standard definition. This allows the slave node to slide and separate from the master surface but not pass through it. Therefore, individual plies can separate but not pass thorough one another.

The complete finite element model of the CST test setup is shown in figure 9. The model consists of the internal fluid of the shock tube and the composite test sample. The fluid within the tube is considered in the simulation so as to capture the fluid structure interaction (FSI) at the interface of the fluid and test plate. As will be shown later, this is a critical interaction to consider as the pressure loading on the plate is not uniform across its face. Only the first 1.01 m (40 in.) of the fluid extending from the test sample towards the charge location is modeled. This was deemed to be acceptable for 2 reasons: (1) the fluid is loaded with the pressure profile measured 0.508 m (20 in.) from the test sample and (2) a non-reflecting boundary layer is applied at the charge side boundary of the fluid domain. The non-reflecting boundary allows the wave that is reflected from the plate to leave the fluid domain but not re-enter. This assumption holds as long as the duration of the plate deformation is small enough such that the wave which is reflected off the plate cannot reach the end of the tube and reflect back to the plate location during this time. A simple calculation shows that the time for a wave to travel from the plate to the end of the tube and back again is 7 ms and the duration of the plate deformation is 5.5 ms. The fluid is modeled with solid elements and a null material definition. The use of the null material allows for the material to be defined with an equation of state (EOS) definition. A linear polynomial EOS is utilized for this model for which only the bulk modulus and density of the water is defined. This allows for an accurate propagation of the pressure wave in the water in a computationally efficient manner. The pressure load is applied as a plane wave at the location of the test pressure transducer. The pressure profile that was measured for the test is applied to

the model. The fluid–structure interaction is handled through the use of a tied-surface-to-surface (LS-DYNA keyword *Contact_Tied_Surface_To_Surface) contact definition. In this method, two contact surfaces (*Set_Segment) are defined for which the nodes are tied together. For the coupling of the fluid and composite plate the two surfaces are: (1) the fluid face where it contacts the plate, and (2) the plate face where it contacts the fluid. The mounting plate is simulated by a nodal constraint set that forces the nodes in the clamped area of the plate, shown in figure 10, to have zero displacement. There is no numerical damping applied to the model.

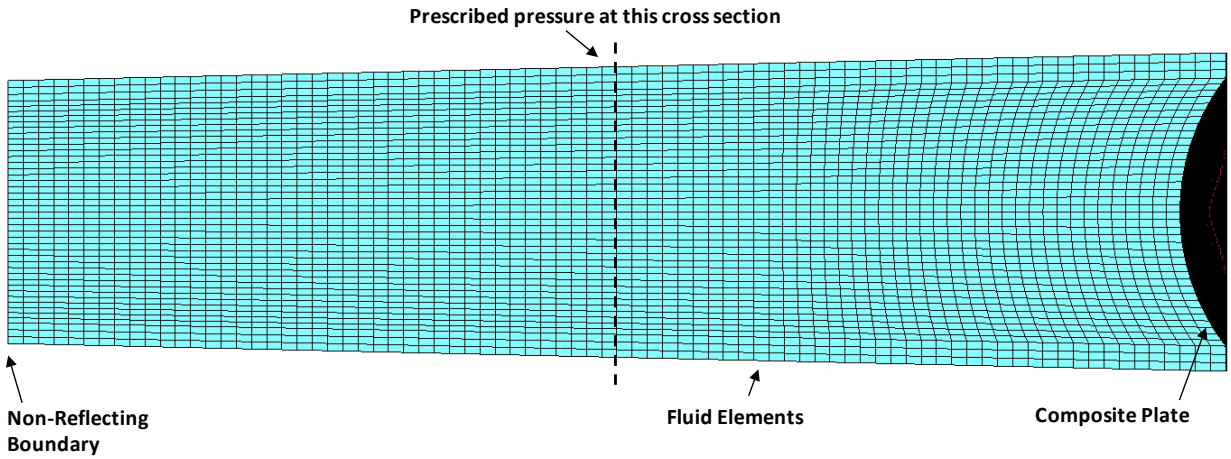

Figure 9 –Finite Element Model of CST

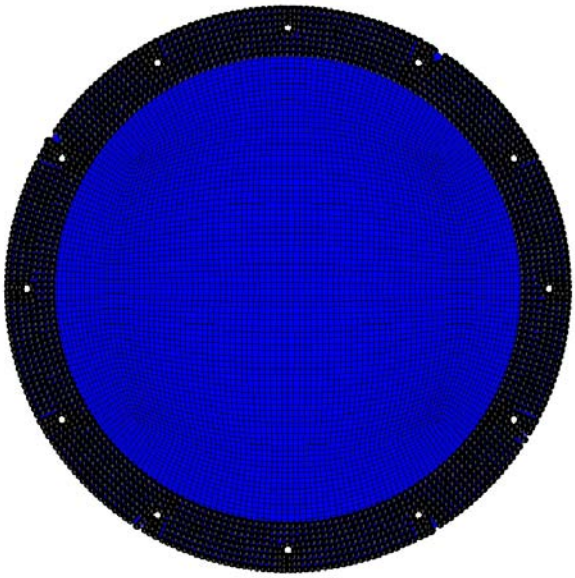

Figure 10 – Composite Plate Clamped Nodes

6. Finite Element Simulation Results

The finite element simulation of the shock tube testing allows for a visual full field representation of the interaction between the pressure wave and the composite plate, whereas the pressure profile obtained from the transducer gives only a single point history. The pressure field in the fluid as it interacts with and loads the plate, for the case of the 1.37 mm (0.054 in.) plate is shown in the left side of figure 11. The associated plate response is shown in the right side of the figure. The time as shown in these figures is the analysis time, with zero taken at the initiation of the pressure field 0.508 m (20 in.) from the test sample. Figure 11 illustrates several key points. First, although the pressure wave is uniform prior to its impact with the test plate, the loading on the plate itself is complex and not uniform. It is evident that there is a low pressure area that develops in the center of the plate while the clamped edge is loaded with high pressure. This can be attributed to the relatively low stiffness of the unsupported area of the plate as compared to the clamped edge of the plate where it is supported by the mounting ring. The

second point is that the loading of the plate and the associated response can be separated into two distinct time regimes. Where the pressure wave interacts with the plate over 0.2 ms, the plate does not start to deform until the wave is nearly fully reflected and takes approximately 5.5 ms to complete.

The plate deformation in the current study can be described as a full inversion, taking approximately 5.5 ms to complete. At 1 ms, a hinge forms at the outer edge of the plate at the clamped boundary. This hinge then continues to propagate towards the center of the plate as seen in the deformation progression images in figure 11. The deformation is completed when the plate has fully inverted itself at 6.5 ms. At this point it is seen that there is a high pressure region that develops at the apex of the inverted shape. During the inversion process of the plate the fluid at the plate boundary is also moving along with the plate surface. Once the inversion of the plate is complete, the velocity is rapidly arrested, resulting in the development of this high pressure region. It is noted that the magnitude of this pressure is small compared to the initial shock wave pressure.

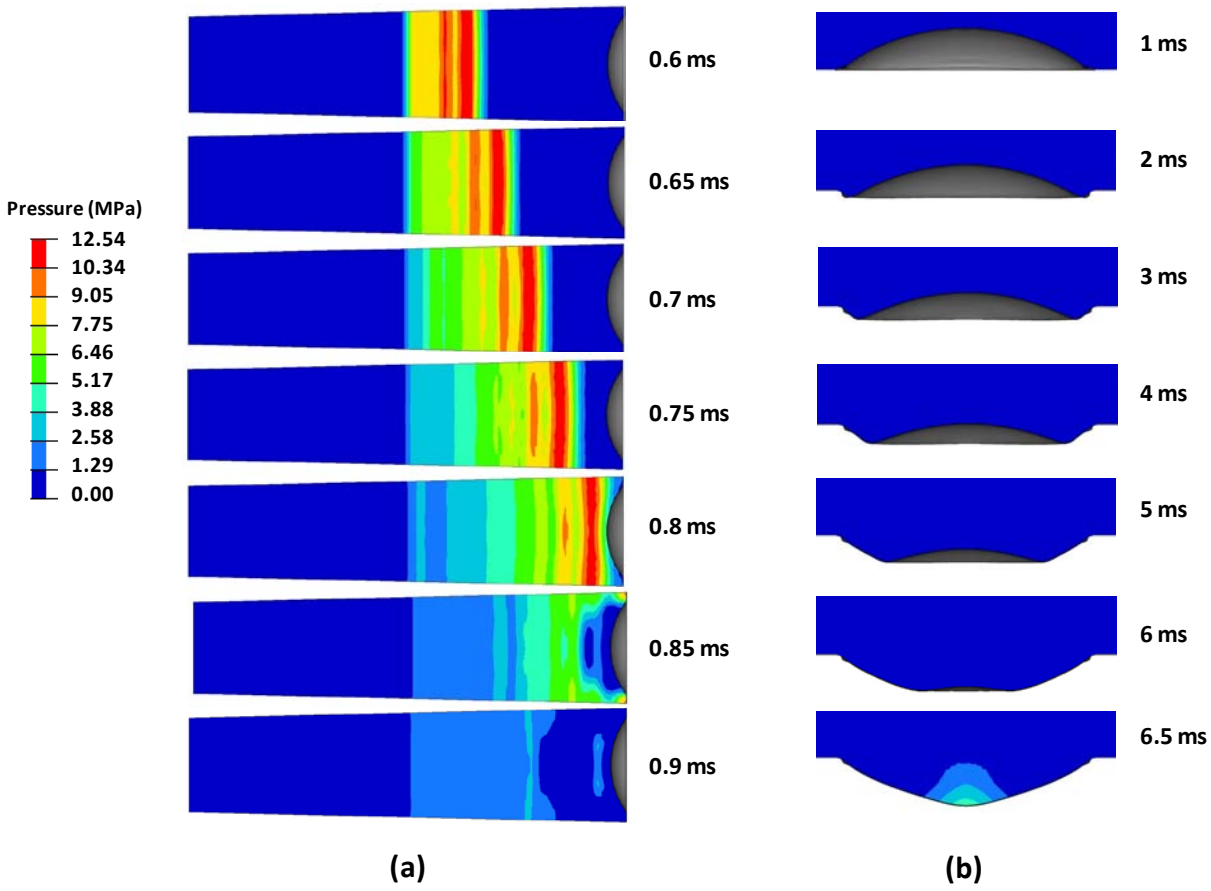

Figure 11 – (a) Fluid Structure Interaction, (b) Plate Deformation Progression

7. Simulation Correlation to Test

The displacement and velocity data that was captured during the experiments is used as a basis to correlate and validate the finite element model results. The quality of the correlation between the test data and numerical results in this study is quantified using the Russell Comprehensive Error measurement. The Russell error technique is one method which evaluates the differences in two transient data sets by quantifying the variation in magnitude and phase. The magnitude and phase error are then combined into a single error measure, the comprehensive error factor. The full derivation of the error measure is provided by Russell [26] with the phase, magnitude, and comprehensive error measures respectively given as:

$$RP = \frac{1}{\pi}\cos^{-1}\left(\frac{\sum c_i m_i}{\sqrt{\sum c_i^2 \sum m_i^2}}\right)$$

$$RM = sign(m)\log_{10}(1 + |m|)$$

$$RC = \sqrt{\frac{\pi}{4}\left(RM^2 + RP^2\right)}$$

In the above equations c_i and m_i represent the calculated (simulated) and measured responses, respectively. Excellent, acceptable, and poor correlation using the Russell error measure is given as: Excellent - RC≤0.15, Acceptable – 0.15<RC≤0.28, and Poor RC>0.28. The definition of these criteria levels are the result of a study that was undertaken to determine the correlation opinions of a team in support of a ship shock trial. A summary of the process used to determine the criteria is presented by Russell [27].

The DIC technique allows for the extraction of a large amount of data from the surface of the plates. The two variables that are used for correlation of the simulations to the experiments are the out of plane displacement and velocity. Time histories are extracted from the DIC data for two points on the measurement surface: (1) the center of the plate, and (2) a point located half way between the center of the plate and the clamped boundary along the vertical axis. Full field data comparisons will be discussed later in the paper. The displacement comparisons are shown in figure 12 and the velocity comparisons are provided in figure 13. A summary of the Russell error for each of these comparisons is provided in table 3. From these graphical comparisons and error summary it is seen that there is a high level of correlation between the experimental results and the computational simulations. It is noted here that the times of the simulation and experiments are arbitrary but are displayed using the simulation time. The two events are

matched temporally by adjusting the experiment time until the first motions of the center point align. This time offset is then held constant for all other comparisons, i.e. there is not a different time offset to align the velocity comparisons.

The displacement comparison shows that the experiment and simulation results agree nearly exactly until 2.5 ms at which point the displacement in the experiment occurs slightly faster than the simulation. This is the same for both the center point and the point halfway between the center and the boundary. It is also seen that the displacement takes place in a linear fashion. The peak deflection is both cases is just under 80 mm for the center point and 55 mm for the point along the vertical axis. In the velocity comparison, it is seen that there is an initial out-of-plane velocity of just less than 20 m/s which then settles to about 10 m/s for the remaining duration of the event. This near constant velocity supports the linearity of the displacement profile. It is seen that the simulation is able to capture the peak velocities seen in the experiments. Overall, it is shown that the Russell error values for the displacement comparisons show excellent correlation as well as the velocity for the point halfway between the center and the boundary. The velocity comparison at the center point falls just outside the excellent agreement criteria but well within the acceptable level (<0.28). Table 3 summarizes the Russell error values for magnitude, phase, and comprehensive for each data comparison.

In addition to the point wise time histories, full field comparisons are made between the experiment and simulations. A comparison of the full field, out of plane displacement evolution is shown in figure 14. From this figure, it is seen that the experiment and simulation show good correlation in terms of the displacement evolution. The experiment shows some un-symmetric behavior in that the displacements are slightly higher along a line at 135 degrees. However, the

values of these displacements are only a few millimeters more than the rest of the plate. As expected, the simulation shows symmetric behavior. It is possible that this would not be the case if initial thickness variations were built into the model. Overall, the displacements over the surface of the plate correlate well between the experiment and the simulation.

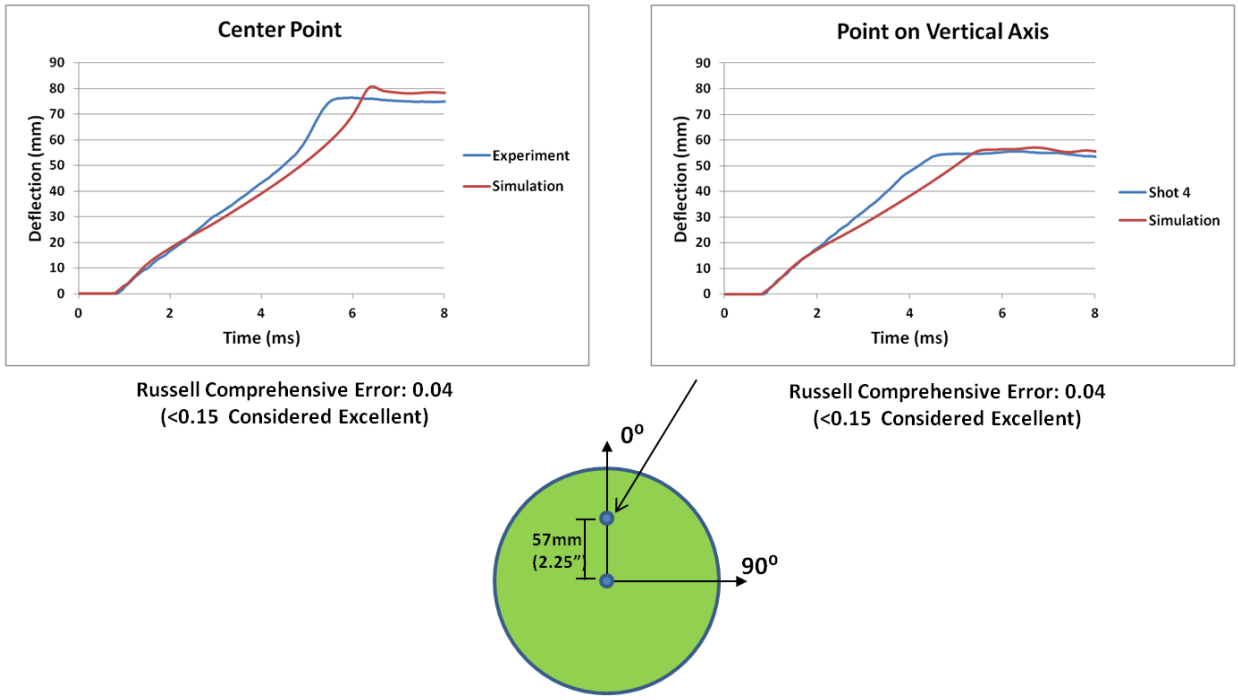

Figure 12 –Time History Deformation Comparison of Experiment and Simulation

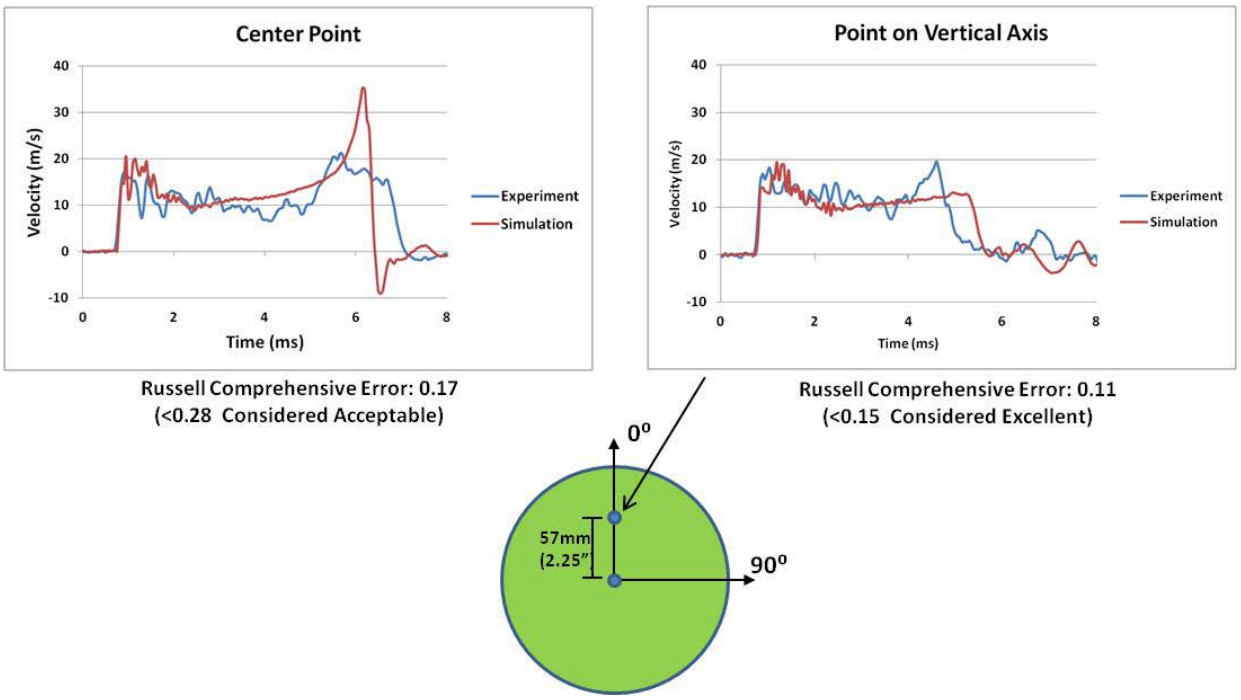

Figure 13 – Time History Velocity Comparison of Experiment and Simulation

Table 3 – Russell Error Summary

	Magnitude Error	Phase Error	Comprehensive Error
Center Point Deflection	0.03	0.03	0.04
Center Point Velocity	0.1	0.16	0.17
Half Way Along Vertical Axis Deflection	0.03	0.03	0.04
Half Way Along Vertical Axis Velocity	0.03	0.12	0.11

RC<0.15 Excellent
.15<RC<0.28 Acceptable
RC>0.28 Poor

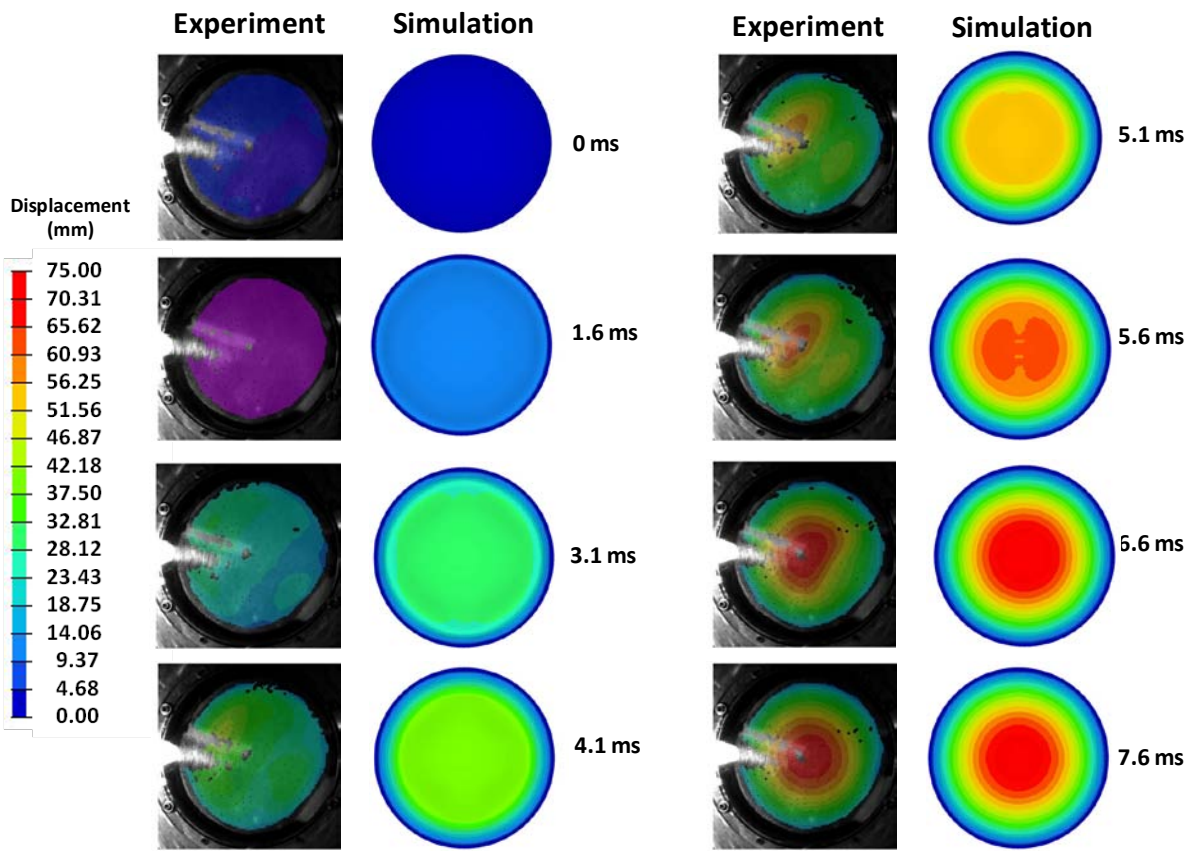

Figure 14 – Full Field Deformation Comparison of Experiment and Simulation

In addition to the transient response correlations, the relationship between the material damage observed during the test and the damage level predicted by the simulations is of interest. In the experiment the main damage mechanism that was observed is delamination between the plies. There was minimal fiber rupture or matrix cracking. The final damage state from the shock test is shown in figure 15a. Here it is seen that the extent of the delamination ranges from approximately 1.27 cm (0.5 in.) in the lower left region of the plate to 5.08 cm (2 in.) at the 3 O'clock position. In the corresponding computational model, figure 15b, the delamination area is highlighted by the black area at the edge of the plate and propagates inwards from the edge 1 cm (0.4 in.). In the simulation results there are also 4 larger delamination zones at the 45°

directions. These areas indicate the weaker material directions (fibers run in the 0° and 90° directions) and extend 3.81 cm (1.5 in.) from the edges. Although the amount of delamination is somewhat larger in the experiment than is observed in the computational model, it is encouraging that the model is able to predict the onset of the delamination itself and propagate it to a comparable distance

In the current model the choice of a delamination criterion was taken to be 36 MPa (5250 lb/in^2) for both tensile and shear stresses. The choice of this value was based on discussions with the Material Sciences Corporation (MSC) who have developed composite damage models currently in use within the LS-DYNA code (Mat_162). Based on these discussions it was determined that the delamination criteria should be set to approximately one-half of the tensile strength of the pure vinyl ester. The degradation by ½ of the tensile strength accounts for voids, and interfacial defects / flaws between the layers of fibers during the manufacturing of the material. Therefore the failure criteria was set to 36 MPa (5,250 lb/in^2) based on the values for the resin provided in table 2. The degradation by one-half was also used in similar shock loading work by LeBlanc et al [19] for an E-Glass/Epoxy laminate. This observation is provided to aid in the development of delamination modeling best practices but is not meant to be definitive. More work is planned into the most efficient way to model the delamination parameters but is outside of the scope of the current study.

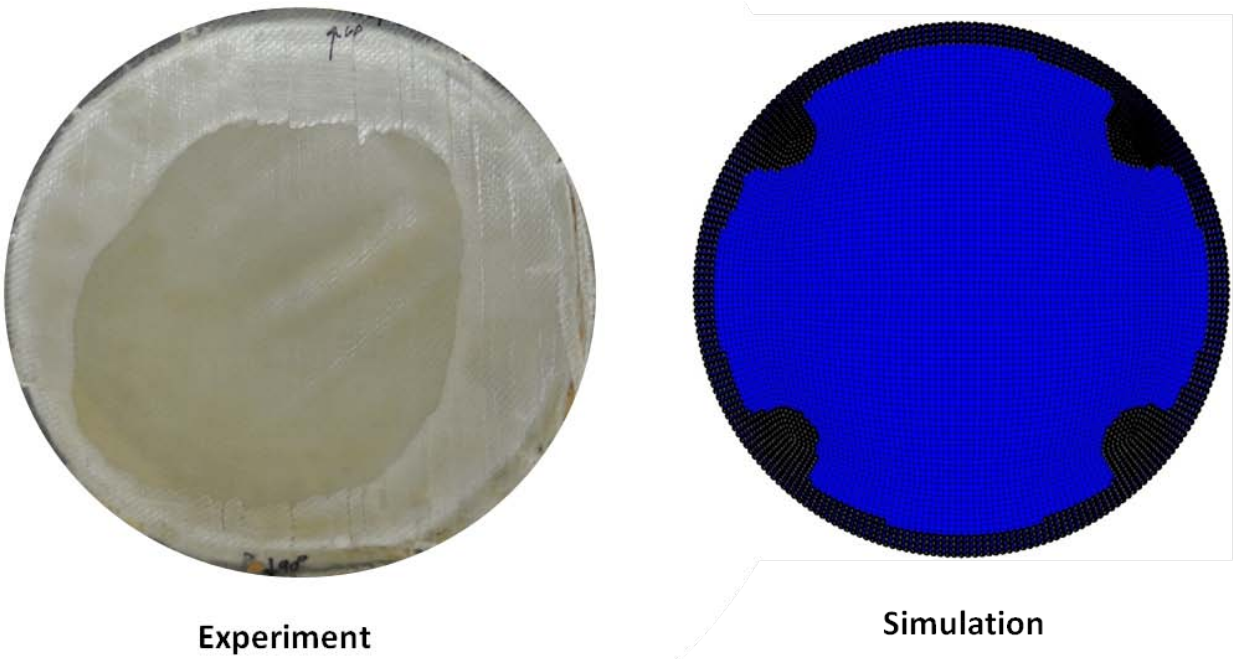

Figure 15 – (a) Material Damage during Test, (b) Material Damage from Simulation

8. Conclusions

A conical shock tube has been used to study the response of curved E-Glass / Vinyl ester composite panels subjected to underwater shock loading. The material is a bi-axial laminate with fibers balanced in the 0 and 90 degree directions. The round plates are curved in shape with the convex surface oriented towards the incoming shock front with fully clamped boundaries. A 3D Digital Image Correlation system is used to capture the full field, transient response of the back (dry) surface of the plates. This allowed for real time recording of the displacement and velocity history of this surface. The displacement and velocity data for the center point and a point halfway between the center and boundary are correlated to the computational models by utilizing the Russell error. The Russell error value for the deflection correlation at these two points is excellent. The velocity correlation at the point halfway between the center and the boundary is also excellent, while the center point velocity has acceptable correlation. The full field displacement evolution is also shown to agree between the experiment and the simulations.

The computational model was also able to predict the onset of delamination damage and predict its growth to a reasonable degree. This work has shown the ability of the LS-DYNA material model Mat_Composite_Failure_Option_Model to realistically model the behavior of a composite material under shock loading conditions. This work has served to show that computational tools can serve to support experimental test results and show promise for use as an alternative to testing to support structural designs utilizing composite materials.

Acknowledgements

The financial support of the Naval Undersea Warfare Center (Division Newport) In-house Laboratory Independent Research program (ILIR) directed by Dr. Anthony Ruffa is greatly acknowledged. Arun Shukla would like to acknowledge the support of Office of Naval Research under ONR Grant No. N00014-10-1-0662 (Dr. Y.D.S. Rajapakse) to the University of Rhode Island. Bruce Booker, Steve Morin, and Brian Ploutz are thanked for their operation of the shock tube facility. The assistance of Nate Gardner and Nicholas Heeder with the DIC setup is acknowledged. Lastly the authors acknowledge LBI Fiberglass of Groton, CT, specifically Peter Legnos and Ricky Menser for the manufacturing of the composite samples for testing.

References

1. Espinosa HD, Lee S, Moldovan N. A Novel Fluid Structure Interaction Experiment to Investigate Deformation of Structural Elements Subjected to Impulsive Loading. Experimental Mechanics 2006; 46:805-824.

2. Nurick G, Olson M, Fagnan J. Levin, A. Deformation and Tearing of Blast Loaded Stiffened Square Plates. International Journal of Impact Engineering 1995; 16:273–291.

3. Nurick G, Shave G. The Deformation and Tearing of Thin Square Plates Subjected to Impulsive Loads - An Experimental Study. International Journal of Impact Engineering 1996; 18:99–116.

4. Tekalur AS, Shivakumar K, Shukla A. Mechanical Behavior and Damage Evolution in E-Glass Vinyl Ester and Carbon Composites Subjected to Static and Blast Loads. Composites: Part B 2008; 39:57-65.

5. Mouritz AP. Ballistic Impact and Explosive Blast Resistance of Stitched Composites. Composites: Part B 2001; 32: 431-439.

6. LeBlanc J, Shukla A, Rousseau C, Bogdanovich A. Shock Loading of Three-Dimensional Woven Composite Materials. Composite Structures 2007; 79:344-355.

7. Jackson M, Shukla A. Performance of Sandwich Composites Subjected to Sequential Impact and Air Blast Loading. Composites: Part B 2010; doi:10.1016/j.compositesb.2010.09.005.

8. Schubel PM, Luo J, Daniel I. Impact and Post Impact Behavior of Composite Sandwich Panels. Composites: Part A 2007; 38:1051-1057.

9. Arora H, Hooper P, Dear JP. Impact and Blast Resistance of Glass Fibre Reinforced Sandwich Composite Materials. In: Proceedings of IMPLAST 2010; October 2010.

10. Matzenmiller A, Lubliner J, Taylor RL. A Constitutive Model for Anisotropic Damage in Fiber-Composites. Mechanics of Materials 1995; 20:125-152.

11. Zako M, Uetsuji Y, Kurashiki T. Finite Element Analysis of Damaged Woven Fabric Composite Materials. Composites Science and Technology 2003; 63:507-516.

12. Dyka CT, Badaliance R. Damage in Marine Composites Caused by Shock Loading. Composites Science and Technology 1998; 58:1433-1442.

13. O'Daniel JL, Koudela KL, Krauthammer T. Numerical Simulation and Validation of Distributed Impact Events. International Journal of Impact Engineering 2005; 31:1013–1038.

14. McGregor CJ, Vaziri R, Poursartip A, Xiao X. Simulation of Progressive Damage Development in Braided Composite Tubes under Axial Compression. Composites: Part A 2007; 38:2247–2259.

15. Gama B, Xiao J, Haque M, Yen C, Gillespie J. Experimental and Numerical Investigations on Damage and Delamination in Thick Plain Weave S-2 Glass Composites under Quasi-Static Punch Shear Loading. Center for Composite Materials, University of Delaware; 2004.

16. Donadon MV, Iannucci L, Falzon BG, Hodgkinson JM, de Almeida SFM. A Progressive Failure Model for Composite Laminates Subjected to Low Velocity Impact Damage. Computers and Structures 2008; 86:1232–1252.

17. Hosseinzadeh R, Shokrieh MM, Lessard L. Damage Behavior of Fiber Reinforced Composite Plates Subjected to Drop Weight Impacts. Composites Science and Technology 2006; 66:61–68.

18. Batra RC, Hassan NM. Response of Fiber Reinforced Composites to Underwater Explosive Loads. Composites: Part B 2007; 38:448–468.

19. LeBlanc J, Shukla A. Dynamic Response and Damage Evolution in Composite Materials Subjected to Underwater Explosive Loading: An Experimental and Computational Study. Composite Structures 2010; 92:2421-2430.

20. Poche L, Zalesak J. Development of a Water-Filled Conical Shock Tube for Shock Testing of Small Sonar Transducers by Simulation of the Test Conditions for the Heavyweight MIL-S-901D (Navy). NRL Memorandum Report 7109, 10 October 1992.

21. Coombs A, Thornhill CK. An Underwater Explosive Shock Gun. Journal of Fluid Mechanics 1967; 29:373-383.

22. Filler WS. Propagation of Shock Waves in a Hydrodynamic Conical Shock Tube. The Physics of Fluids 1964; 7:664-667.

23. Tiwari V, Sutton MA, McNeill SR. Assessment of High Speed Imaging Systems for 2D and 3D Deformation Measurements: Methodology Development and Validation. Experimental Mechanics 2007; 47:561-579.

24. Tiwari V, Sutton MA, McNeill SR, Xu S, Deng X, Fourney WL, Bretall D. Application of 3D Image Correlation for Full-Field Transient Plate Deformation Measurements During Blast Loading. International Journal of Impact Engineering 2009; 36:862-874.

25. Chan S, Fawaz Z, Behdinan K, Amid R. Ballistic Limit Prediction using a Numerical Model with Progressive Damage Capability. Composite Structures 2007; 77:466–474.

26. Russell DM. Error Measures for Comparing Transient Data, Part I: Development of a Comprehensive Error Measure, Part II: Error Measures Case Study. In: Proceedings of the 68th Shock and Vibration Symposium; 3-6 November 1997.

27. Russell DM. DDG53 Shock Trial Simulation Acceptance Criteria. In: 69th Shock and Vibration Symposium; 12-19 October 1998.

CHAPTER 4

RESPONSE OF E-GLASS / VINYL ESTER COMPOSITE PANELS TO UNDERWATER EXPLOSIVE LOADING: EFFECTS OF LAMINATE MODIFICATIONS

by

James LeBlanc and Arun Shukla

Is being prepared for submission to International Journal of Impact Engineering

Corresponding Author: James LeBlanc

Naval Undersea Warfare Center (Division Newport)

1176 Howell Street

Newport, RI, 02841

Phone: +1-401-832-7920

Email Address: James.M.LeBlanc@Navy.Mil

Abstract

The response of E-Glass / Vinyl ester curved composite panels subjected to underwater explosive loading has been studied. Three laminate constructions have been investigated to determine their relative performance when subjected to shock loading. These constructions are: (1) a baseline 0°/90° biaxial layup, (2) a 0°/90° biaxial layup that includes a thin glass veil between plies, and (3) a 0°/90° biaxial layup that has a coating of polyurea applied to the back face. The work consists of experimental work utilizing a water filled, conical shock tube facility. The samples are round panels with curved midsections, and are approximately 2.54 mm in thickness. The transient response of the plates is measured using a three-dimensional (3D) Digital Image Correlation (DIC) system, including high speed photography. This ultra high speed system records full field shape and displacement profiles in real time. The results show that the performance of the baseline laminate is improved when coated with the polyurea material, but conversely, is degraded by the inclusion of the glass veils between plies.

1. Introduction

Composite materials have been widely used in a variety of applications in the marine, automotive, and transportation industries. These materials offer the advantages of high strength to weight ratios, reduced maintenance costs, and improved corrosion resistance. Recently, there has been an increased interest in composite materials for use in military applications including land vehicles (structural components and armor solutions), advanced ship hull designs, and submarine components. The use of these materials in wartime environments requires that they not only be able to withstand the loads produced by everyday use but also those imparted from explosions and high speed projectile impact. Currently, the response of these materials at static

and quasi-static loading rates is well established. However, the response at the high strain rates that shock and ballistic events can induce is not well understood. This leads to an inherent conservative approach to be taken when these structures are designed and constructed. Typically this results in structures which do not fully realize the weight savings afforded by these materials. The focus of the current research is on the response of composite materials subjected to underwater explosions, UNDEX.

Historically, there have been two experimental methodologies used to impart shock loading conditions to structures: (1) explosives and (2) shock tubes. Although the use of explosives offers an ease of use, there are associated deficiencies such as spherical wave fronts and pressure signatures which are often spatially complex and difficult to capture. Shock tubes offer the advantage of plane wave fronts and wave parameters that are easily controlled and repeated. The current study utilizes a water filled, conical shock tube that replicates the free field pressure wave expansion of an underwater explosion.

The response of materials subjected to shock and impact loading has been studied over a wide range of loading rates. The effect of shock loading on stainless steel plates subjected to underwater impulsive loads has been presented by Espinosa et al [1]. Nurick et al [2,3] have studied the effects of boundary conditions on plates subjected to blast loading and identified distinct failure modes depending on the magnitude of the impulse and standoff. The response of E-Glass and Carbon based composite laminates under shock and explosive loading (including the effects of heat generation during combustion) has been presented by Tekalur et al [4]. Mouritz [5] studied the effectiveness of adding a light weight, through thickness stitching material to increase the damage resistance of composites. LeBlanc et al [6] have studied the effects of shock

loading on three-dimensional woven composite materials. Recently, there has been an increased interest in the study of the effect of shock loading on sandwich structures. These studies include the effects of shock and impact loading conditions (Jackson et al [7], Schubel et al [8], Arora et al [9]).

The use of polyurea materials to enhance the failure resistance of materials subjected to explosive loading has become a topic of interest. Polyurea is a synthetic, high strength / high elongation coating that is typically spray cast onto existing structures to increase their resistance to shock and ballistic/shrapnel loading events such as those of a bomb blast. The armed forces have begun to investigate the suitability of these materials for use on military and naval vehicles such as Humvees, troop carriers and ship hulls, Hodge [10]. Research efforts have focused on the use of polyurea coatings on steel plates, composite plates, and as inner layers of sandwich composites. Amini et al [11, 12, 13] have studied the effects of monolithic and polyurea coated steel plates subjected to impulsive loads and showed that polyurea has a positive damage mitigation effect when applied to the back face of the material. They also found that polyurea can enhance the loading and damage levels if applied on the impact side of the plates. In this study it was shown that coating the front face of the panels with the polyurea increased the amount of impact energy transmitted to the plate as compared to when the back face was coated. Gardner et al [14] studied the effect of polyurea in sandwich composites. It was observed that when a layer of polyurea is placed between the foam core and the back face of the sandwich the blast resistance is improved, while conversely if the polyurea is placed between the front face and the foam core the performance is degraded.

2. Composite Material

Three composite material constructions are utilized in this study: (1) 0°/90° biaxial layup, (2) 0°/90° biaxial layup with a glass veil between plies, and (3) 0°/90° biaxial layup with a coating of polyurea. All of the composite material in the study is E-Glass / Vinyl ester. The panels are manufactured using the vacuum assisted resin transfer molding (VARTM) process with a vinyl ester resin, AOC Hydropel R015-AAG-00. All panels were manufactured by LBI Fiberglass located in Groton, CT.

The baseline laminate (1) is a balanced construction of 0° and 90° continuous fibers with the two layers being stitched together rather than woven. The areal weight of the dry fabric is 0.406 kg/m^2 (12 oz/yd^2). The baseline panels in the study consist of 6 plies of the fabric, with each ply oriented in the same direction, i.e. the 0° fibers in each ply are parallel. The finished part has a thickness of 2.54 mm (0.10 in.), areal weight of 4.25 kg/m^2 (126 oz/yd^2), and a fiber content of 63% by weight.

The second laminate (2) which is studied is a modified version of the baseline (1). This layup includes the addition of a lightweight glass veil in between layers of the 0°/90° fabric. The addition of the glass veil layers would have increased the overall part thickness and areal density, so in an effort to maintain these parameters only 5 layers of the 0°/90° fabric, and correspondingly 4 layers of the veil are utilized in these parts. This laminate is meant to aid in the understanding of what the best laminate choice is (when shock is a concern) if part thickness and areal weight are concerns. The dry glass veil has an areal weight of 0.054 kg/m^2 (1.62 oz/yd^2). The finished part has a thickness of 2.54 mm (0.10 in.), areal weight of 4.32 kg/m^2 (128 oz/yd^2), and a fiber content of 60% by weight. This construction is being investigated because

although fiberglass cloths of continuous, oriented fibers have high in-plane strengths when the fibers are oriented in the loading direction, they can suffer from low through thickness strength, meaning they are susceptible to delamination damage. The incorporation of a glass veil of chopped fibers is meant to serve as a resin rich layer to improve the inter-laminar strength of the laminates. The practice of alternating plies of fiberglass cloth and chopped strand mats has historically been used in the boat building industry [15, 16]. This practice is common enough that many manufactures of fiberglass reinforcing fabrics make products which are combinations of continuous unidirectional fibers with a chopped mat / veil backing.

The final laminate construction (3) utilized in this study is identical to the baseline laminate; however the back face of the panel is coated with polyurea. This laminate is chosen to represent what would typically be found in a real world application where structures are retrofitted (spray coated) with this material as opposed to being incorporated into the original design (Hodge [10]). The polyurea material is applied to the composite panel after manufacturing and is not part of the infusion process. A 4 mm (0.160 in.) thick layer of the material is applied to the back face (concave) of the panels resulting in a total part thickness of 6.6 mm (0.26 in.) and an areal weight of 8.31 kg/m^2 (246 oz/yd^2). The polyurea is sprayed on the panels and then post cured for 48 hours at a temperature of 160°F. In the current study the polyurea is only applied to the back face of the composite panels. This location is chosen based on the prior work by Amini et al [11, 12, 13] and Gardner et al [14]. These studies have shown that applying the polyurea layer on the back face of shock loaded panels and sandwich composites results in improved performance while, locating the material on the front face can degrade performance.

The polyurea material that is used for coating the panels is Dragonshield-BC available from Specialty Products, Inc. of Lakewood, WA. This is a 2 part material that can be spray applied to a wide range of surface materials. The product is typically used for blast mitigation and fragment containment in applications ranging from walls, structures, and vehicle protection. The manufacturer provides a tensile strength of over 37.9 MPa (5500 lb/in^2) and an elongation of 344%.

A summary of the panel thicknesses and areal weights is provided in table 1, and a schematic of the laminate designs are shown in figure 1. The mechanical properties for the 0°/90° baseline and 0°/90° laminate with glass veil inter-laminar plies are provided in tables 2 and 3. Comparing the values in these tables it is seen that the introduction of the glass veils between plies reduces the in-plane tensile modulus and strengths by 35% and 34% respectively.

Table 1 – Thickness and Areal Weight of Laminates

	Thickness, mm (in)	Areal Weight, kg/m^2 (oz/yd^2)
0°/90° Baseline Laminate	2.54 (0.10)	4.25 (126)
0°/90° with Inter-Laminar Veils	2.54 (0.10)	4.32 (128)
0°/90° Baseline with Polyurea	6.6 (0.26)	8.31 (246)

Table 2 – 0°/90° Baseline Laminate - Mechanical Properties (ASTM 638)

	MPa (lb/in^2)
Tensile Modulus (0°)	15.8e3 (2.3e6)
Tensile Modulus (90°)	15.8e3 (2.3e6)
Tensile Strength (0°)	324 (47,000)
Tensile Strength (90°)	324 (47,000)

Table 3 – 0°/90° Laminate with Inter-Laminar Glass Veils -Mechanical Properties (ASTM 638)

	MPa (lb/in^2)
Tensile Modulus (0°)	10.3e3 (1.5e6)
Tensile Modulus (90°)	10.3e3 (1.5e6)
Tensile Strength (0°)	213 (31,000)
Tensile Strength (90°)	213 (31,000)

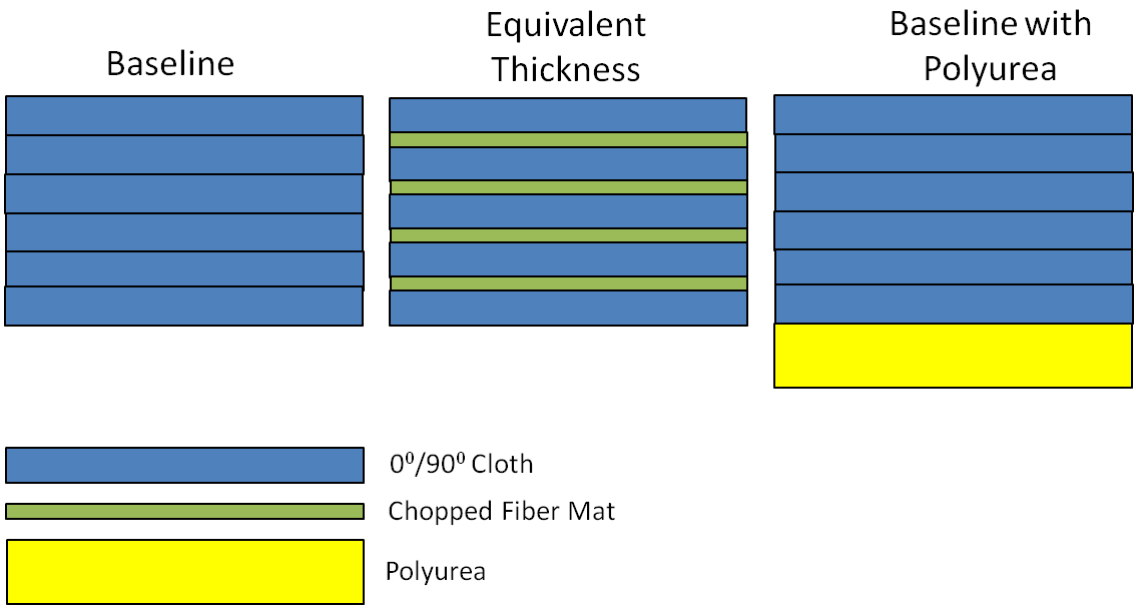

Figure 1 – Composite Plate Construction - Schematic

The geometry of the plates consists of a curved midsection with a flat boundary as shown in figure 2. The convex face of the plate represents the mold line in the manufacturing process and has a radius of curvature of 18.28 cm (7.2 in.), an outer diameter of 26.54 cm (10.45 in.), and the curved portion of the plate is 22.86 cm (9 in.) in diameter.

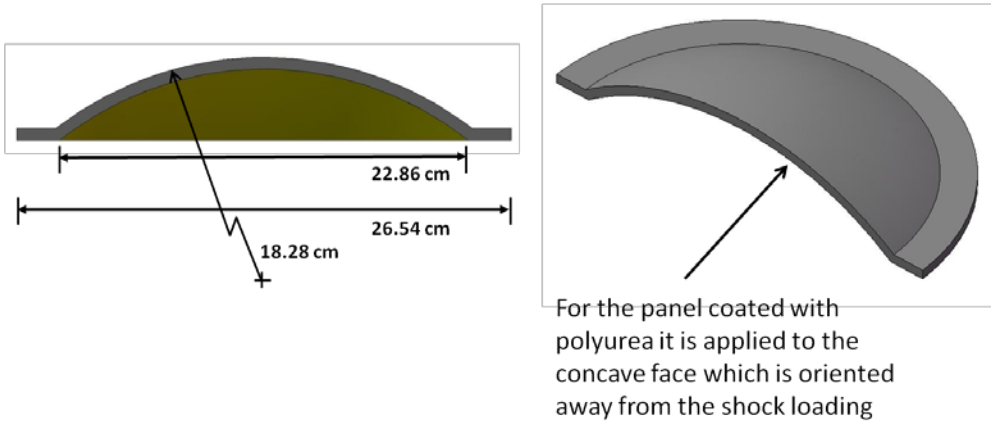

Figure 2 – Composite Plate Geometry (Section View)

3. Shock Loading Apparatus

A conical shock tube (CST) facility located at the Naval Undersea Warfare Center, Division Newport was utilized in the shock loading of the composite materials. The shock tube is a horizontally mounted, water filled tube with a conical internal shape, Figure 3. The tube geometry represents a solid angle segment of the pressure field that results from the detonation of a spherical, explosive charge, Figure 4. In an open water environment the pressure wave expands from the charge location as a spherical wave. In the shock tube the rigid wall acts to confine the expansion of the pressure wave in a manner that simulates a conical sector of the pressure field. In order to compare free field and shock tube pressure values, it is useful to define an amplification factor which is the ratio between the volume of a spherical charge to the volume of the conical sector charge and is defined by Poche and Zalesak [17] as:

$$AF = \frac{1}{sin^2\left(\frac{\alpha}{4}\right)}$$

α is the cone angle

This equation assumes perfectly rigid wall conditions which are not fully realized. Therefore, the actual amplification factor is less than the calculated value and is typically reported as an effective weight amplification factor. This is defined by Poche and Zalesak [17] as the ratio between the weight of a spherical charge, W, required to produce the same peak pressure at a given standoff distance as that produced in the shock tube by a segment of charge weight, w. The reduction in the amplification factor is typically attributable to elastic deformation of the shock tube walls. Further discussion on the development and history of the water filled conical shock tube is provided by references 18 and 19.

The internal cone angle of the tube is 2.6 degrees. The tube is 5.25 m (207 in.) long from the charge location to the location of the test specimen and internally contains 98.4 L (26 gal.) of water at atmospheric pressure. The pressure shock wave is initiated by the detonation of an explosive charge at the breech end of the tube (left side of figure) which then proceeds down the length of the tube. Peak shock pressures from 10.3 MPa (1500 lb/in^2) to 20.6 MPa (3000 lb/in^2) can be obtained depending on the amount of explosive charge. A typical pressure profile obtained from the use of the tube is shown in figure 5. This figure illustrates the rapid pressure increase associated with the shock front followed by the exponential decay of the wave. This profile was obtained using a M6 Blasting Cap – 1.32g (.00292 lb) TNT Equivalency and is measured 0.508 m (20 in.) from the impact face of the plate. The length of the tube is sufficient so that plane wave conditions are nearly established at the specimen.

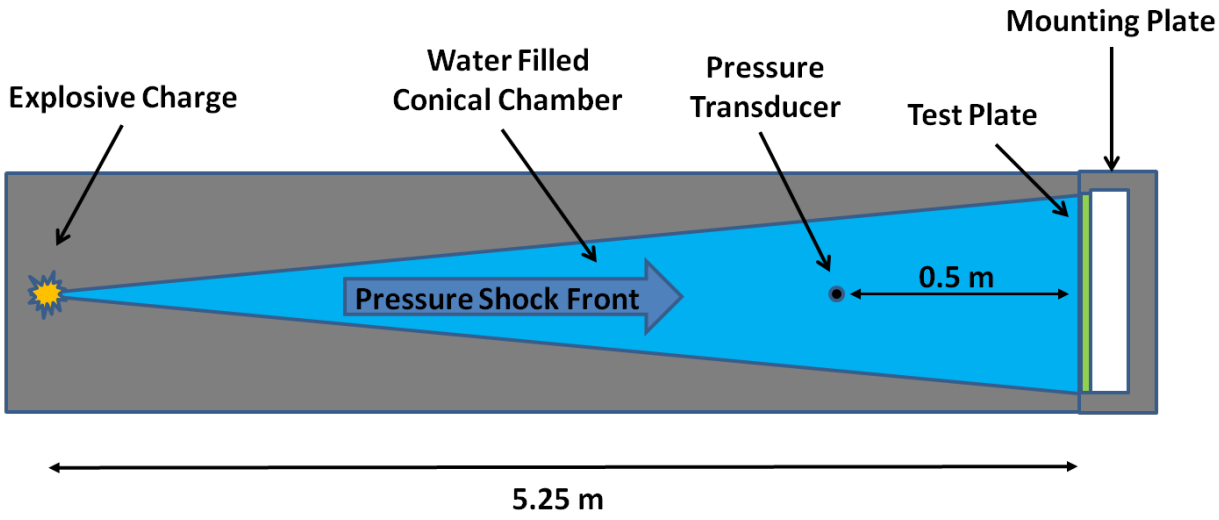

Figure 3 – Conical Shock Tube Schematic (not to scale)

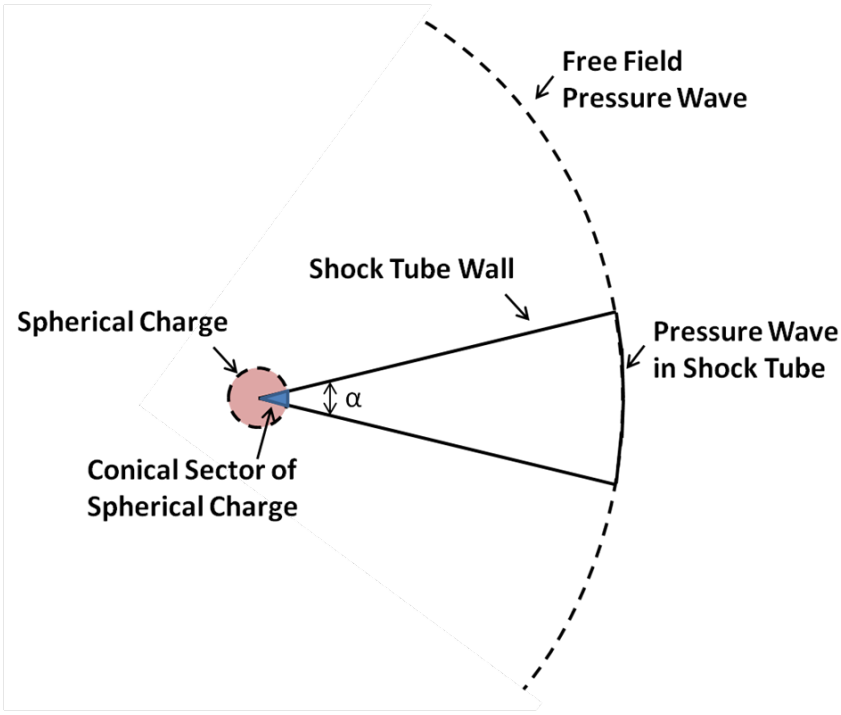

Figure 4 – Explosive Charge in Shock Tube (Poche and Zalesak, 1992)

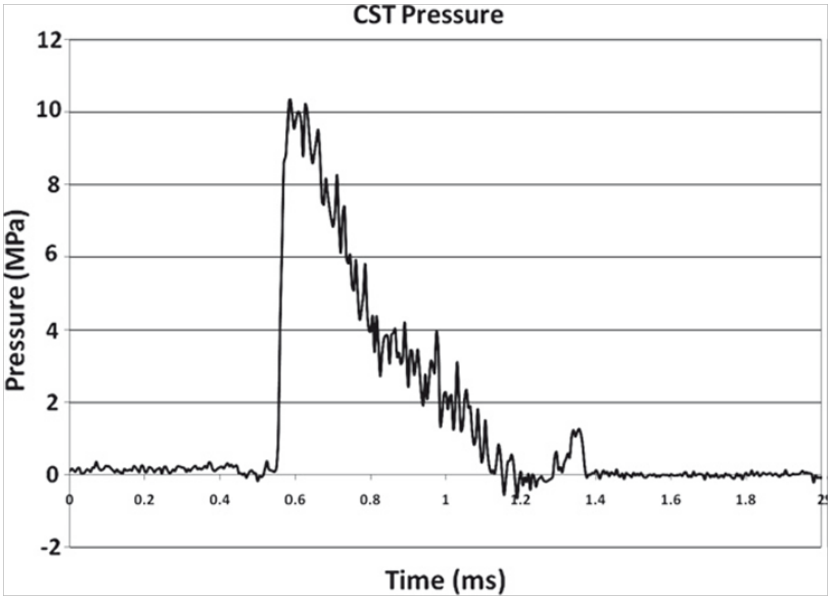

Figure 5 – Typical Pressure Profile Generated in the Conical Shock Tube

A mounting fixture has been designed so the test specimens are air backed with fully clamped edges. The specimens are 26.54 cm (10.45 in.) in overall diameter with a 22.86 cm (9 in.) unsupported middle section. The mounting arrangement is shown in figure 6. The

specimens are mounted with the convex surface towards the incoming shock fronts. This is chosen so that the experiment will represent geometries commonly used in underwater applications with curved surfaces typically facing into the fluid (i.e. submersible vehicle hull forms).

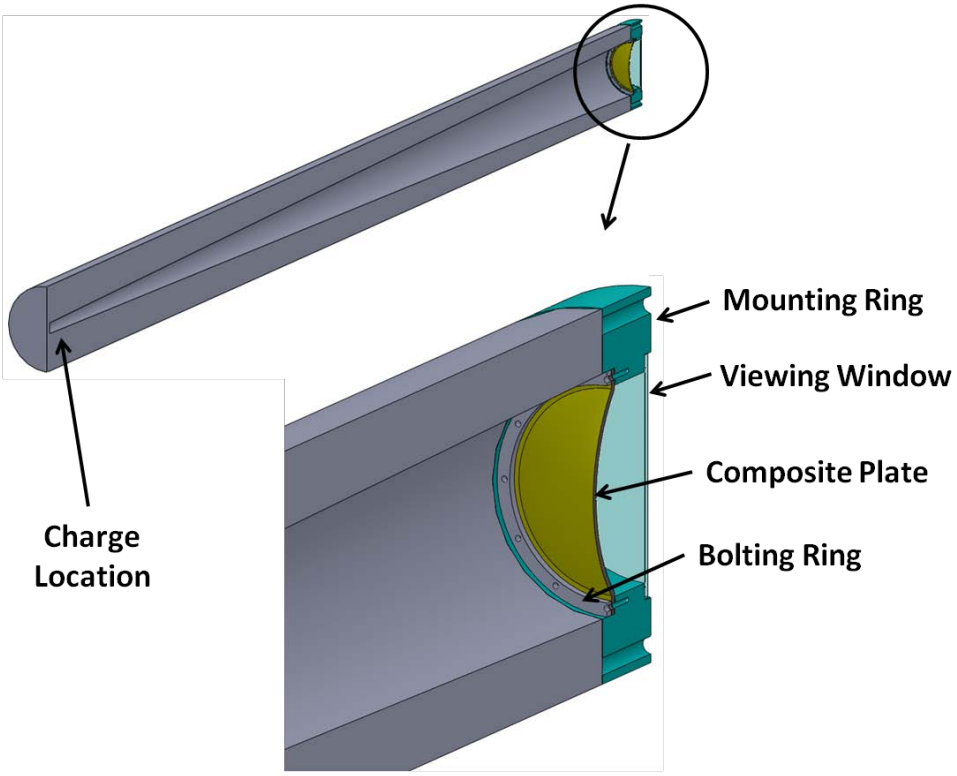

Figure 6 – Shock Tube Mounting Configuration

4. Experimental Procedure

Shock testing of the composite material has been performed with the CST utilizing a fixed end cap. The use of the fixed end cap configuration allows the plate to absorb the full energy level of the shock and sustain a suitable level of damage. The tube can also be configured with a sliding piston end cap (LeBlanc et al. [20]) to lower the level of energy the plate absorbs, but is not utilized in this study. All experiments were performed two times to ensure repeatability. High speed photography coupled with a 3D digital image correlation system is utilized to capture the back face transient response during the shock event. This

system offers the advantage that it is a noncontact measurement technique which gives full field information and eliminates the difficulties of strain gages debonding from the specimens at high shock levels and large plate flexures. The explosive charge used in the study is an M6 blasting cap with a net TNT equivalence of 1.32grams. This yields peak pressures at the sensor location (.508 m in front of the test specimen) of approximately 11 MPa (1600 lb/in^2).

The Digital Image Correlation (DIC) technique is used to capture the transient response of the back face (dry) of the plates. DIC is a non-intrusive, optical technique for capturing the full field, transient response of the panels through the use of high speed photography and specialized software. Capturing the three dimensional response of the plates requires that 2 cameras be used in a stereo configuration. To record the transient response with this system the cameras must be calibrated and have synchronized image recording throughout the event. The calibration of the cameras is performed by placing a grid containing a known pattern of dots in the test space where the composite sample is located during the experiment. This grid is then translated and rotated in and out of plane while manually recording a series of images. As this grid pattern is predetermined, the coordinates of the center of each dot is extracted from each image. The coordinate locations of each dot extracted uniquely for each camera allows for a correspondence of the coordinate system of each camera (Tiwari et al [21]). The DIC is then performed on the image pairs that are recorded during the shock event. Prior to the experiment, the back face of the sample is painted white and then coated with a randomized speckle pattern, Figure 7. The post processing is performed with the VIC-3D software package (Correlated Solutions) which matches common pixel subsets of the random speckle pattern between the deformed and un-deformed images. The matching of pixel subsets is used to calculate the three dimensional location of distinct points on the face of the panel throughout time. This technique

has been applied as a full field measurement technique in many applications including shock loading (Tiwari, et al [22])

Two high speed digital cameras, Photron SA1, are positioned behind the shock tube, figure 7. The use of two cameras allows for the out-of-plane behavior to be captured. If a single camera is utilized the data would be limited to the in-plane results. The distance from the lens of the camera to the specimen is 1.44 m (57 in.) and each camera is angled at approximately 7° with respect to the symmetry plane, figure 8. A frame rate of 20,000 was used with an inter-frame time of 50μs.

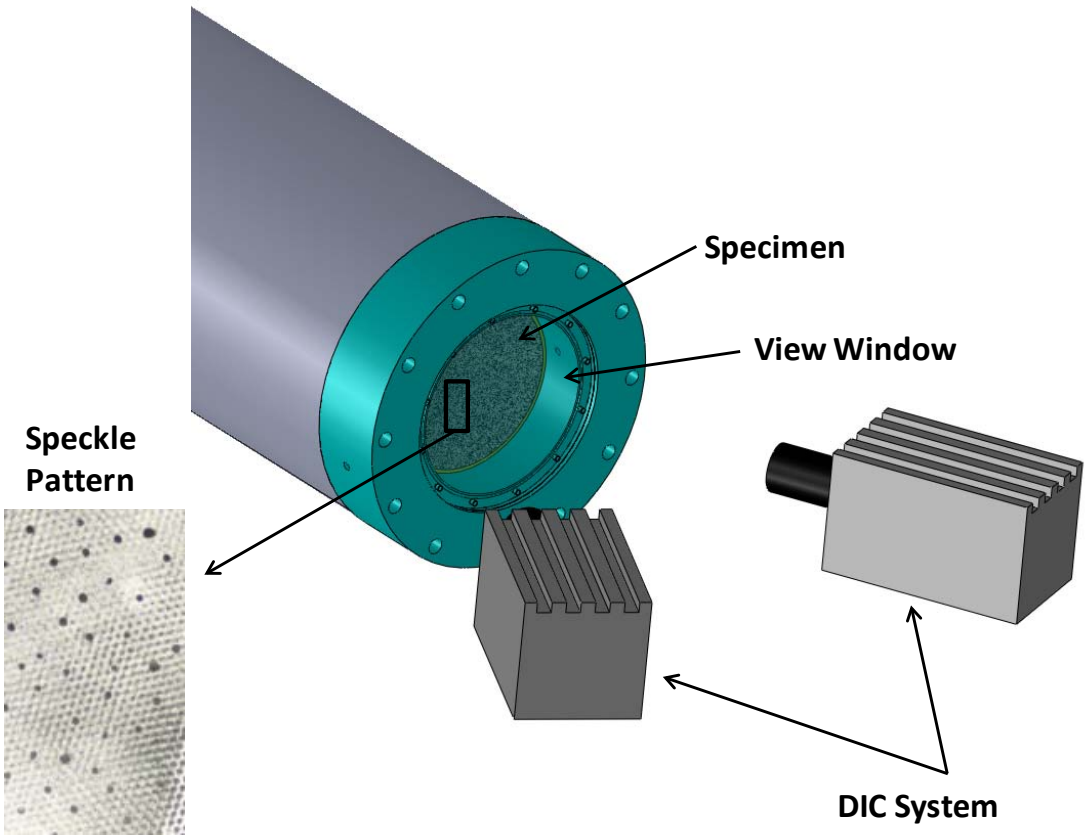

Figure 7 –Digital Image Correlation Schematic

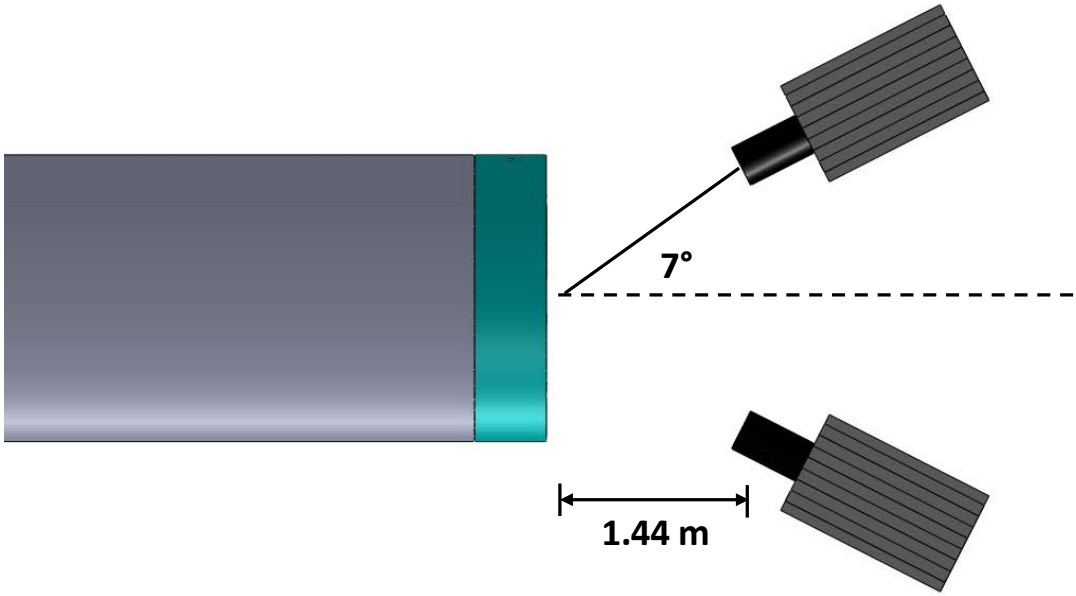

Figure 8 –Digital Image Correlation Setup (Not to Scale)

5. Results

The determination of the effectiveness of the two laminate modifications in comparison to the baseline laminate will focus on deformation and velocity time histories, as well as the level of post mortem damage. The deformation and velocity histories are presented for distinct points on the back face of the panels, and are extracted from the DIC post processed data. The post mortem damage levels are assessed from visual observations of the damage mechanisms.

The pressure profile obtained from the experiment with the baseline laminate is shown in figure 9. The pressure history can be separated into three distinct time regimes. The first is the initial shock front which has time duration of less than 1 ms from peak pressure to full decay to ambient. The second set of pressure effects arrives at the pressure transducer at approximately 10.5 ms after the initial shock front. This secondary wave is formed when the velocity of the plate is brought to rest. During the initial deformation of the plate, the water that contacts the plates moves along with the plate surface. When the movement of the plate is brought to rest,

the momentum of this water causes it to compress against the plate and a high pressure wave is developed. This wave then propagates down the length of the tube and is reflected back towards the plate. The time delay from this secondary wave reaching the transducer, traveling down the tube, and arriving back at the transducer is expected to be on the order of 5.5ms based on the distance of travel from the transducer to the charge location. This time delay is clearly seen in figure 9. The bubble pulse for the charge weight and conditions that are used in this study is expected to be on the order of 30 ms, and is confirmed by the high pressures seen in the pressure profiles at this time. From figure 10 it is seen that the initial peak pressure for each shot is nearly identical. It is important to note the absence of a reflection of the incident pressure wave in the pressure signal. This is attributable to the similar acoustic impedance values of the water and the composite plate as well as the fluid structure interaction of a plane wave with a curved surface. Consider the case of a dilatation wave arriving at the interface between two dissimilar materials (Water-Composite interface). The wave will be partially transmitted into the plate and partially reflected back into the water. The magnitudes of the reflected (A_2) and transmitted (A_4) waves as a function of the incident wave (A_1) are given as:

$$A_2 = A_1 - A_4$$

$$A_4 = \left(A_1 + A_2\right)\frac{C_{1A}\rho_A}{C_{1B}\rho_b}$$

Where C_1 and ρ are the longitudinal wave speed and the density of the water (A) and the Composite (B). For the water the wave speed and density are 1500 m/s and 1000 kg/m^3 and for the composite material the values are 3064 m/s and 1680 kg/m^3. These parameters yield a reflected wave magnitude that is 55% of the incident wave. The development of these equations (Sadd, 2009) assume that the surfaces are perfectly bonded with matching of displacements and stresses at the interface. It is likely that these conditions are not fully realized with one of the

mediums being water which carries no shear stress, and has the possibility of separating from the composite forming a cavitiation region during the initial deformation of the plate. The development of cavitiation at the water / plate interface has been observed by Espinosa et al. (2006) for experiments with steel plates. If perfect matching conditions are not fully realized then the reflected wave has the possibility of further magnitude reduction from the analytical value of 55%. Furthermore, these equations assume a flat interface normal to the incident wave. In the current configuration the wave is interacting with a convexly curved surface which will act to disperse the wave front, further reducing the magnitude of the reflected wave that the pressure transducer would measure. Previous work has observed similar reduced reflection waves. Experiments performed by Espinosa (2006) with steel plates measured reflected waves on the order of 60% of the incident, whereas the theory predicts a value on the order of 95% reflection.

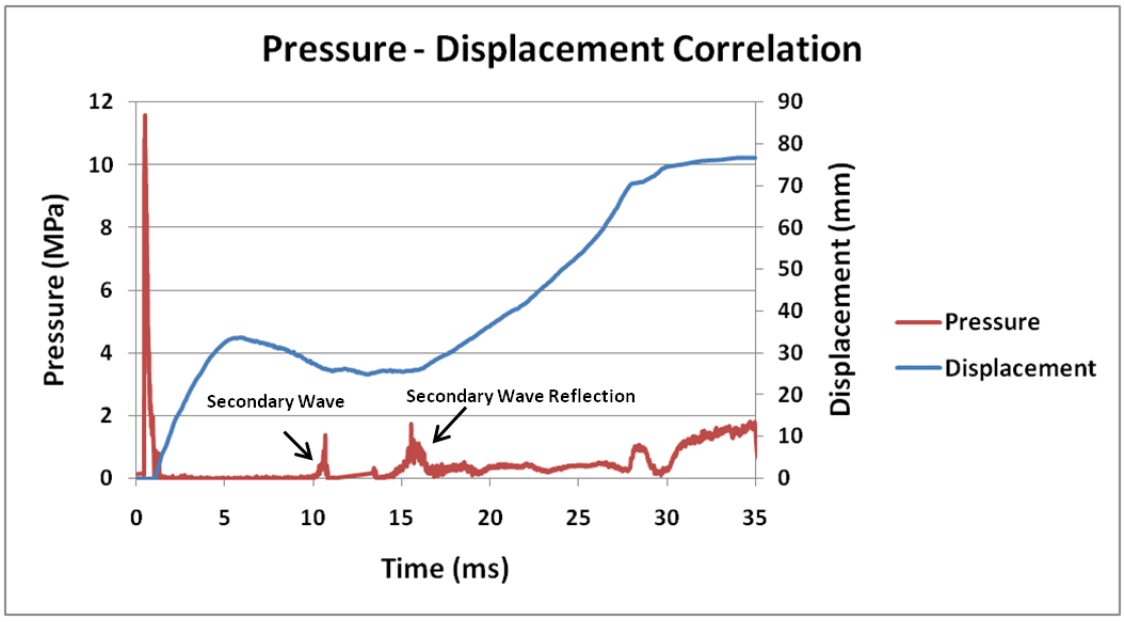

Figure 9 – Pressure – Deformation History Correlations

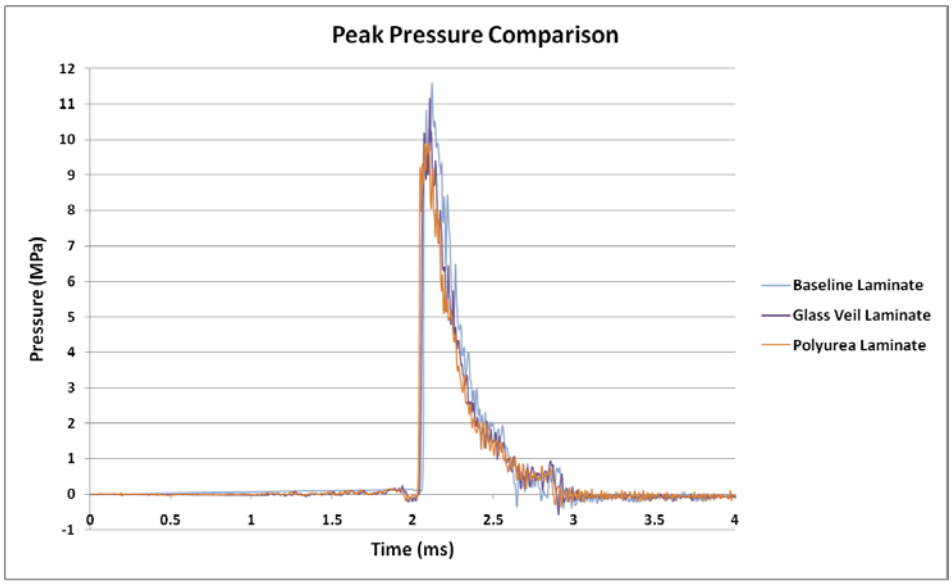

Figure 10 – Pressure Profiles (Peak Pressure Comparison) obtained from CST

The center point deformation time history along with the corresponding pressure profile for the case of the base line laminate is shown in figure 9. It is seen in this figure that the initial shock causes a deformation of the center point (0–5 ms), a small recovery (5–10 ms), and finally a temporary arresting of the motion (10–15 ms). After this arresting of the motion, the secondary pressure wave arrives (15 ms) and restarts the deformation process of the plate. The effect of the secondary pressure wave is sufficient to carry the deformation process to full inversion of the plate. A similar trend is seen for the other two laminates in this study.

The comparison of the displacement –time history for the three laminates is shown in figure 11. The top plot shows the deflection for the center point and the bottom plot shows the deflection for a point located halfway between the center and the clamped edge along the horizontal axis. Using the baseline laminate as a reference, the panel which is coated with polyurea on the back face shows a distinct performance increase in terms of the displacement sustained after the arrival of the first pressure peak. Conversely, the performance is degraded when glass veil is incorporated between plies but the panel thickness is maintained constant.

After the first pressure peak the baseline laminate sustains a center point displacement of 33.5 mm (1.31 in.) while the deflection for the polyurea sample is 11 mm (0.43 in.), a decrease of 67%. In the case of the veil laminate the center point displacement is 48 mm (1.88 in.), an increase of 43% over the baseline. In table 3 it was shown that the this laminate has a 34% reduction in modulus over the baseline, which likely is the cause for this reduction on deformation behavior, especially since the primary loading mechanism is flexure. In all cases it is seen that the effects of the secondary pressure waves are sufficient to continue the displacement to full plate inversion. This is attributable to the plates being weakened and partially inverted by the initial peak pressure effect.

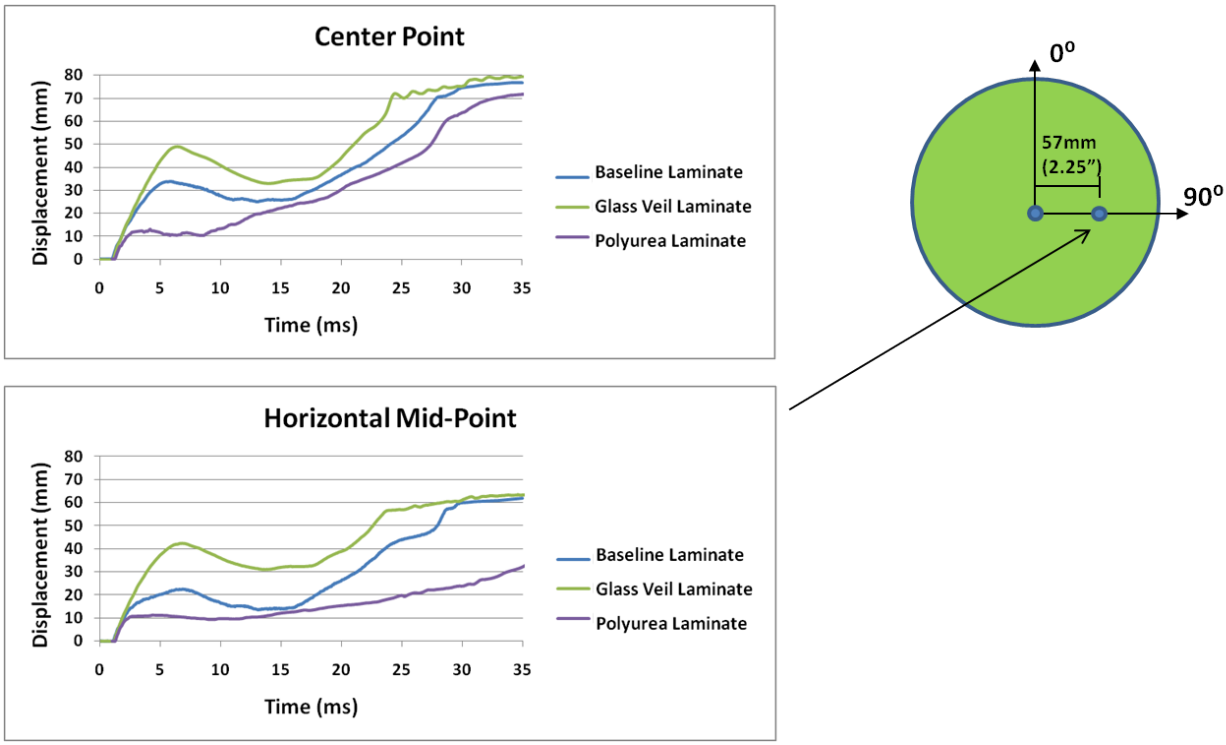

Figure 11 –Time History Deformation Comparison

The velocity time history comparison for the center point of each of the three laminates is shown in figure 12. The top plot of this figure shows the velocity history for the total time

duration of the event, whereas the bottom plot focuses on the velocity resulting from the initial shock pressure. From the bottom figure it is seen that the magnitude of the kick off velocity for each of the laminates is nearly the same, approximately 16 - 17 m/s (52.5 – 55.7 ft/s). There is a difference, however, in the time that it takes for the velocity to decay back to zero for each of the panels. The velocity of the baseline laminate fully decays over 4.5 ms while the panel with polyurea decays faster, taking only 2.4 ms to return to rest. Conversely, the panel with the glass veil layers takes 5.5 ms, 1 ms longer than the baseline panel. An alternative way to compare the decay rate of the velocity is to represent the initial velocity profile as an exponential function as shown below and compute the decay constant, θ, from an exponential curve fit for each panel. The decay constants respectively for the baseline, polyurea, and the glass veil panels are: -1.9 sec, -2.6 sec, and -1.0 sec.

$$V(t) = V_{max} e^{\frac{t}{\theta}}$$

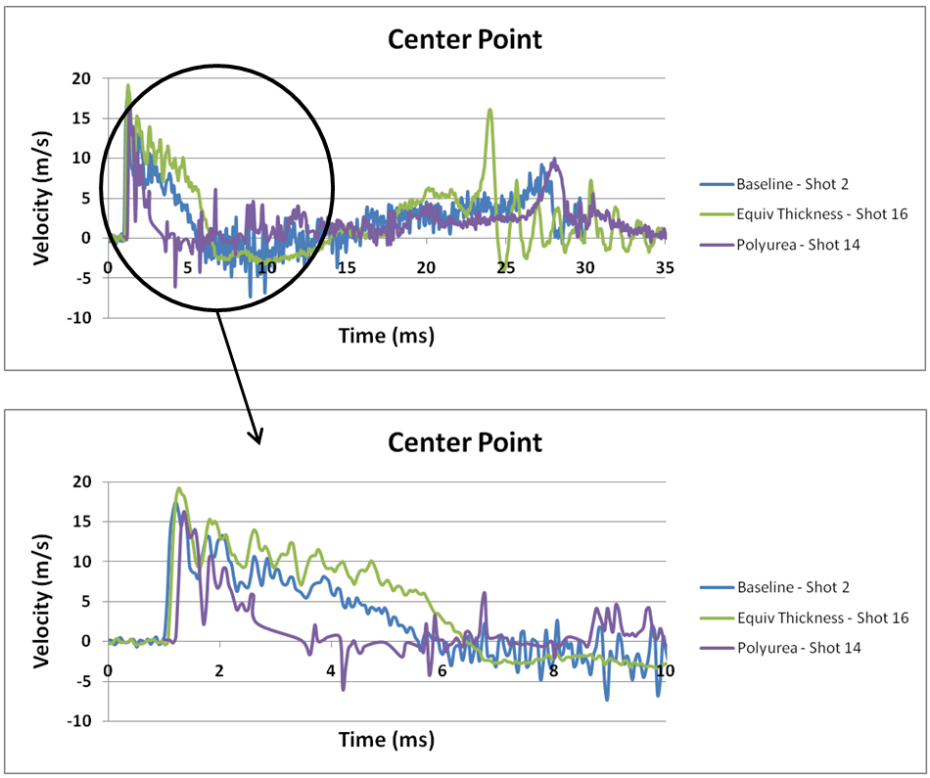

Figure 12 –Velocity History Deformation Comparison

The final damage states of the three laminates are shown in figure 13. From this figure it is seen that for all of the laminates the primary damage mechanism is delamination, indicated by the lighter regions of the plates. There is minimal matrix cracking or fiber breakage observed in any of the panels. There is a small 76.2 mm (3 in.) crack towards the center of the baseline panel but this is limited to the surface of the plate and is does not extend through the thickness of the laminate. It is important to note that these are the final states of damage after the entire shock event occurs, including the secondary deformation process later in time. It was not possible to separate which damage occurs during the initial shock loading and which occurs as a result of the secondary deformation process. Similarly it is not known what the exact damage state after the initial deformation process is and how this initial damage state compares between the three laminates. The only conclusion that can be drawn from these figures is that among the three laminates the final level of damage is comparable, and consists primarily of delamination. This

indicates that for these loading conditions and plate geometries, the inclusion of glass veils between plies does not improve the delamination performance of the composite laminate as compared to the baseline.

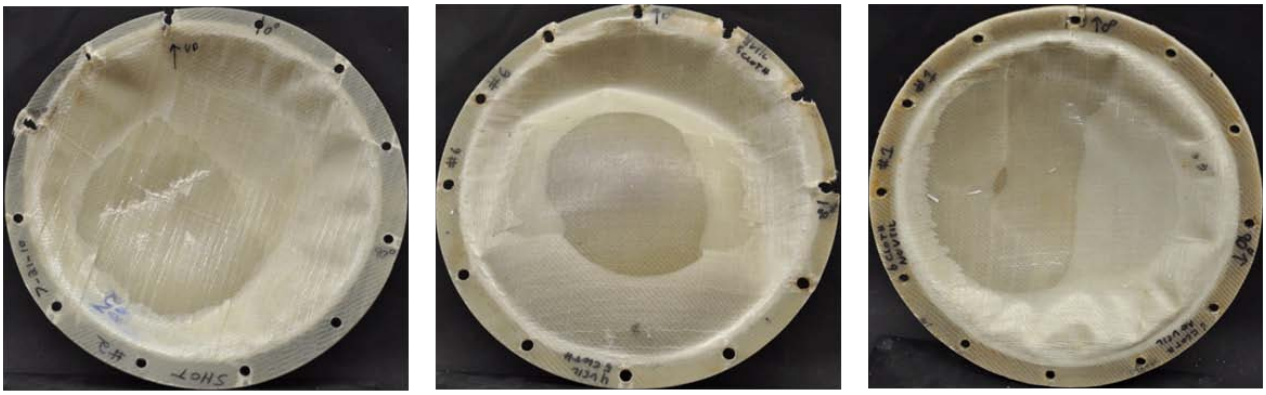

Figure 13 – Material Damage Comparison

6. Conclusions

A conical shock tube has been used to study the response of curved E-Glass / Vinyl ester composite panels subjected to underwater shock loading. Three laminate constructions have been investigated and consist of (1) a baseline 0°/90° biaxial layup, (2) a 0°/90° biaxial layup that includes a thin glass veil between plies, and (3) a 0°/90° biaxial layup that has a coating of polyurea applied to the back face. The round plates are curved in shape with the convex surface oriented towards the incoming shock front with fully clamped boundaries. A 3D Digital Image Correlation system is used to capture the full field, transient response of the back (dry) surface of the plates. This allowed for real time recording of the displacement and velocity history of this surface.

The deformation and velocity time histories at several unique points on the back face of the sample are used to evaluate the effectiveness of each laminate subjected to shock loading conditions. Using the deformation response to the initial peak pressure it was shown that the polyurea reduced the center point deflection by 67%, while the inclusion of glass veils increased the deflection by 43%. In all cases it is seen that the effects of the secondary pressure waves are sufficient to continue the displacement to full plate inversion. It is also observed that the magnitude of the kickoff velocity for all panels was the same at around 16 m/s, however the polyurea panel showed the fastest decay of this peak velocity back to zero. Overall damage levels in each of the panels were comparable but it was not possible to separate which damage occurs during the initial shock loading and which occurs as a result of the secondary deformation process. The results show that the performance of the baseline laminate is degraded by the inclusion of the glass veils between plies but improved when the back face is coated with the polyurea material.

Acknowledgements

The financial support of the Naval Undersea Warfare Center (Division Newport) In-house Laboratory Independent Research program (ILIR) directed by Dr. Anthony Ruffa is greatly acknowledged. Arun Shukla would like to acknowledge the support of Office of Naval Research under ONR Grant No. N00014-10-1-0662 (Dr. Y.D.S. Rajapakse) to the University of Rhode Island. Bruce Booker, Steve Morin, and Jim Sinclair are thanked for their operation of the shock tube facility. The assistance of Nate Gardner, Nicholas Heeder, and Ryan Sekac with the DIC setup is acknowledged. Lastly the authors acknowledge Specialty Products, Inc. , specifically Shere Bush, for providing the polyurea material used in this study.

References

1. Espinosa HD, Lee S, Moldovan N. A Novel Fluid Structure Interaction Experiment to Investigate Deformation of Structural Elements Subjected to Impulsive Loading. Experimental Mechanics 2006; 46:805-824.

2. Nurick G, Olson M, Fagnan J. Levin, A. Deformation and Tearing of Blast Loaded Stiffened Square Plates. International Journal of Impact Engineering 1995; 16:273–291.

3. Nurick G, Shave G. The Deformation and Tearing of Thin Square Plates Subjected to Impulsive Loads - An Experimental Study. International Journal of Impact Engineering 1996; 18:99–116.

4. Tekalur AS, Shivakumar K, Shukla A. Mechanical Behavior and Damage Evolution in E-Glass Vinyl Ester and Carbon Composites Subjected to Static and Blast Loads. Composites: Part B 2008; 39:57-65.

5. Mouritz AP. Ballistic Impact and Explosive Blast Resistance of Stitched Composites. Composites: Part B 2001; 32: 431-439.

6. LeBlanc J, Shukla A, Rousseau C, Bogdanovich A. Shock Loading of Three-Dimensional Woven Composite Materials. Composite Structures 2007; 79:344-355.

7. Jackson M, Shukla A. Performance of Sandwich Composites Subjected to Sequential Impact and Air Blast Loading. Composites: Part B 2010; doi:10.1016/j.compositesb.2010.09.005.

8. Schubel PM, Luo J, Daniel I. Impact and Post Impact Behavior of Composite Sandwich Panels. Composites: Part A 2007; 38:1051-1057.

9. Arora H, Hooper P, Dear JP. Impact and Blast Resistance of Glass Fibre Reinforced Sandwich Composite Materials. In: Proceedings of IMPLAST 2010; October 2010.

10. Hodge N. Military Experimenting with ‘Spray On’ Armor for Humvees. Defense Today 2004; 25

11. Amini MR, Isaacs JB, Nemat-Nasser S. Experimental Investigation of Response of Monolithic and Bilayer Plates to Impulsive Loads. International Journal of Impact Engineering 2010; 37:82-89

12. Amini MR, Simon J, Nemat-Nasser S. Numerical Modeling of Effect of Polyurea on Response of Steel Plates to Impulsive Loads in Direct Pressure-Pulse Experiments. Mechanics of Materials 2010; 42:615-627

13. Amini MR, Isaacs JB, Nemat-Nasser S. Investigation of Effect of Polyurea on Response of Steel Plates to Impulsive Loads in Direct Pressure-Pulse Experiments. Mechanics of Materials 2010; 42:628-639

14. Gardner N, Wang E, Kumar P, Shukla A. Blast Mitigation in a Sandwich Composite Using Graded Core and Polyurea Interlayer. Experimental Mechanics; In Process

15. Geer D. Boat Strength for Builders, Designers, and Owners. International Marine 2000. ISBN 0-07-023159-1

16. Casey D. This Old Boat. International Marine 2009. ISBN 978-0-07-147794-9

17. Poche L, Zalesak J. Development of a Water-Filled Conical Shock Tube for Shock Testing of Small Sonar Transducers by Simulation of the Test Conditions for the Heavyweight MIL-S-901D (Navy). NRL Memorandum Report 7109, 10 October 1992.

18. Coombs A, Thornhill CK. An Underwater Explosive Shock Gun. Journal of Fluid Mechanics 1967; 29:373-383.

19. Filler WS. Propagation of Shock Waves in a Hydrodynamic Conical Shock Tube. The Physics of Fluids 1964; 7:664-667.

20. LeBlanc J, Shukla A. Dynamic Response and Damage Evolution in Composite Materials Subjected to Underwater Explosive Loading: An Experimental and Computational Study. Composite Structures 2010; 92:2421-2430.

21. Tiwari V, Sutton MA, McNeill SR. Assessment of High Speed Imaging Systems for 2D and 3D Deformation Measurements: Methodology Development and Validation. Experimental Mechanics 2007; 47:561-579.

22. Tiwari V, Sutton MA, McNeill SR, Xu S, Deng X, Fourney WL, Bretall D. Application of 3D Image Correlation for Full-Field Transient Plate Deformation Measurements During Blast Loading. International Journal of Impact Engineering 2009; 36:862-874.

CHAPTER 5

CONCLUSIONS AND FUTURE WORK

1. CONCLUSIONS

This research has studied the dynamic response and damage evolution of composite materials when subjected to underwater explosive loading conditions. The work consisted of both experimental work and computational simulations to aid in the understanding of the behavior of these materials. The objective of the study was to develop a better understanding of the shock response of composite materials leading to more efficiently designed structures. The relevant findings resulting from the present study are presented below.

(1) An experimental methodology has been developed which subjects composite plates of both flat and curved geometries to shock loading resulting from an underwater explosion. A conical shock tube facility is utilized which replicates the free field expansion of pressure waves resulting from the explosion. The plates are air backed and held with fully clamped boundary conditions. The dynamic response of the back face of the specimens is captured through the use of strain gages and digital image correlation. The use of digital image correlation allowed for the capture of the full field deformation and velocity histories.

(2) A modeling methodology has been developed that is able to accurately simulate the response of the composite material as observed during the experiments. The modeling is performed utilizing the commercially available LS-DYNA explicit finite element code. The finite element models consist of both the water within the conical shock tube and the composite plate. The models are able to capture the fluid structure interation between the water and the plates as well as the transient response of the plates.

Additionally the models are able to simulate the onset of material damage including both in-plane and through thickness mechanisms.

(3) The results from the shock experiments and the computational simulations have been correlated using both the dynamic response histories as well as the final damage states. The time histories obtained from the strain gages and the digital image correlation results have been correlated to the simulation results using the Russell Error. This is a method which evaluates the differences in two transient data sets by quantifying the variation in magnitude and phase. The correlation between the strain, deflection, and velocities for the respective experiments were found to fall within the acceptable criteria with some comparisons being excellent. Additionally, comparisons between the final material damage state in the experiment and the simulation were agreeable both in terms of the type and extent of the individual mechanisms.

(4) The effects of laminate modifications were studied to determine the effectiveness of each on improving the response to shock loading. Three laminate constructions were investigated: (1) a baseline 0°/90° biaxial layup, (2) a 0°/90° biaxial layup that includes a thin glass veil between plies, and (3) a 0°/90° biaxial layup that has a coating of polyurea applied to the back face. It was found that coating the back face of the material with a layer of polyurea improved the damage mitigation performance of the composite plates, while conversely including a glass veil between plies degraded the material performance.

2. FUTURE WORK

The current investigation has provided a basis for experimental and computation techniques which can be applied to the study of the dynamic response of composite materials subjected to

underwater explosive loading conditions. There however, remains a significant body of work to be completed in this area before the dynamic response of these materials matures to an equivalent level of understanding as that for metallic materials. This work includes further experimental and computational studies as well as work which correlates the two. This will effectively lead to validated modeling practices that can be applied during the design phase of composite structures. The proposed potential future projects are summarized as follows:

1. Perform small scale underwater explosive experiments in which the charge is located much closer to the composite plates than what was performed in this study. In the current study the standoff distance was large compared to the plate geometry, whereas future work should examine the effects of charge standoffs which are smaller than the plate dimensions. At smaller standoff distances the pressure wave will have a much more spherical shape when it interacts with the plates as opposed to the current study where near planar conditions were achieved and the plate was loaded over its entire surface area. Smaller standoffs will examine the localized effects of UNDEX loading as only a portion of the plate surface may be loaded.
2. Conduct shock experiments in which the complexity of the geometry of the test articles is further increased. In the current study plates that were flat or had a smooth curve to them were utilized. More complex geometries could include oblong spheroids, cylinders, and plates with abrupt angle changes. The goal should be to incorporate real world design shapes into the test article geometry. The current finite element modeling methodology should also be expanded to simulate these experiments to ensure it is able to accurately simulate the geometrical effects.

3. Conduct an experimental and computational study to more effectively model delamination damage and determine the appropriate governing parameters. The current study utilized a tiebreak surface to surface contact definition to model the ply interfaces where the delamination value was taken to be percentage of the resin properties. This modeling methodology has the potential to be improved through other representations of this interface including the use of cohesive elements or constraint sets. An experimental method should be employed to provide a basis to which the simulations can be compared to and validated against.
4. Investigate the effects of underwater explosive loading on other materials and laminate constructions. In the current study E-Glass was used as the structural fibers in all of the laminates. The performance of other materials such as S-Glass, Carbon, and Kevlar should be examines as well as the possibility of hybrid materials such as Glass / Carbon constructions. The performance of these materials needs to be understood as they inherently have different characteristics. For example carbon fibers have higher tensile strengths and modulus but fail much more catastrophically than glass fibers which have more elongation. Additionally the response of other laminate constructions should be examined. The current research utilized laminates which were constructed using individual layers of continuous fibers. There now exist three dimensional (3D) fabrics which include through thickness fibers which are inter-woven through the cloth. These through thickness fibers may improve the performance of the laminates in terms of reducing the delamination damage.
5. Conduct an investigation into the response of submerged composite structures to high hydrostatic pressures. This would provide insight as to how a composite structure would implode as compared to a corresponding metallic structure. For example the implosion

process for metallic cylinders is well understood including collapse pressure and final shape. However there is little understanding of how a composite cylinder of equivalent strength would collapse.

BIBLIOGRAPHY

Amini, M.R., Isaacs, J.B., Nemat-Nasser, S., "Experimental Investigation of Response of Monolithic and Bilayer Plates to Impulsive Loads", *International Journal of Impact Engineering*, 37, 2010, pp: 82-89

Amini, M.R., Simon, J., Nemat-Nasser, S., "Numerical Modeling of Effect of Polyurea on Response of Steel Plates to Impulsive Loads in Direct Pressure-Pulse Experiments", *Mechanics of Materials*, 42, 2010, pp: 615-627

Amini, M.R., Isaacs, J.B., Nemat-Nasser, S., "Investigation of Effect of Polyurea on Response of Steel Plates to Impulsive Loads in Direct Pressure-Pulse Experiments", *Mechanics of Materials*, 42, 2010, pp: 628-639

Arora, H., Hooper, P., Dear, J.P., "Impact and Blast Resistance of Glass Fibre Reinforced Sandwich Composite Materials", *Proceedings of IMPLAST 2010,* October 2010.

Batra, R.C., Hassan, N.M., "Response of Fiber Reinforced Composites to Underwater Explosive Loads", *Composites: Part B,* 38, 2007, pp: 448–468.

Bogdanovich, A., Singletary, J., Mohamed, M., "A new generation of composites reinforced with 3-D woven fabric performs", *Proceedings of the 22nd international SAMPE Europe conference*, Paris, France, March 27–29, 2001

Casey, D., *This Old Boat,* International Marine, 2009. ISBN 978-0-07-147794-9

Chan, S., Fawaz, Z., Behdinan, K., Amid, R., "Ballistic limit prediction using a numerical model with progressive damage capability", *Composite Structures*, 77, 2007, pp: 466–474.

Coombs, A., Thornhill, C.K., "An Underwater Explosive Shock Gun", *Journal of Fluid Mechanics*, 29, 1967, pp: 373-383

Donadon, M.V., Iannucci, L., Falzon, B.G., Hodgkinson, J.M., de Almeida, S.F.M., "A Progressive Failure Model for Composite Laminates Subjected to Low Velocity Impact Damage", *Computers and Structures*, 86, 2008, pp: 1232–1252.

Dyka, C.T., Badaliance, R., "Damage in Marine Composites Caused by Shock Loading", *Composites Science and Technology*, 58, 1998, pp: 1433-1442.

Espinosa, H.D., Lee, S., Moldovan, N., "A Novel Fluid Structure Interaction Experiment to Investigate Deformation of Structural Elements Subjected to Impulsive Loading", *Experimental Mechanics*, 46, 2006, pp: 805-824.

Filler, W.S., "Propagation of Shock Waves in a Hydrodynamic Conical Shock Tube", *The Physics of Fluids,* 7, 1964, pp: 664-667

Franz, T., Nurick, G., Perry, M., "Experimental Investigation into the Response of Chopped-Strand Mat Glassfibre Laminates to Blast Loading", *International Journal of Impact Loading*, 27, 2002, pp: 639- 667.

Gama, B., Xiao, J., Haque, M., Yen, C., Gillespie, J., "Experimental and numerical investigations on damage and delamination in thick plain weave S-2 glass composites under quasi-static punch shear loading", Center for Composite Materials, University of Delaware 2004.

Gardner, N., Wang, E., Kumar, P., Shukla, A., "Blast Mitigation in a Sandwich Composite Using Graded Core and Polyurea Interlayer", *Experimental Mechanics*; In Process

Geer, D., *Boat Strength for Builders, Designers, and Owners*, International Marine, 2000. ISBN 0-07-023159-1

Hodge, N., "Military Experimenting with 'Spray On' Armor for Humvees", *Defense Today*, 25, 2004

Hosseinzadeh, R., Shokrieh, M.M., Lessard, L., "Damage Behavior of Fiber Reinforced Composite Plates Subjected to Drop Weight Impacts", *Composites Science and Technology*, 66, 2006, pp: 61–68.

Jacinto, A., Ambrosini, R., Danesi, R., "Experimental and Computational Analysis of Plates Under Air Blast Loading", *International Journal of Impact Engineering*, 25, 2001, pp: 927 – 947.

Jackson, M., Shukla, A., "Performance of Sandwich Composites Subjected to Sequential Impact and Air Blast Loading", *Composites: Part B*, 42, 2011, pp: 155-166

LeBlanc, J., Shukla, A., Rousseau, C., Bogdanovich, A., "Shock loading of three-dimensional woven composite materials", *Composite Structures*, 79, 2007, pp: 344-355.

LeBlanc, J., Shukla, A., "Dynamic Response and Damage Evolution in Composite Materials Subjected to Underwater Explosive Loading: An Experimental and Computational Study", *Composite Structures*, 92, 2010, pp: 2421-2430.

Matzenmiller, A., Lubliner, J., Taylor, R.L., "A Constitutive Model for anisotropic damage in fiber-composites", *Mechanics of Materials*, 20, 1995, pp: 125-152.

McGregor, C.J., Vaziri, R., Poursartip, A., Xiao, X., "Simulation of progressive damage development in braided composite tubes under axial compression", *Composites: Part A*, 38, 2007, pp: 2247–2259.

Mouritz, A.P., "The effect of underwater explosion shock loading on the fatigue behaviour of GRP laminates", *Composites*, 26, 1995, pp: 3-9

Mouritz, A.P., “Ballistic Impact and Explosive Blast Resistance of Stitched Composites”, *Composites: Part B*, 32, 2001, pp: 431-439.

Nurick, G., Olson, M., Fagnan, J., Levin, A., “Deformation and Tearing of Blast Loaded Stiffened Square Plates” *International Journal of Impact Engineering*, 16, 1995, pp:273–291.

Nurick, G., Shave, G., “The Deformation and Tearing of Thin Square Plates Subjected to Impulsive Loads - An Experimental Study”, *International Journal of Impact Engineering*, 18, 1996, pp: 99–116.

O’Daniel, J.L., Koudela, K.L., Krauthammer, T., “Numerical Simulation and Validation of Distributed Impact Events”, *International Journal of Impact Engineering*, 31. 2005, pp: 1013–1038.

Poche, L., Zalesak, J., “Development of a Water-Filled Conical Shock Tube for Shock Testing of Small Sonar Transducers by Simulation of the Test Conditions for the Heavyweight MIL-S-901D (Navy)”, *NRL Memorandum Report 7109*, 10 October 1992.

Russell, D.M., “Error measures for comparing transient data, Part I: Development of a comprehensive error measure, Part II: Error measures case study”, *Proceedings of the 68th Shock and Vibration Symposium*, 3-6 November 1997.

Russell, D.M., “DDG53 Shock trial simulation acceptance criteria”, *69th Shock and Vibration Symposium*, 12-19 October 1998.

Sadd, M.H., “Wave Motion and Vibration in Continous Media”, University of Rhode Island, Kingston, RI, 2009

Schubel, P.M., Luo, J., Daniel, I., “Impact and Post Impact Behavior of Composite Sandwich Panels”, *Composites: Part A*, 38, 2007, pp: 1051-1057.

Stoffel, M., Schmidt, R., Weichert, D., “Shock Wave Loaded Plates”, *International Journal of Solids and Structures*, 38, 2001, pp: 7659- 7680.

Tekalur, A.S., Shivakumar, K., Shukla, A., “Mechanical Behavior and Damage Evolution in E-Glass Vinyl Ester and Carbon Composites Subjected to Static and Blast Loads”, *Composites: Part B*, 39, 2008, pp: 57-65.

Tekalur, A.S., Bogdanovich, A.E., Shukla, A., “Shock loading response of sandwich panels with 3-D woven E-glass composite skins and stitched foam core”, *Composites Science and Technology*, 69, 2009, pp: 736-753

Tiwari, V., Sutton, M.A., McNeill, S.R., "Assessment of High Speed Imaging Systems for 2D and 3D Deformation Measurements: Methodology Development and Validation", *Experimental Mechanics*, 47, 2007, pp: 561-579.

Tiwari, V., Sutton, M.A., McNeill, S.R., Xu, S., Deng, X., Fourney, W.L., Bretall, D.. "Application of 3D Image Correlation for Full-Field Transient Plate Deformation Measurements During Blast Loading", *International Journal of Impact Engineering* , 36, 2009, pp: 862-874.

Wang, L., "Unloading Waves and Unloading Failures in Structures Under Impact Loading", International Journal of Impact Engineering, 30, 2004, pp: 889-900

Wierzbicki, T., Nurick, G., "Large Deformation of Thin Plates Under Localized Impulsive Loading", *International Journal of Impact Engineering*, 18, 1996, pp: 899 – 918.

Williams, K.V., Vaziri, R., "Application of a damage mechanics model for predicting the impact response of composite materials", *Computers and Structures*, 79, 2001, pp: 997 – 1011.

Xiao, J., Gama, B., Gillespie, J., "Progressive damage and delamination in plain weave S-2 glass / SC-15 composites under quasi-static punch-shear loading", *Composite Structures*, 78, 2007, pp: 182-196.

Yuan, F.,Tsai, L., Prakash, V., Rajendran, A.M., Dandeka, D., "Spall strength of glass fiber reinforced polymer composites" *International Journal of Solids and Structures*, 44, 2007, pp: 7731–7747.

Zako, M., Uetsuji, Y., Kurashiki, T., "Finite Element Analysis of Damaged Woven Fabric Composite Materials", *Composites Science and Technology*, 63, 2003, pp:507-516.

Zaretsky, E., deBotton, G., Perl, M., "The response of a glass fibers reinforced epoxy composite to an impact loading", *International Journal of Solids and Structures*, 41, 2004, pp: 569–584.